Rabaptin5 is recruited to endosomes by Rab4a and Rabex5 to regulate endosome maturation

Inauguraldissertation

zur

Erlangung der Würde eines Doktors der Philosophie

vorgelegt der

Philosophisch-Naturwissenschaftlichen Faktultät

der Universität Basel

von

Simone Kälin

aus Einsiedeln (SZ)

Basel, 2014

Genehmigt von der Philosophisch-Naturwissenschaftlichen Fakultät auf Antrag von

Prof. Dr. Martin Spiess

Prof. Dr. Kurt Ballmer

Basel, den 18. Februar 2014

Prof. Dr. Jörg Schibler

Dekan

Acknowledgments

I would like to express my sincerest thanks to the following people:

Martin Spiess for giving me the opportunity to work on this project and for his continuous support.

My thesis committee members, **Kurt Ballmer** and **Markus Rüegg**, for your time, helpful discussions and advice.

David Hirschmann for data contributions and experimental advice

Nicole Beuret, who had always an open ear for technical questions and for always offering a helping hand.

All the past and present members of the Spiess group for a great working atmosphere, answering questions, giving input and relaxing coffee and lunch breaks: **Cristina Baschong, Julia Birk, Dominik Buser, Erhan Demirci, Franziska Hasler, Sonja Huser, Tina Junne, Lucyna Kocik, Deyan Mihov and Barry Shortt**.

Andrijana Kriz and Philipp Berger for introducing me to the MultiLabel system

Aurélien Rizk for helping me with the quantitation of the endosome size

Summary

Membrane trafficking between organelles is fundamental to the existence of eukaryotic cells. A multitude of proteins is involved in membrane trafficking, acting as building blocks for transport carriers, regulators of transport, and targeting and fusion factors. One important group of regulators are the Rab GTPases. They serve as multifaceted organizers of almost all membrane trafficking related processes in eukaryotic cells. In their active state, Rab proteins bind to effectors to mediate their function. One of these effector proteins is Rabaptin5, an early endosome protein with binding sites for Rab4, Rab5, the Rab5 GDP/GTP exchange factor Rabex5, as well as for the clathrin coat adaptor AP1. Rabaptin5 is considered to be the prototype of a Rab effector mediating a positive feedback loop by binding to active Rab5 and bringing along Rabex5, which activates further Rab5, thus maintaining endosomal fusion activity. Via the separate Rab4 interaction domain, Rabaptin5 has been proposed to function as a molecular linker between Rab5 and Rab4 to coordinate endocytic and recycling traffic.

In the present study, we analysed the function of Rabaptin5 in more detail by mutagenesis of the different interaction domains or motifs and expression of the mutant proteins in HeLa cells. We identified two independent Rab4 binding domains in the N-terminal half of the protein and two cooperating sequences binding to Rab5a. Deletion of the Rab4 and Rabex5 binding domains, respectively, abolished endosome recruitment of Rabaptin5 mutants. Inactivation of Rab4a and Rabex5 by siRNA-mediated silencing, respectively, completely prevented membrane binding of wildtype Rabaptin5, confirming the requirement for Rab4a and Rabex5 and excluding indirect structural effects of the deletions. Interestingly, deletion of either one of the two Rab5 binding domains showed no effect on endosome recruitment, but induced giant endosomes positive for markers of early endosomes like Rab4a, Rab5a, and transferrin, but also for the late endosomal markers Rab7a and the ESCRT component CHMP2B, suggesting the formation of early/late endosomal chimeras. The complete disruption of the Rabaptin5/Rab5a interaction produced giant endosomes with only late endosomal properties.

Our results clearly contradict the widely accepted feedback model, in which Rab5 controls its own activity. They rather indicate that Rabaptin5 is recruited to endosomes by Rab4a-GTP and Rabex5, which locally activates Rab5a by nucleotide exchange. At the same time, activated Rab5a appears to inhibit or moderate Rabaptin5 driven endosome maturation, since deletion of the Rab5 binding domains on Rabaptin5 induces a premature maturation process. The mechanism of Rabaptin5 driven endosome maturation remains to be clarified by further investigation.

Table of contents

Introduction

1. Intracellular transport

Membrane traffic in higher eukaryotes is a fundamental function. Every cell takes up external molecules, communicates with the world around it and quickly responds to changes in its environment. To fulfil these tasks, cells continually adjust the composition of their plasma membrane in rapid response to need. An extensive internal membrane system is used to add and remove cell-surface proteins integrated in the plasma membrane. Through the process of exocytosis, the secretory pathway delivers newly synthesized proteins, carbohydrates and lipids to the plasma membrane and the cell exterior. Through endocytosis, the opposite process, plasma membrane lipids, integral proteins and extracellular fluid is internalized and can be recycled or sent for degradation. Great progress has been made in the last decades to understand the basic mechanisms of protein transport, although a lot of the details of the different pathways are still missing. There are two major processes to transfer cargo from one organelle to another, called vesicular transport and organelle maturation.

1.1. Vesicular transport

Of the different cargo transfers between organelles, the vesicular transport is the best studied. The different types of vesicles are classified according to their proteins building the coat, the best studied of which are COPI, COPII, and clathrin coated vesicles. The vesicular transport hypothesis states that cargo is selectively incorporated into vesicles and transported from a donor compartment to a specific acceptor compartment. Specific coat proteins recognize cargo proteins and recruit other proteins to deform the membrane leading in pinching off a vesicle. The vesicle is actively transported along cytoskeletal filaments to the acceptor compartment where fusion occurs (Fig. 1) (Bonifacino and Glick, 2004; Spang, 2008)

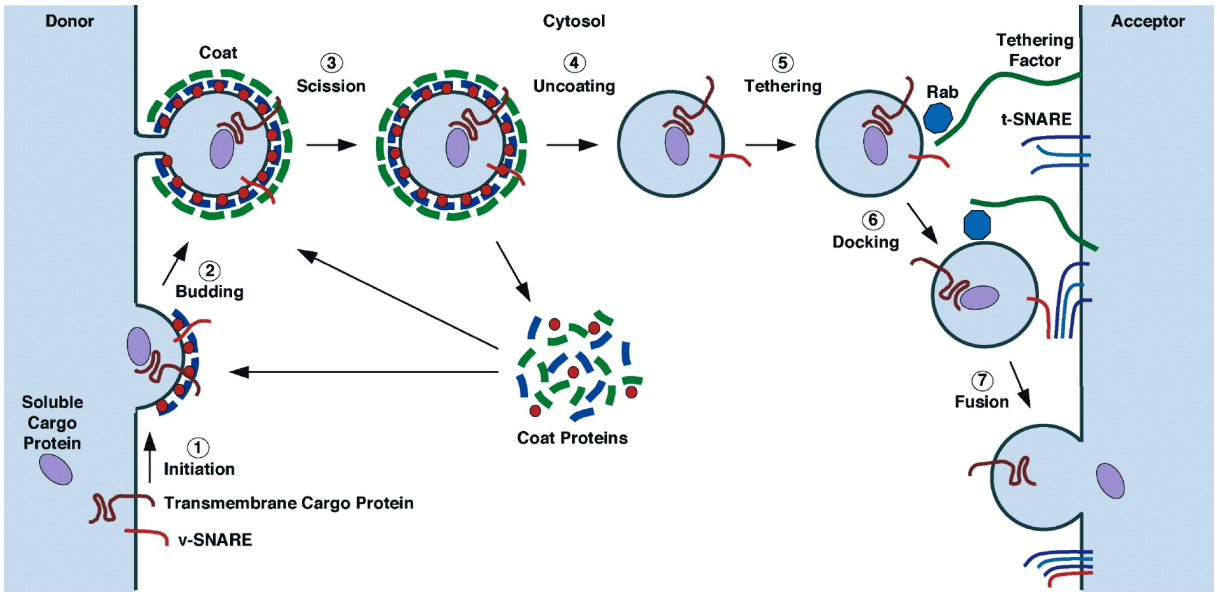

Fig. 1. **Steps of vesicle budding and fusion**
Vesicluar transport occurs in the following steps: coat initiation (1), budding (2) and scission (3), followed by uncoating (4), tethering (5), docking (6) and fusion (7) (Bonifacino and Glick, 2004)

1.1.1. Clathrin coated vesicles

Clathrin coated vesicles (CCVs) are the best characterized transport carriers and the first to be discovered (Pearse, 1976). They form at the plasma membrane, TGN and endosomes and have a large variety of associated proteins. The main component of CCVs is clathrin itself, which forms a mechanical scaffold on the vesicle surface (Edeling et al., 2006). The formation of these vesicles is a complex process and requires a regulated interplay between clathrin, its adaptors, cargo proteins and accessory factors.

1.1.1.1. Clathrin

Clathrin monomers assemble into triskelia, which form a lattice around the central membrane vesicle. Each clathrin protein consists of three trimerized heavy chains (CHCs) and three clathrin light chains (CLCs) (Ungewickell and Branton, 1981). The heavy chain can be subdivided into a C-terminal proximal domain at the trimerization zone, a middle domain forming a typical knee and a N-terminal globular domain (Fig. 2), which provide the structural backbone of the clathrin lattice. The light chains bind primarily to the proximal leg portion of the heavy chain with some interaction near the trimerization domain and they are thought to regulate the formation and disassembly of the clathrin lattice by changing their conformation to either stabilize or destabilize the clathrin cage (Brodsky, 2012).

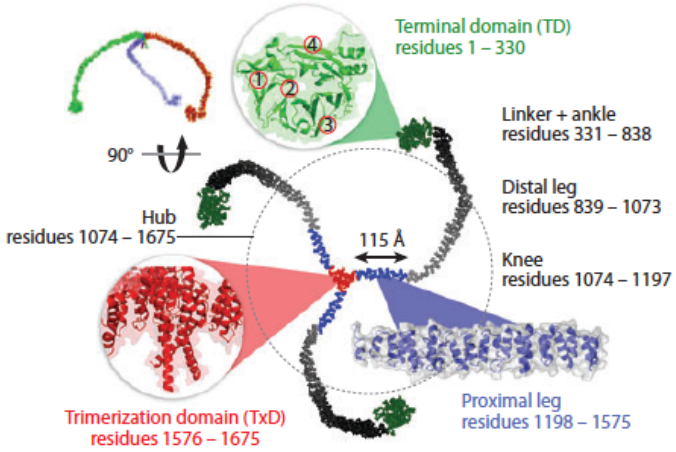

Fig. 2. **Structure of clathrin heavy chain**
A representation of a clathrin triskelion, which highlights the various domains using different colours. A single clathrin heavy chain is subdivided into the C-terminal proximal domain (red), the middle domain forming the knee (blue and grey) and the N-terminal globular domain (green) (Brodsky, 2012).

Although purified clathrin triskelia can spontaneously assemble into cages at low pH (Keen et al., 1979), adaptor proteins are necessary to form a clathrin coated vesicle *in vivo*. These adaptors bind to the N-terminal domain of clathrin. The first identified clathrin binding motive was the clathrin binding box (Dell'Angelica et al., 1998), a short consensus sequence of LΦXΦ[DE] (Φ is a bulky hydrophobic amino acid, X is a polar amino acid). Sequence analysis of different clathrin binding proteins revealed additional binding motifs like DLL (Morgan et al., 2000) or the W box motif (Miele et al., 2004).

1.1.1.2. ARF proteins

ADP ribosylation factors (ARFs) are a family of small GTPases that regulate membrane traffic and organelle structure in eukaryotic cells. The function of ARF requires a switch between GDP- and GTP-bound forms. Hydrolysis of bound GTP is mediated by GTPase activating proteins (GAPs), whereas the exchange of GDP for tri-phosphate nucleotide is mediated by guanine nucleotide exchange factors (GEFs). The GTP-bound ARF undergoes a conformational change, leading to an exposure of a myrostoyl tail, which anchors the protein in the membrane. There, the ARFs generate binding sites for adaptor proteins. There are six mammalian ARF proteins named ARF1 to ARF6 (D'souza-Schorey and Chavrier, 2006).

In many clathrin mediated transport pathways in the cell, ARF proteins are the first recruiters of adaptor and coat proteins as well as lipid-modifying enzymes. ARF1 is required for the

recruitment of the adaptor proteins AP1, AP3, AP4 and GGAs to the TGN (Boehm et al., 2001; Dell'Angelica et al., 2000; Stamnes and Rothman, 1993), but is also involved in clathrin assembly at endosomes (Pagano et al., 2004; van Dam et al., 2002). At the Golgi, ARF1, 3, 4 and 5 are all present and seem to have redundant functions since RNAi knockdown of the individual ARFs showed no effect on Golgi function (Volpicelli-Daley et al., 2005). ARF6 is found on the plasma membrane and is implicated in regulation of endosomal trafficking and the structural organization of the cell surface (D'Souza-Schorey et al., 1995). It is involved in clathrin independent endocytosis (Donaldson and Jackson, 2011) and thought to regulate clathrin mediated endocytosis (Poupart et al., 2007), although this still is highly debated and not clear.

1.1.1.3. Adaptor proteins

Adaptors represent a diverse group of proteins recognizing different classes of cargo receptor. The best characterized are a family of closely related proteins called the adaptor proteins (APs) comprising AP1, AP2, AP3, AP4 and AP5. Each of these five classes are localized to different intracellular compartments and vary in their receptor specificity (Hirst et al., 2013). Each AP complex is composed of two large subunits (~100kDa) called adaptins (a β-class adaptin, and one of either an α-,γ-,δ-,ε- or ζ-adaptin), a medium μ-subunit (~50kDa) and a small σ-subunit (~20kDa). The two large subunits can be subdivided into a C-terminal appendage domain connected to the N-terminal core domain via an unstructured flexible linker sequence (Kirchhausen, 1999). Adaptor complexes are organized in a typical structure with a core consisting of the small and medium subunit and the N-terminal trunk domains of the large subunits. All five APs bind directly to cytosolic sorting signals in transmembrane cargo proteins and have different subcellular localization. Whereas AP1 and AP2 are components of clathrin vesicles, AP4 and AP5 seem to act independently of clathrin (Hirst et al., 1999; 2011). In HeLa cells, AP2 together with AP1 and AP3 are the most abundant, whereas AP4 and AP5 are 1-2 order of magnitude less frequent (Fig. 3) (Hirst et al., 2013).

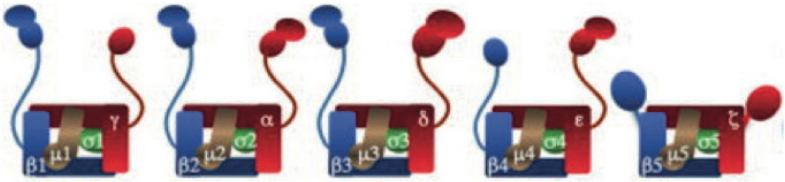

Adaptor	AP-1	AP-2	AP-3	AP-4	AP-5
Scaffold	Clathrin	Clathrin	Clathrin?	?	SPG11?
Lipid	PI(4)P	$PI(4,5)P_2$	PI(3)P	?	?
GTPase	Arf/Arfrp1	Arf?	Arf	Arf	?
Signals	YxxΦ [DE]xxxL[LI]	YxxΦ [DE]xxxL[LI]	YxxΦ [DE]xxxL[LI]	YxxΦ Yx[FYL][FL]E	?
Localization	TGN/ Endosomes	Plasma membrane	Endosomes	TGN	Late endosomes

Fig. 3. **AP complexes**
Schematic representation of the members of the heterotetrameric adaptor protein complexes and a summary of their properties. The colours represent the homology among the corresponding subunits (Canagarajah et al., 2013).

AP1

AP1 consists of two isoforms, which only differ in their μ_1-subunit (Ohno et al., 1999). AP1A is ubiquitously expressed and involved in the assembly of clathrin coated vesicles at the TGN and endosomes (Traub et al., 1993), while AP1B is only found in polarized cells (Ohno et al., 1999), where it mediates basolateral cargo sorting in epithelial cells (Fölsch et al., 1999). AP1A was believed to be responsible for anterograde transport from the TGN to endosomes (Doray et al., 2002). In addition, AP1A was shown to function at early endosomes where it is important for the recycling of cargo to the plasma membrane (Pagano et al., 2004). Other studies using cells derived from μ1A knockout mice show an involvement of AP1A in retrograde transport of cargo from endosomes to the TGN (Meyer et al., 2000).

AP2

AP2 is the best characterized adaptor complex and mediates the formation of CCVs from the plasma membrane for endocytosis (Owen et al., 2004). Knockout of AP2 is embryonically lethal showing its critical role in cell homeostasis (Mitsunari et al., 2005).

AP2 interacts with clathrin through the clathrin box motif in the β_2 hinge (Haar et al., 2000) and through interactions with the appendage domains (Owen et al., 2000). The appendage

domains are also responsible for the recruitment of a large number of accessory and regulatory proteins. The trunk of the α-subunit was shown to bind phosphoinositol-4,5-bisphosphate ($PI(4,5)P_2$) and phosphoinositol-3,4,5-triphosphate ($PI(3,4,5)P_3$) (Gaidarov et al., 1996), which is responsible for the targeting of AP2 to the plasma membrane (Gaidarov and Keen, 1999). Membrane recruitment of AP2 is favoured by the binding to cargo sorting signals. The medium μ-subunit recognizes tyrosine-based and dileucine sorting signals in the cargo receptors. The phosphorylation of a threonine residue in the μ-subunit by its kinase AAK1 induces a conformational change that exposes the binding sites. Its open conformation is further stabilized by binding of μ_2 to $PI(4,5)P_2$ allowing simultaneous interaction with sorting signals and the lipid bilayer (Olusanya et al., 2001; Ricotta et al., 2002).

AP3

AP3 was identified in mammals on the basis of structural homology with AP1 and AP2 (Pevsner et al., 1994). Two isoforms of AP3 exist: AP3A is ubiquitously expressed, while AP3B is found in neuroendocrine cells where it is involved in the biogenesis of synaptic vesicles from endosomes (Nakatsu and Ohno, 2003).

Immunofluorescence and electron microscopy localized AP3A on the TGN and endosomes (Dell'Angelica et al., 1997). It is believed that AP3A traffics cargo from the TGN or early endosomes to late endosomes or lysosomes (Nakatsu and Ohno, 2003). Localization of AP3A to its target membrane is highly dependent on ARF1, since ARF1 mutants locked in their GDP-bound form prevent binding of AP3 to organelles (Ooi et al., 1998). The interaction between AP3A and clathrin is highly debated. Studies showed that clathrin was not involved in AP3-containing vesicles and AP3 may use another scaffolding protein (Hirst and Robinson, 1998). Another group, on the other hand, could show that the β_3-subunit can interact with clathrin and also showed a colocalization with clathrin on endosomes (Dell'Angelica et al., 1998).

AP4

AP4 is ubiquitously expressed in human tissue (Dell'Angelica et al., 1999) and even though it has a low abundance compared to the other adaptor proteins in the cell, AP4 seems to play an important role, since mutations in humans lead to severe neurological symptoms (Hirst et al., 2013). According to immunofluorescence microscopy AP4 is mainly located at the TGN colocalizing with TGN46 (Hirst et al., 1999). It is proposed that AP4 mediates anterograde trafficking between the TGN and the endosomes, since a study could show that a depletion of AP4 resulted in the redistribution of the amyloid precursor protein APP from endosomes to

the TGN (Burgos et al., 2010). Alternatively AP4 might be involved in the direct transport between the TGN and the plasma membrane (Simmen et al., 2002).

Compared to the β-subunits of the other AP complexes, no clathrin binding motifs seem to be present on the β_4-subunit. Consistent with this observation is that AP4 does not colocalize with clathrin and is not detectable in clathrin coated vesicles purified from pig brain (Hirst et al., 1999). Like AP1 and AP3, AP4 is targeted to the TGN by ARF1 because treatment of cells with brefeldin A disrupted the signal at the TGN (Boehm et al., 2001).

AP5

AP5 was only discovered in 2011, hence relatively little is known about its function (Hirst et al., 2011). In cells expressing GFP-tagged AP5, a punctate staining was observed that was concentrated in the perinuclear region and colocalizing with late endosomal/lysosomal markers (Hirst et al., 2011).

Taking into account the low level of sequence similarity in the hinge and appendage regions of the ζ- and β_5-subunits relative to the other large adaptins, AP5 does not associate with clathrin. During the discovery of AP5, SPG11 and SPG15 were co-immunoprecipitated. SPG15 harbours a FYVE domain that can bind to the endosomal phosphoinositide-3-phosphate (PI(3)P). SPG11, on the other hand, shares salient features of domain organization with clathrin heavy chain implying a role of SPG11 as a membrane scaffold (Hirst et al., 2013).

1.1.1.4. GGAs

Another family of clathrin adaptor proteins are the Golgi-localizing, γ-adaptin ear homology domain, ARF-binding proteins (GGA). There are three GGAs in mammals, GGA1, GGA2 and GGA3, which are monomeric and ubiquitously expressed. They are organized into four distinct domains: a VHS domain (found in Vps27, Hrs and Stam), a GAT domain (found in GGAs and TOM1), a hinge domain rich in prolines and serines, and a GAE domain (similar to the γ-adaptin ear domain) (Fig. 4) (Nakayama and Wakatsuki, 2003).

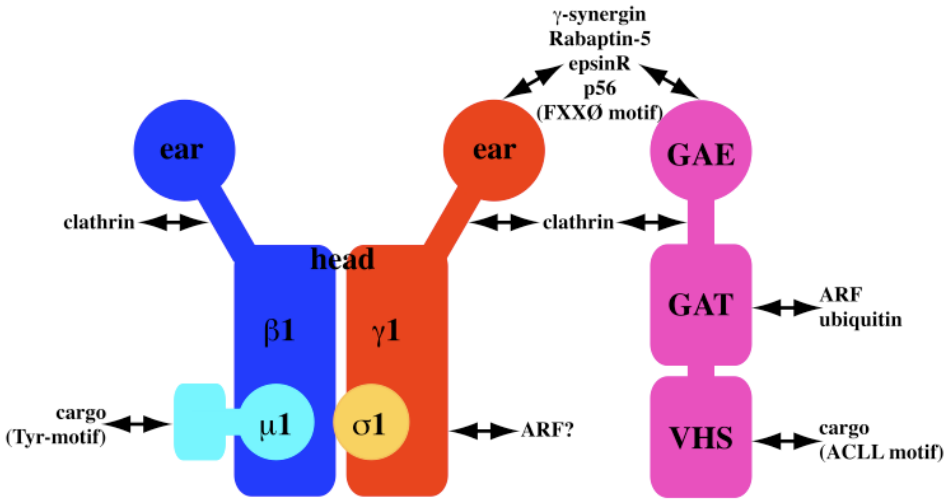

Fig. 4. **Domain organization of GGAs and AP1**

The structure of GGAs is similar to the γ_1-subunit of AP1. The sequences and proteins that bind to each domain are indicated with arrows. GGAs are recruited to membranes via the interaction with ARF in the GAT domain. The VHS domain is responsible for cargo recognition, the hinge region for clathrin recruitment and the GAE domain for interaction with accessory proteins (Nakayama and Wakatsuki, 2003).

VHS domains of mammalian GGAs recognize the acidic amino acid cluster-dileucine (ACLL) sequences within the cytoplasmic domains of transmembrane proteins found in the TGN (Puertollano et al., 2001). Through interaction with activated ARF, the GAT domain is responsible for targeting of GGAs onto TGN membranes. However it is unlikely that the specific TGN association of GGAs is determined solely by their interaction with ARF (Takatsu et al., 2002). The hinge region binds clathrin via type I clathrin-binding motifs (Dell'Angelica, 2001). The GAE domains of GGAs and the ear domain of γ-adaptin have been shown to share several binding partners. These accessory proteins include Rabaptin5 (Mattera et al., 2003), γ-synergin (Hirst et al., 2000), epsinR (Hirst et al., 2003) and enthoprotin (Wasiak et al., 2002).

GGAs are involved in the packaging of the mannose-6-phosphate receptor (M6PR) and its ligands into clathrin coated vesicles at the TGN to deliver them to early or late endosomes. Coated buds and vesicles containing GGAs together with clathrin, AP1 and M6PRs have been observed at the TGN (Doray et al., 2002; Puertollano et al., 2001) but they were not enriched in purified clathrin coated vesicles (Hirst et al., 2000). A recent study proposes that GGAs act together with AP1 to transport hydrolase-receptor complexes in the anterograde direction, from the TGN to endosomal compartments, since purified CCVs from AP1 knocksideways cells were strongly depleted from GGA2 (Hirst et al., 2012).

In addition, GGAs have an ubiquitin binding site on the GAT domain. They are proposed to play a role in the sorting of ubiquitinated proteins towards lysosomal degradation by sequestering these proteins to sites of clathrin coated vesicle formation (Pelham, 2004).

1.1.2. Clathrin mediated endocytosis

Clathrin mediated endocytosis involves the uptake of transport receptors with their cargo molecules from the plasma membrane to endosomes. Formation of CCVs can be generally divided into 5 stages: initiation, cargo selection, coat assembly, scission and uncoating (McMahon and Boucrot, 2011).

Initiation/Nucleation

Clathrin coated vesicle formation starts with the generation of a membrane invagination called a coated pit. Which proteins are responsible for the initiation step is highly debated. One study could show with single molecule imaging that endocytic sites begin with the simultaneous plasma membrane binding of two AP2 adaptors and one clathrin triskelion (Cocucci et al., 2012). Another study, however, implies that AP2 may not be required at the earliest stages of endocytosis, but that initiation involves the following three factors: FCH domain only (FCHO) proteins, EGFR pathway substrate 15 (EPS15) and intersectins (Henne et al., 2010; Stimpson et al., 2009). FCHOs contain a F-BAR domain that is able to induce membrane curvature. EPS15 and intersectins are involved in recruiting clathrin adaptor proteins to the membrane (Fig. 5).

Cargo selection

After clathrin, the adaptor AP2 is the most abundant component of clathrin coated vesicle formation at the plasma membrane. AP2 binds $PI(4,5)P_2$, which is specific for the plasma membrane, and motifs in the cytoplasmic tails of cargo proteins (McMahon and Boucrot, 2011). In addition, cargo specific accessory adaptor proteins link AP2 to cargo molecules, which are not directly recognized by AP2 (Fig. 5).

Clathrin coat assembly

As soon as the cargo is sequestered to the nucleation site, the clathrin coat starts to assemble. Clathrin triskelia are directly recruited to sites with high adaptor concentration on the membrane through the interaction with adaptors and clathrin-binding accessory factors. The polymerization of clathrin is thought to stabilize membrane curvature, but is not directly inducing membrane bending (McMahon and Boucrot, 2011). Further accessory proteins like

epsins and amphiphysin are recruited to the edge of the forming vesicle where they induce further membrane invagination by their specialized curvature domains (Fig. 5).

Vesicle scission

BAR domain containing proteins, like amphiphysin, endophilin and sorting nexin 9, which are located at the vesicle neck, are recruiting the mechanochemical enzyme dynamin (Ferguson et al., 2009; Sundborger et al., 2011). Dynamin forms a helical collar around the neck of the invaginating vesicle and undergoes a GTP hydrolysis dependent conformational change (Sever, 2002). The mechanism of the membrane cleavage is still not absolutely clear.

Uncoating and coat recycling

After scission, the clathrin coat is most probably incomplete across the zone where the vesicle neck was attached, leaving a defect in the clathrin cage (McMahon and Boucrot, 2011). At this position auxilin can bind to clathrin (Massol et al., 2006) and recruit HSP70, an ATPase catalysing clathrin disassembly (Schlossman et al., 1984). Conversion of $PI(4,5)P_2$ to PI(4)P mediated by the phosphatase synaptojanin is required for uncoating (Cremona et al., 1999), but how the mechanism really works is not clear. The uncoating process releases the clathrin machinery for reuse in a new cycle (Fig. 5)

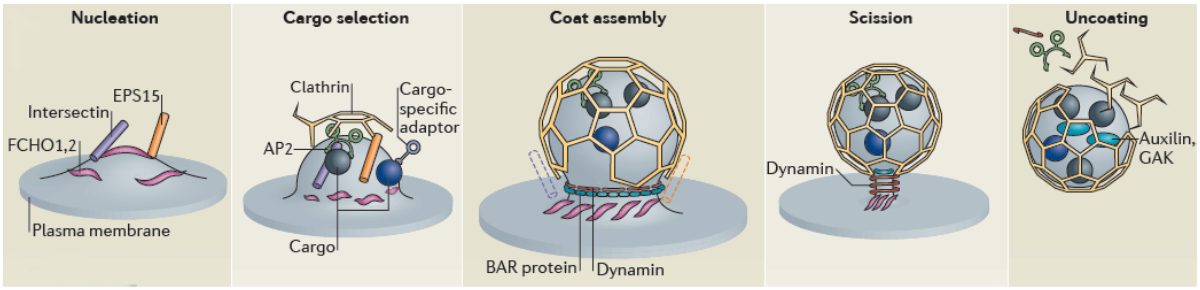

Fig. 5. **Assembly and disassembly of a clathrin coat.**
The five steps of clathrin vesicle formation: Clathrin coated pit formation is either initiated by AP2 directly or indirectly via FCHOs and EPS15. The adaptor AP2 then interacts with cargo and other coat components like clathrin. Clathrin polymerizes on the membrane, which leads to membrane deformation. The coat formation is stabilized by accessory factors. After coat assembly, dynamin pinches off the vesicle. In a further step, clathrin is quickly uncoated by the combined action of the ATPase HSP70 and auxilin (McMahon and Boucrot, 2011).

1.2. Organelle maturation

In addition to vesicular transport some organelles undergo a so-called maturation process, where they change their identity by replacing their associated proteins or altering the luminal pH. During the maturation process, cargo molecules do not need to leave the lumen of the organelle. Typical examples include the cisternal maturation in the Golgi apparatus and the maturation of early to late endosomes.

1.2.1. Cisternal maturation in the Golgi

The Golgi apparatus is composed of stacks of membrane-bound structures known as cisternae and can be divided into the cis-, medial- and trans-cisternae plus the Trans Golgi Network (TGN) (Glick and Luini, 2011). Secretory proteins from the ER enter the Golgi at the cis-face, are transported through the Golgi where they are modified and exit at the trans-face.

How the secretory proteins are transported through the Golgi is still not absolutely clear. For many years, there was the idea that Golgi cisternae are stable compartments, where the cargo is transported from one cisternae to the next in anterograde vesicles (Rothman and Wieland, 1996). This view is more and more replaced by the cisternal maturation model (Fig. 6). In this model, new cisternae assemble at the cis-face of the Golgi from ER-derived vesicles, progress through the Golgi stack and disintegrate at the TGN by forming transport carriers (Glick and Malhotra, 1998). Resident Golgi proteins are recycled from older to younger cisternae by retrograde transport in COPI vesicles (Rabouille and Klumperman, 2005). Important evidence for cisternal maturation is the progressive transport of large procollagen fibers, which are too large to fit into a transport vesicle, through the Golgi (Bonfanti et al., 1998). In addition, the bulky soluble protein procollagen was observed to move through the Golgi stack at the same rate as the smaller transmembrane glycoprotein VSV-G (Mironov et al., 2001).

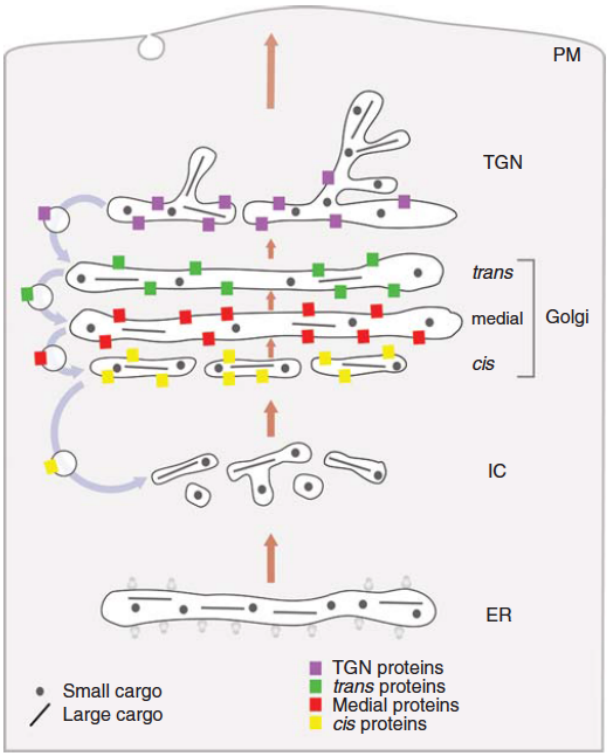

Fig. 6. **Cisternal maturation model**

Golgi cisternae are transient structures formed de novo form ER-derived vesicles. A newly formed cisterna matures from cis to trans and breaks into transport carriers at the TGN. Maturation is driven by the retrograde transport of resident Golgi proteins by COPI vesicles (Glick and Luini, 2011).

2. Endocytic pathway

2.1. Endocytosis

Endocytosis is a basic cellular process and plays a role in nutrient acquisition, antigen presentation, clearance of apopotic cells, receptor regulation and controlling the lipid and protein composition of the plasma membrane. There are several pathways for internalizing cargo from the cell surface (Fig. 7). Some of them are constitutive, whereas others are triggered by specific signals. They typically involve the formation of small vesicles. The best-studied type of endocytosis is clathrin mediated endocytosis as described in a previous chapter. Other, clathrin independent internalization routes include actin based macropinocytosis and phagocytosis, as well as caveolin dependent endocytosis.

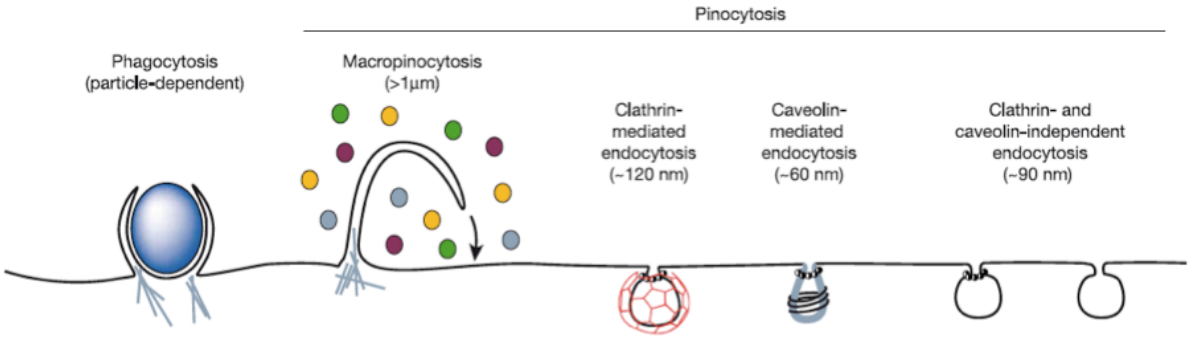

Fig. 7. **Pathways of entry into the cell.**
Large particles can be taken up by phagocytosis, whereas fluid uptake occurs by macropinocytosis. A lot of cargo is also taken up by clathrin or caveolin mediated endocytosis. However, numerous cargo can be endocytosed by less characterized mechanisms independent of clathrin or caveolin (Conner and Schmid, 2003).

Endocytosed molecules, including recycling receptors with their bound ligand and down-regulated receptors, are delivered to early endosomes. In this compartment ligand and recycling receptor are often separated from each other and encounter different destinies. The ligands and down-regulated receptors are destined for destruction in lysosomes along with other soluble content of the endosome, while recycling receptors are transported back to the plasma membrane (Gruenberg, 2001). In mammalian cells several recycling receptors like the low density lipoprotein (LDL) and the transferrin receptor (TfR) cycle between the plasma membrane and the early endosome (Trowbridge et al., 1993).

2.2. The endosomal/lysosomal system

The endocytic compartment can be morphologically subdivided into early endosomes, late endosomes with its multivesicular appearance and lysosomes. The term 'early endosomes' actually describes two distinct endosomal organelles: the sorting and recycling endosomes (Maxfield and Mcgraw, 2004).

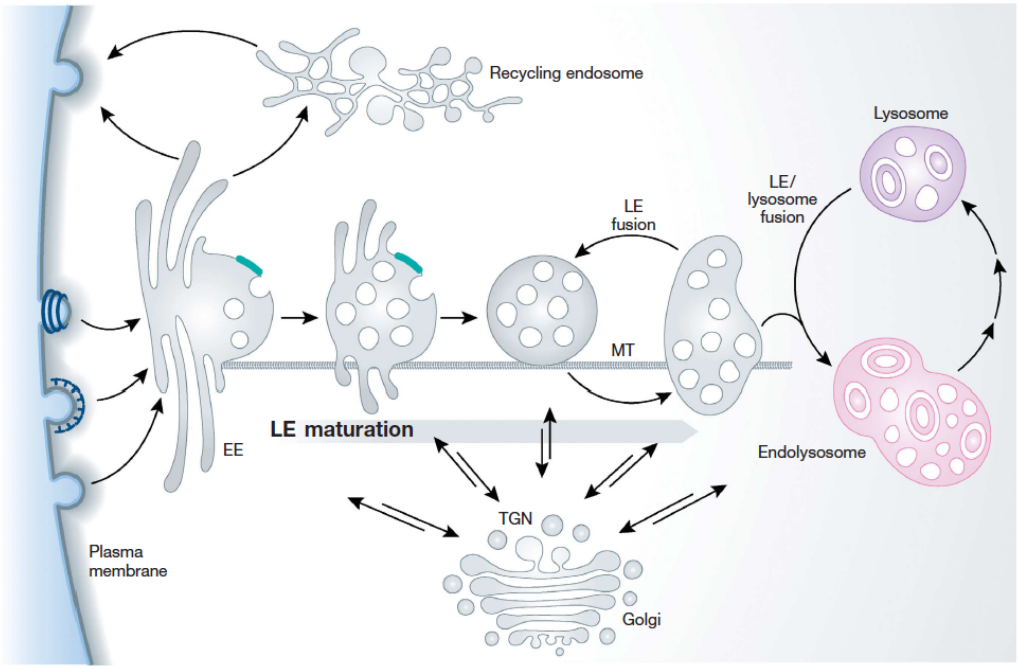

Fig. 8. **The endosomal/lysosomal system.**
Endocytosed material is first delivered to sorting endosomes. Once the ligand and the receptor encounter the lower pH in the lumen of the sorting endosome, the pH-sensitive ligands dissociate from their receptors. While most receptors are recycled back directly or indirectly via recycling endosomes to the plasma membrane, ligands and down-regulated receptors stay in the sorting endosome, which mature into late endosomes. Late endosomes fuse with lysosomes where its content is degraded (Huotari and Helenius, 2011).

2.2.1. Sorting endosomes

Sorting endosomes are defined as the first endocytic compartment to accept incoming cargo internalized from the plasma membrane. Endocytic vesicles are presumed to fuse with each other to form primary sorting endosomes. These structures in turn undergo homotypic membrane fusion and grow (Mills et al., 1999). Sorting endosomes are located in the peripheral cytoplasm close to the plasma membrane and have a slightly acidic lumen with a pH of around 6 (Fig. 8). They consist of regions of thin tubular extensions (~60 nm diameter) and a globular part (~400 nm diameter) which has membrane invaginations and give rise to a multivesicular appearance (Gruenberg, 2001). The globular part matures into late endosomes,

while the tubular extensions convert into recycling endosomes (Mellman, 1996). As their name implies, an important function of the sorting endosome is to target molecules to their correct destination. There are three possible ways: recycling to the plasma membrane, degradation in the lysosome or retrieval to the TGN. In the endolysosomal system proteins can either travel to late endosomes and later lysosomes or are recycled back to the plasma membrane either directly from the sorting endosome (fast pathway) or indirectly via recycling endosomes (slow pathway) (Hao and Maxfield, 2000; van Dam et al., 2002). Due to the moderately acidic pH in the sorting endosome lumen, pH-sensitive ligands can dissociate from their receptors. While most of the receptors are recycled back to the plasma membrane, the ligands and down-regulated receptors accumulate in the vesicular region of the sorting endosome which leads to the degradative pathway (Jovic et al., 2010).

Sorting endosomes are positive for Rab5 and early endosome antigen 1 (EEA1). In addition, Rab4 is also localized to sorting endosomes (van der Sluijs et al., 1991), but likewise to Rab11-positive recycling endosomes (Trischler et al., 1999). Organelles are defined by their lipid composition. Sorting endosomes are enriched in phosphoinositol-3-phosphate (PI(3)P) helping to manifest its identity (Behnia and Munro, 2005).

In the globular part of the sorting endosome, intraluminal vesicle (ILV) formation already begins. The cytosolic surface of the sorting endosome membrane has characteristic plaques containing clathrin and components of the endosomal sorting complex required for transport (ESCRT), which is responsible for the sorting of ubiquitinated membrane proteins into ILVs (Raiborg and Stenmark, 2002).

2.2.2. Recycling endosomes

As mentioned above, there are two main routes to recycle receptors back to the cell surface: Either via the fast recycling directly form the sorting endosomes or via the slow recycling indirectly over the recycling endosomes (Fig. 8). Recycling endosomes are mainly a collection of tubular structures associated with microtubules, which are thought to be pinched off from the main body of the sorting endosomes. They have a perinuclear localization in the cell and are less acidic than sorting endosomes (pH 6.4-6.5) (Taguchi, 2013). Specific surface proteins such as Rab11 can be used as a marker for recycling endosomes (Trischler et al., 1999). A well-studied receptor using the slow recycling pathway is the low density lipoprotein receptor (LDLR). LDL is released from the LDLR in the sorting endosomes and transported to the lysosomes, while the receptor recycles back to the plasma membrane via recycling endosomes (Maxfield and Mcgraw, 2004).

2.2.3. Late endosomes

Late endosomes are derived from the vacuolar domains of sorting endosomes. How the conversion occurs is still under debate. The classical model envisages a vesicular transport between the two endosomes. Endosomal carrier vesicles would serve as transporters of cargo from sorting endosomes to late endosomes (Vonderheit and Helenius, 2005). This view is more and more challenged by the maturation model. Here the sorting endosome is transformed into a late endosome by a Rab conversion (discussion in further detail later), which predicts no vesicular transport (Rink et al., 2005).

Late endosomes formed in the peripheral cytoplasm from sorting endosomes move to the perinuclear area of the cell (Huotari and Helenius, 2011). Mature late endosomes are typically round or oval and have a diameter of 250-1000nm. Their lumen has a pH of 5-6 and they are located near the nucleus. Late endosomes are defined to be Rab7 and PI(3,5)P_2 positive and already contain some hydrolases, but they are not able to digest all the material. Therefore proteins destined for degradation are transported further to lysosomes.

Newly formed late endosomes undergo a multitude of changes by the time they fuse with lysosomes having almost no similarities with sorting endosomes anymore. The maturation process involves the following main steps (Huotari and Helenius, 2011) (Fig. 8):

1. Rab conversion: Rab5 is exchanged with Rab7. This process will be discussed in further detail in the Rab conversion chapter.

2. Formation of intraluminal vesicles (ILVs): Ubiquitinated cargo recruits the ESCRT machinery that induces inward-budding of membrane containing specific membrane proteins and lipids destined for degradation.

3. Acidification: The luminal pH drops from 6.5 to 5-6 through the action of V-ATPases.

4. Phosphoinositiol conversion: PI(3)P is converted to PI(3,5)P_2.

5. Loss of recycling with the plasma membrane

6. Gain of lysosomal hydrolases and membrane proteins: Many newly synthesized acid hydrolases are delivered to late endosomes after they are tagged with mannose-6-phosphate (M6P) in the Golgi and then bind mannose-6-phosphate receptor (M6PR) in the TGN. In the late endosomes, the hydrolases dissociate from the receptors as a result of the low pH and the receptors are recycled back to the TGN.

2.2.4. Lysosomes

The mechanism of transfer of endocytosed material from endosomes to lysosomes is controversial. There are four possible models: maturation model, vesicular transport model, kiss-and-run model and hybrid model (Luzio et al., 2007). The kiss-and-run model describes a continuous cycle of transient contacts between late endosomes and lysosomes, while in the hybrid model the two organelles fuse to form a hybrid organelle, followed by a fission event (Fig. 9).

Lysosomes are the main site for intracellular digestion and are organelles of heterogeneous size. They have a perinuclear localisation and Lamp1 is a typical marker. Two classes of proteins are essential for the function of lysosomes: acid hydrolases and integral lysosomal membrane proteins (LMPs). Lysosomes contain about 50 types of acid hydrolases including proteases, nucleases, glycosidases, lipases, phosholipases, phosphatases and sulfatases. The lysosome with a luminal pH of 5.0 to 5.5 provides the environment for optimal hydrolase activity. The hydrolases are mainly transported via the M6P receptors to late endosomes and reache the lysosomes via the endocytic pathway.

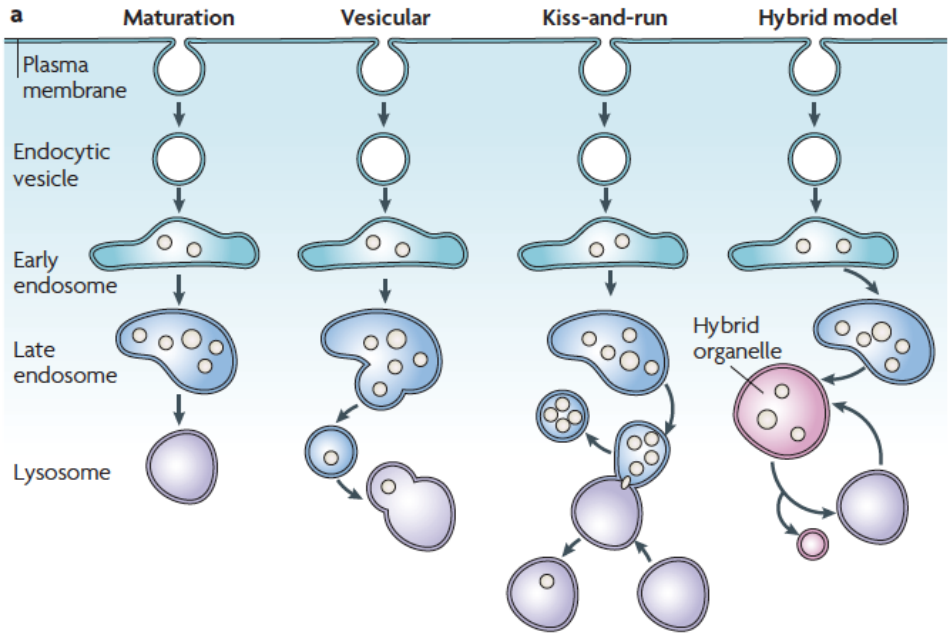

Fig. 9. **Delivery to lysosomes**
Different models have been proposed to explain the transport from late endosomes to lysosomes. In the first model late endosomes mature into lysosomes, while in the second model a vesicular transport between the two organelles takes place. In the third model, late endosomes and lysosomes can partially fuse to allow exchange of content before they separate again (kiss-and-run model). In the last model, late endosomes and lysosomes fuse to a hybrid organelle (Luzio et al., 2007).

The mammalian lysosome contains around 25 LMPs. They are mainly located in the lysosomal limiting membrane and have diverse functions like lysosomal acidification, protein import from the cytosol, membrane fusion and transport of degradation products to the cytosol. The most famous LMPs are the lysosome associated membrane proteins (LAMPs) (Saftig and Klumperman, 2009). Not so much is known about the transport of LMPs to lysosomes. A fraction of the LMPs that exit the TGN reaches the plasma membrane over the secretory pathway and travel then to the lysosomes via the endocytic pathway. But there are also direct ways from the TGN to the endolysosomal system.

3. Retrograde transport from endosomes to the TGN

Retrograde transport from endosomes to the TGN is only partially involved in the endocytic pathway since this pathway is mainly used by endogenous membrane-bound proteins like acid hydrolase receptors, which cycle between endosomes and the TGN. However, to some extent, these proteins are also present at the plasma membrane. Following their internalization into early endosomes, they return to the TGN showing the existence of a plasma membrane-endosome-TGN pathway (Fig. 10) (Bonifacino and Rojas, 2006).

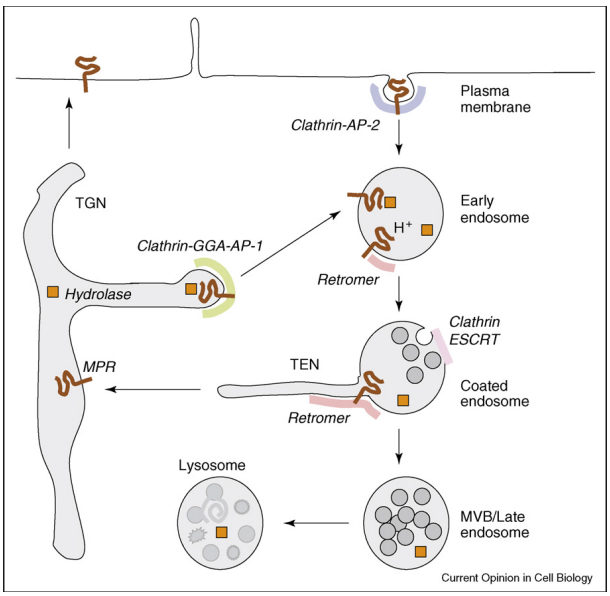

Fig. 10. **Sorting of an acid hydrolase receptor**
Mannose-6-phosphate receptor (M6PR), a typical acid hydrolase receptor, cycles between the TGN and endosomes. Clathrin coats mediate exit of M6PR bound to hydrolases from the TGN. In the endosomes, the hydrolases dissociate from the M6PRs as a result of the low pH and the receptors are recycled back to the TGN via the retromer complex. A small subset of M6PR is also present at the plasma membrane, where it is internalized and joins the pool of the recycling M6PR in the endosomes (Bonifacino and Hurley, 2008).

Cargos like acid-hydrolase receptors, transmembrane enzymes and SNARES are transported from endosomes to the TGN by the retromer complex. In mammalian cells, the retromer complex consists of sorting nexin (SNX) dimers and a VPS26-VPS29-VPS35 trimer (McGough and Cullen, 2011). SNX proteins form specific homo- or heterodimers via their BAR-domains, which induces high membrane curvature and are recruited to endosomal membranes by binding to PI(3)P with their Phox-homology (PX)-domains (Bonifacino and Hurley, 2008). The VPS26-VPS29-VPS35 complex is then recruited through interactions with the N-termini of the SNXs. The VPS35 subunit is responsible for the selection of retrograde cargo proteins into retromer coated membrane domains (Bonifacino and Rojas, 2006).

There are also other retrograde transport mechanisms such as clathrin mediated transport. Clathrin coated carriers are involved in transport of Shiga toxin and the TGN markers TGN38 and TGN46 from endosomes to the TGN (Saint-Pol et al., 2004).

4. Multivesicular body formation

Multivesicular bodies (MVBs) are late endosomes containing intraluminal vesicles (ILVs). A subset of transmembrane proteins and lipids are sorted into these vesicles. Upon fusion with the lysosome, the ILVs are exposed to hydrolases and are degraded (Babst, 2011). The proteins inducing intraluminal vesicle formation form the endosomal sorting complex required for transport, short ESCRT. The ESCRT machinery consists of four sub-complexes: ESCRT-0, -I, -II and -III plus several accessory components (Table 1) (Raiborg and Stenmark, 2009).

Table 1 | ESCRT subunits

Complex	Yeast protein	Metazoan protein	Mammalian synonym	Ubiquitin-binding domain	Selected interacting proteins (metazoan)
ESCRT-0	Vps27	Hrs	NA	UIM	Clathrin, Eps15b
	Hse1	STAM1, 2	NA	UIM (VHS)	AMSH, UBPY
ESCRT-I	Vps23	Tsg101	NA	UEV	NA
	Vps28	Vps28	NA	NA	NA
	Vps37	Vps37A, B, C, D	NA	NA	NA
	Mvb12	Mvb12A, B	NA	NA	NA
ESCRT-II	Vps22	Vps22	EAP30	NA	NA
	Vps25	Vps25	EAP20	NA	NA
	Vps36	Vps36	EAP45	GLUE	NA
ESCRT-III	Vps2	Vps2A,B	CHMP2A,B	NA	NA
	Vps20	Vps20	CHMP6	NA	NA
	Vps24	Vps24	CHMP3	NA	AMSH, UBPY
	Vps32 (Snf7)	Vps32A, B, C	CHMP4A,B,C	NA	NA
Vps4	Vps4	Vps4A, B	SKD1A,B	NA	NA
	Ist1	Ist1	NA	NA	NA
	Did2 (Vps46)	Vps46A, B	CHMP1A,B	NA	NA
	Vta1	Vta1	LIP5	NA	NA
	Vps60 (Mos10)	Vps60	CHMP5	NA	NA
Other	Bro1 (Vps31)	Alix, HD-PTP	NA	NA	AMSH, UBPY

NA, not applicable. In an attempt to simplify, we have mainly used the Vps names of ESCRT subunits, although alternative names exist, especially in mammalian cells, as indicated. Certain mammalian proteins, such as Hrs, Tsg101 and Alix, have such well-established names that their Vps names have been omitted. Note that the assignment of accessory proteins to Vps4 rather than to ESCRT-III is arbitrary in the light of our incomplete understanding of their functions.

Table 1: **ESCRT subunits and accessory components** (Raiborg and Stenmark, 2009)

Studies on endosomal membranes have suggested that late endosomes contain lipid rafts rich in cholesterol and sphingomyelin (Sobo et al., 2007), but are also enriched in phosphoinositol-3-phosphate (PI(3)P). It is proposed that intraluminal vesicles are formed from these lipid rafts, since the vesicles contain a high amount of cholesterol (Möbius et al., 2003). This model is also supported by the fact that HRS, a subunit of ESCRT-0, can bind to PI(3)P (Raiborg et al., 2001b) and sort ubiquitinated membrane proteins into these domains. Membrane proteins destined for degradation are mono-ubiquitinated at multiple sites or polyubiquitinated via the ubiquitin-lysine 63. Both subunits of ESCRT-0 possess several motifs interacting with ubiquitin (MIU) (Hirano et al., 2006), which strengthen overall ubiquitin binding. Enhanced complex sorting function was also shown by the binding of HRS to clathrin through a C-terminal clathrin box motif (Fig. 11a) (Raiborg et al., 2001a).

ESCRT-I and ESCRT-II are likely to function when ubiquitin-containing cargo has already been concentrated by ESCRT-0. These two complexes also have one ubiquitin binding motif and it has been proposed that cargo could be handed over from one complex to the other,

but the mechanism is not clear yet (Raiborg and Stenmark, 2009). In addition to the role in cargo sorting, ESCRT-I might contribute to membrane deformation. ESCRT-I in yeast spans about 25 nm, which is approximately the size of ILVs in yeast (Kostelansky et al., 2007). ESCRT-III is so far the best-characterized component of the whole machinery that can drive membrane deformation. *In vivo*, high levels of the ESCRT-III subunit VPS32/CHMP4 causes the formation of curved polymeric spirals on membranes (Hanson et al., 2008). These spirals are able to induce negative curvature in the membrane, which gives rise to membrane tubules that are extruded away from the cytoplasm (Fig. 11b). During this process, cargo is deubiquitinated by Doa4, which is recruited by ESCRT-III. Deubiquitination mediates the recycling of ubiquitin, thereby avoiding depletion of the cellular ubiquitin pool (Swaminathan et al., 1999).

How membrane abscission occurs, is still not clear. One possible model is that ESCRT-III assembles into circular arrays and narrows the neck of the invaginating vesicle. The ATPase VPS4 may then drive abscission through removal of individual ESCRT-III subunits at the neck of the invagination (Fig. 11c) (Henne et al., 2011).

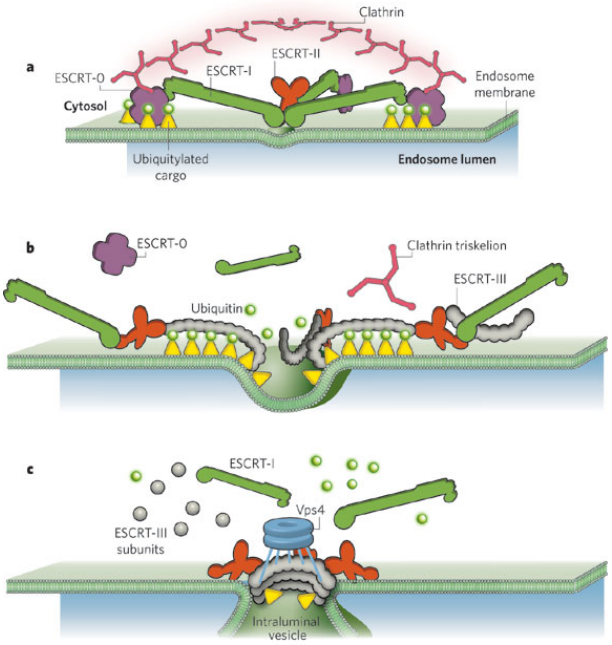

Fig. 11. **MVB formation**

a) Initial recognition of ubiquitinated cargo is mediated by ESCRT-0, which concentrates in lipid rafts containing PI(3)P and clathrin microdomains. b) ESCRT-III induces negative curvature in the membrane, which gives rise to membrane tubules that are extruded away from the cytoplasm. c) Together with ESCRT-III VPS4 causes scission of the vesicles. (Saksena et al., 2009)

5. Rab proteins

The transfer of contents between distinct membrane-enclosed organelles is fundamental to the existence of eukaryotic cells. Central in ensuring that cargoes are delivered to their correct destinations are the Rab proteins, a ubiquitously expressed family of small monomeric Ras-like GTPases (Stenmark, 2009). 11 Rabs have been identified in yeast Saccharomyces cerevisiae and over 60 in mammalian cells (Grosshans et al., 2006). Like other GTPases, Rabs switch between two conformations, an inactive form bound to GDP (guanosine diphosphate), and an active form bound to GTP (guanosine triphosphate). GDP to GTP exchange is catalysed by guanine nucleotide exchange factors (GEFs), which facilitate GDP release. The high cytosolic concentration of GTP ensures that GTP quickly binds as soon as GDP is released from the Rab (Zerial and McBride, 2001). GTP hydrolysis is driven by the intrinsic GTPase activity of the Rab protein itself but also catalyzed by a GTPase-activating protein (GAP) (Stenmark, 2009). Rabs also undergo a membrane insertion and extraction cycle that is partially coupled to the nucleotide cycle. Rabs are anchored via prenyl groups on two cysteines in the C-terminus. Upstream of the prenyl anchor is a hypervariable region that highly differs between Rab proteins, which plays a role in correct membrane targeting (Chavrier et al., 1991).

GDP dissociation inhibitor (GDI) recognizes GDP-bearing Rabs, binds the hydrophobic, insoluble prenyl groups and carries the Rab proteins through the cytoplasm to its appropriate target membrane (Pfeffer, 2013). Membrane attachment of Rab proteins requires the function of a GDI displacement factor (GDF). Once dissociated from GDI the lipid prenyl groups can then insert into the membrane, anchoring the Rab proteins at the cytoplasmic face of a vesicle or the target membrane (Grosshans et al., 2006). The active membrane-bound Rabs are then able to fulfil their various functions in membrane traffic by binding to specific factors called effectors. By definition, effector proteins can only bind to their specific Rab proteins in their GTP bound form (Fig. 12).

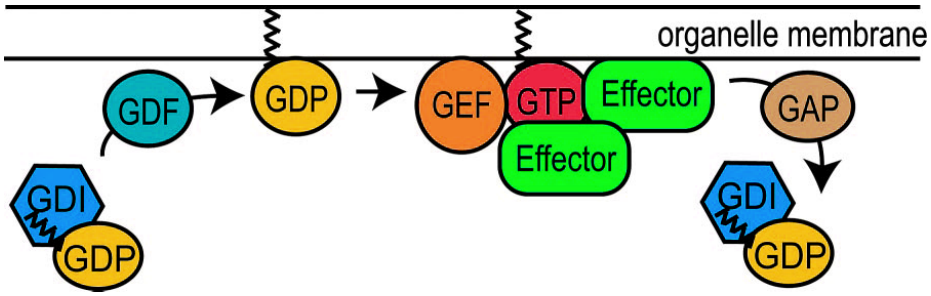

Fig. 12. **Scheme of the Rab-GTP/GDP cycle.**
Conversion of the GDP-bound Rab into the GTP-bound form occurs through GEFs. The active Rab-GTP is recognized by effector proteins, which can then fulfil their function. The active form is converted back to inactive Rab-GDP through GTP hydrolysis, which is stimulated by GAPs. Inactive Rab is then bound to GDI, which masks the prenyl group and keeps the Rab in a soluble cytosolic form. With the help of GDF, the Rab protein gets membrane attached again and the cycle can start form the begining (Gross-hans et al., 2006).

The highly selective distribution of specific Rabs on the membranes makes them ideal molecular markers for identifying each membrane type and guiding vesicular traffic between them. Specific Rab proteins have been shown to regulate the following for steps in transport reactions: vesicle budding, uncoating, motility, and fusion (Stenmark, 2009).

Vesicle budding

It has been shown that several Rab GTPases are involved in cargo specific coat assembly during vesicle budding. A prime example involves Rab9 at late endosomes. Rab9 recruits its effector TIP47, which binds to the cytosolic tail of mannose-6-phosphate receptor (M6PR) and is required for the transport of the receptor from late endosomes to the TGN (Díaz and Pfeffer, 1998).

Uncoating

Rab proteins also participate in vesicular uncoating. Endocytic vesicles from the plasma membrane contain among other components the adaptor complex AP2 and Rab5. AP2 needs to be phosphorylated at its μ_2-subunit to interact with cargo and requires the binding to $PI(4,5)P_2$ to be recruited to the membrane. After scission of the vesicle from the plasma membrane, Rab5 binds to its effector GAPVD1 which coordinates uncoating by promoting dephosphorylation of μ_2-subunit and increasing $PI(4,5)P_2$ turnover (Semerdjieva et al., 2008).

Motility

Vesicles are often actively transported through the cell by using either actin- or microtubule-dependent motors. Some motor proteins can directly bind to Rab proteins. Rab6-GTP binds to the microtubule motor Rabkinesin6 and thus promotes the delivery of vesicles from the Golgi to the ER (Echard et al., 1998). More often, Rabs indirectly interact with motor proteins. Rab27a, for example, recruits the effector melanophillic to melanosomes. Melanophilic in turn binds to the motor myosin Va, thereby shuttling the melanosomes towards the cell periphery (Kuroda and Fukuda, 2004).

Vesicle fusion

In the last step of vesicle transport, Rab tethering effectors are involved. Rab5 is essential for homotypic early endosome fusion as well as heterotypic endocytic vesicle to endosome fusion. It indirectly influences this processes by recruiting the tethering effector EEA1 and Rabenosyn5, which in turn interact with SNARE proteins (Nielsen et al., 2000; Simonsen et al., 1999).

In the next chapters, some Rab proteins involved in the endolysosomal system are explained in further detail.

5.1. Rab5

Rab5 is involved in several different functions and is localized to early endosomes, clathrin coated vesicles, and the plasma membrane. Its traditional role lies in targeting plasma-membrane-derived vesicles to endosomes and in homotypic fusion between early endosomes (Bucci et al., 1992; Gorvel et al., 1991). Rab5 is a rate-limiting component in membrane docking or fusion in the early endocytic pathway. A GTPase-deficient mutant, Rab5Q79L, stimulates endocytosis and early endosome fusion leading to enlarged early endosomes, whereas a mutant with a greater affinity for GDP, Rab5S34N, inhibits these processes (Stenmark et al., 1994).

The role of Rab5 on the plasma membrane was for a long time neglected. A small fraction of Rab5 is localized to the plasma membrane and several *in vitro* studies indicate that Rab5 contributes directly to clathrin mediated endocytosis. Ligand uptake during *in vitro* endocytosis depends on the presence of Rab5-GDP bound to GDI (McLauchlan et al., 1998), whereas Rab5-GDP bound to GDI undergoes GDP/GTP exchange when incubated with purified clathrin coated vesicles (Horiuchi et al., 1995). Rab5 also affects protein sorting within endosomes (de Renzis et al., 2002) and is involved in the attachment and movement of early endosomes along microtubules (Nielsen et al., 1999).

On endosomes, a lot of different Rab5-interacting proteins were found. These proteins include Rabaptin5 (Stenmark et al., 1995), Rabenosyn5 (Nielsen et al., 2000), Vps34 (Christoforidis et al., 1999b) and EEA1 (Christoforidis et al., 1999a).

5.2. Rab4

The monomeric GTPase Rab4 is associated with early endosomes and is supposed to regulate recycling from endosomes to the plasma membrane. However, its role in this recycling process is not absolutely clear. Overexpression of wildtype Rab4 reduces the intracellular accumulation of the tracer horse radish peroxidase and transferrin receptors are redistributed from endosomes to the plasma membrane (Mohrmann and van der Sluijs, 1999). It also blocks iron discharge by preventing the delivery of transferrin to acidic early endosomes, instead causing transferrin accumulation in a population of nonacidic vesicles and tubules. Rab4 thus appears to control the function or formation of recycling endosomes (van der Sluijs et al., 1992). In an *in vitro* study, depletion of Rab4 from cytosol blocked the formation of recycling vesicles, indicating that Rab4 is required to generate endosome-derived vesicles (Pagano et al., 2004). siRNA mediated knockdown of Rab4 in HeLa cells showed contradicting results. In one study transferrin receptor recycling was enhanced by Rab4 knockdown (Deneka et al., 2003), while the recycling rate was decreased in another study (Yamamoto et al., 2010).

Rab4-GTP is membrane bound while Rab4-GDP has a cytosolic distribution. To see if this is important, chimeric Rab4 proteins were created in which the carboxyl-terminal prenylation motif was replaced by the transmembrane domain of cellubrevin (Mohrmann, 2002). Due to this replacement the protein was permanently attached to the membrane. The chimeric Rab4 was still properly targeted to early endosomes and bound GTP to the same extent as wildtype Rab4, but recycling of the transferrin receptor was less efficient than with wildtype Rab4. This indicated that Rab4 function requires on-going cycles of association and dissociation with the membrane (Mohrmann, 2002).

As with many other Rabs, Rab4 interacts with specific effectors like Rabaptin5 (Vitale et al., 1998), Rabenosyn5 (de Renzis et al., 2002) and Rabip4 (Fouraux et al., 2004).

5.3. Rab11

By immunofluorescence and electron microscopy it was shown that Rab11 colocalizes with internalized transferrin in recycling endosomes of CHO and BHK cells (Ullrich et al., 1996). Rab11 is involved in recycling of receptors to the plasma membrane because early steps of uptake of transferrin were not affected by overexpressing Rab11. Dominant negative Rab11S25N inhibited transport of internalized transferrin from recycling endosomes to the plasma membrane and caused fragmentation of this compartment. Transfection of the dominant positive Rab11Q70L lead to compaction of the recycling endosome, but also inhibited transferrin recycling (Ullrich et al., 1996). Ren et al. (1998) used a low temperature block to inhibit transport between sorting and recycling endosomes. They could show that Rab11S25N inhibits transferrin recycling, whereas Rab11Q70L and wildtype Rab11 did not have this effect (Ren et al., 1998). It seems that the active Rab11-GTP is required for the exit of the transferrin receptor.

In addition to these reports linking Rab11 activity to endocytic pathways, other reports suggested a role for Rab11 in biosynthetic exocytic membrane traffic. In PC12 cells, Rab11 was detected in association with TGN and TGN-derived secretory vesicles (Urbé et al., 1993). In BHK cells, overexpression of dominant-negative Rab11S25N decreased delivery of the basolaterally targeted vesicular stomatitis virus (VSV) G protein from the Golgi to the cell surface (Chen et al., 1998), and expression of wildtype Rab11 accelerated delivery of new protease-activated receptors to kidney epithelial cell surfaces following trypsin exposure (Roosterman et al., 2003)

5.4. Rab7

Rab7 is associated primarily with late endosomes and is the only Rab protein that is at least partially localized to lysosomes (Méresse et al., 1995). Wildtype Rab7 allowed normal transport of VSV G protein from the plasma membrane to late endosomes, while a dominant negative mutant caused an accumulation of VSV G protein in early endosomes. Further was shown that Rab7 function was not required for early internalization of cargo, but was crucial in downstream degradative events (Feng et al., 1995). Another study showed a marked inhibition of the degradation of low density lipoproteins (LDL) in cells expressing a dominant negative Rab7 (Vitelli et al., 1997). Press et al. (1998) observed that dominant negative Rab7 caused a redistribution of mannose-6-phosphate receptor (M6PR) from its late endosomal localization to early endosomes (Press et al., 1998). In summary, all the data suggest a key role of Rab7, downstream of Rab5, in regulating membrane transport leading from early to late endosomes.

6. Rab GEFs

As described above, Rab GEFs enhance the release of GDP from Rab proteins, thereby facilitating nucleotide exchange. A recent study has shown that Rab GEFs can provide the minimal machinery needed to target one Rab to a specific membrane in the cell. For this, Rab GEFs were fused to mitochondrial outer membrane targeting sequences and the effect on different Rabs were observed. With this approach, it was possible to specifically target a selection of Rab proteins to their cognate GEFs at mitochondria (Blümer et al., 2013).

6.1. Rabex5

Rabex5 is a guanine nucleotide exchange factor (GEF) for Rab5 on early endosomes and was originally identified as an interaction partner of Rabaptin5 (see chapter Rab effectors). They form a stable complex and are coimmunoprecipitated with one another. That is why Horiuchi et al. (1997) named the protein Rabex5 for Rabaptin5-associated exchange factor for Rab5. Rabex5 contains multiple functional domains. In the middle of the protein resides the GEF catalytic core, which consists of a VPS9 domain and an adjacent N-terminal helical bundle. A coiled-coil domain downstream of the GEF domain mediates the binding to Rabaptin5, whereas a zinc-finger domain at the N-terminus is shown to bind ubiquitin (Fig. 12).

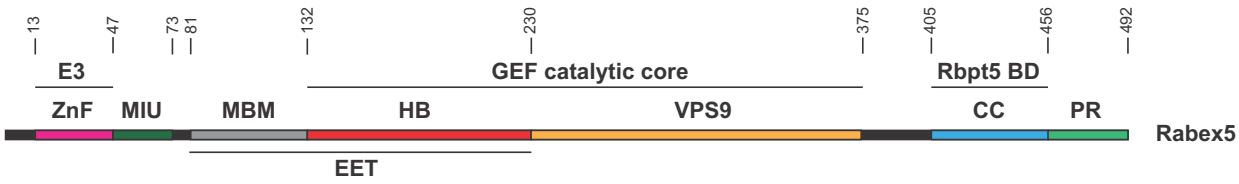

Fig. 13. **Domain organization of Rabex5**

At the N-terminus, the zinc-finger motif (ZnF) and the motif interacting with ubiquitin (MIU) are located. In the middle is an early endosome targeting (EET) domain consisting of the membrane-binding motif (MBM) and the helical bundle (HB). The GEF catalytic core in cludes the helical bundle (HB) and the VPS9 module. The C-terminus comprises the coiled-coil domain (CC) interacting with Rabaptin5 followed by a proline-rich region (PR).

The middle sequence of Rabex5 shares high sequence homology with VPS9, which is the GEF for the yeast homologue of Rab5 (Horiuchi et al., 1997). The structure of the catalytic core was solved showing an N-terminal bundle domain (HB) and the VPS9 domain. In addition, Rabex5 did not only show catalytic activity for Rab5 but also for the closely related Rab21. Furthermore, four amino acids could be identified, that are essential for the GEF activity: Asp313, Pro317, Tyr354 and Thr357 (Delprato et al., 2004).

Full-length Rabex5 shows very little GEF activity *in vitro* and requires interaction with Rabpatin5, a Rab5 effector, to gain full activity (Lippé et al., 2001) or endosomal membrane association (Zhu et al., 2007). In a yeast two-hybrid assay, Mattera et al. (2006) could show that Rabex5 binds to Rabaptin5 via a coiled-coil domain downstream of the GEF catalytic core. In an attempt to crystalize the Rabex5 GEF catalytic core in complex with nucleotide-free Rab21, an autoinhibitory element in an amphiphatic helix located near the C-terminus of the VPS9 domain was discovered. This autoinhibitory element overlaps with the Rabaptin5 binding site. Autoinhibition could be released by binding of Rabaptin5 to this element (Delprato and Lambright, 2007), also explaining the higher GEF activity of Rabex5 complexed to Rabaptin5 as shown by Lippe et al (2001).

Another study showed that Rabex5 could be targeted to early endosomes independent of Rabaptin5. They identified an early endosome targeting (EET) domain composed of a membrane targeting motif (MBM) and the helical bundle (HB) also used by the GEF catalytic core. Mutants missing the Rabaptin5 binding domain were able to recruit to early endosomes and activate Rab5 independently of Rabaptin5 *in vivo* (Zhu et al., 2007).

In addition to its function as a Rab5 GEF, Rabex5 also binds ubiquitin and undergoes ubiquitin binding-dependent monoubiquitination (Lee et al., 2006; Mattera et al., 2006; Penengo et al., 2006). The N-terminal zinc-finger (ZnF) motif has ubiquitin ligase activity (Lee et al., 2006; Mattera et al., 2006), while the following motif interacting with ubiquitin (MIU) binds ubiquitin (Lee et al., 2006; Penengo et al., 2006). Mattera et al. (2008) demonstrated that ubiquitin binding is essential for Rabex5 recruitment to endosomes and that monoubiquitinated Rabex5 is enriched in the cytosol. They proposed a model where ubiquitin binding-dependent monoubiquitination results in dissociation of Rabex5 from endosomes to the cytosol thereby causing an intramolecular binding of the ubiquitin to the ZnF/MIU domains. Deubiquitination of Rabex5 releases this interaction allowing again endosome recruitment (Mattera and Bonifacino, 2008).

In summary, the data suggests three different ways of Rabex5 recruitment to endosomes: First via the Rab5 effector Rabaptin5, second via the early endosome targeting domain, and finally by binding to ubiquitinated cargo. To what extend each pathway contributes to the final picture is not clear yet.

6.2. RME6

While Rabex5, the GEF that is mainly required to activate Rab5 on early endosomes, is well-characterized, not much is known about GEFs acting at the plasma membrane. In 2005, Sato et al. characterized RME6 as a novel nucleotide exchange factor for Rab5 at the plasma membrane. RME6 was identified in a screen for C. elegans mutants that are defective in receptor-mediated endocytosis. As for Rabex5, RME6 possesses a Vps9 GEF domain. Its specificity for Rab5-GDP was shown by yeast two-hybrid and co-immunoprecipitation experiments with dominant negative Rab5 (Sato et al., 2005). It could be shown that RME6 colocalized with clathrin at the plasma membrane and that localization of RME6 to the plasma membrane disappeared when clathrin was silenced (Sato et al., 2005), suggesting that RME6 localization depends on recruitment to clathrin coated structures. Vesicle formation and subsequent removal of the clathrin coat occurred normally in RME6 mutants but fusion of the vesicle with early endosomes was inhibited by the lack of active Rab5 (Sato et al., 2005).

7. Rab effectors

The activated Rab proteins bind to soluble factors that act as effectors to transduce the signal of the Rab GTPase (Zerial and McBride, 2001). By definition Rab effectors recognize the GTP-bound form of a Rab GTPase. Many different effector proteins have been identified and characterized through a variety of approaches. Various modes of Rab coordination by Rab effectors have been proposed (Fig. 14) (Stenmark, 2009): Firstly, a positive feedback loop, where one Rab protein recruits it own GEF, thus maintaining the membrane's Rab identity. Secondly, effector coupling, where the effector of one Rab also interacts with another and thereby coordinates or couples different Rab domains or Rab activities in the same membrane. Thirdly, activation coupling, where one Rab recruits the GEF of a second Rab protein in a feedforward manner, and finally, Rab conversion, where the first Rab recruits the GEF of the second which then recruits a GTPase activating protein (GAP) for the first, thereby completing the full transition from one Rab identity of the membrane to the next.

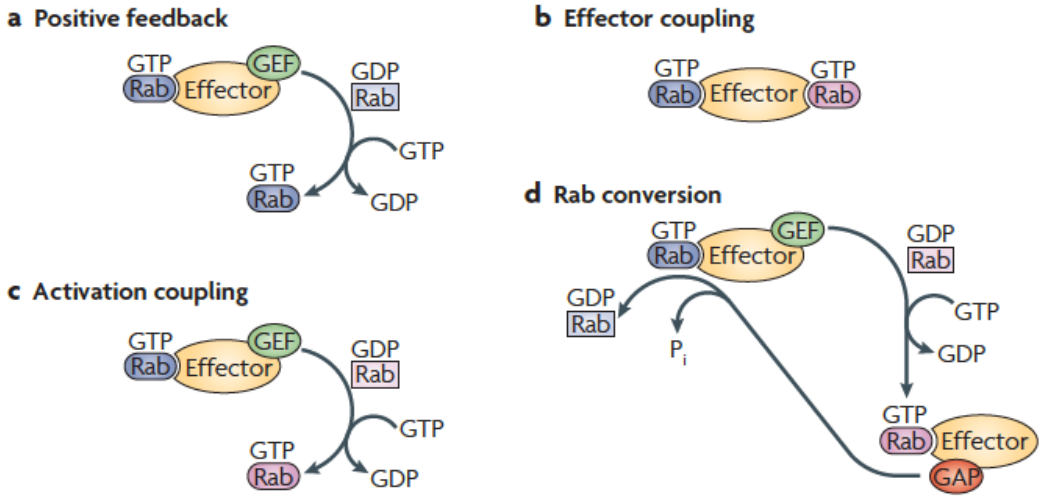

Fig. 14. **Coordination of Rab functions by effector proteins**

a) Positive feedback: One Rab protein recruits it own GEF

b) Effector coupling: The effector of one Rab also interacts with another Rab

c) Activation coupling: One Rab recruits the GEF of a second Rab

d) Rab conversion: The first Rab recruits the GEF of the second which then recruits a GAP for the first

7.1. Rabaptin5

Rabaptin5 is generally considered the prime example of a Rab effector involved in positive feedback and effector coupling. It is a cytosolic protein recruited to transferrin-positive endosomes and consists of 862 amino acid residues. There are several Rabaptin5 isoforms (Rabaptin5α, Rabaptin5γ, Rabpatin5δ) in human cells as a result of differential splicing varying only in small insertions or deletions (Korobko et al., 2002). It was found that Rabaptin5 dimerizes through N- and C-terminal sequences predicted to form coiled coil structures (Fig. 15). Coiled-coil domains consist of seven amino acid repeats where positions one and four are non-polar and positions five and seven are mainly polar. Their overall secondary structure is α-helical and the interaction between two helices result in efficient burial of the hydrophobic side-chains at their interface (Vitale et al., 1998).

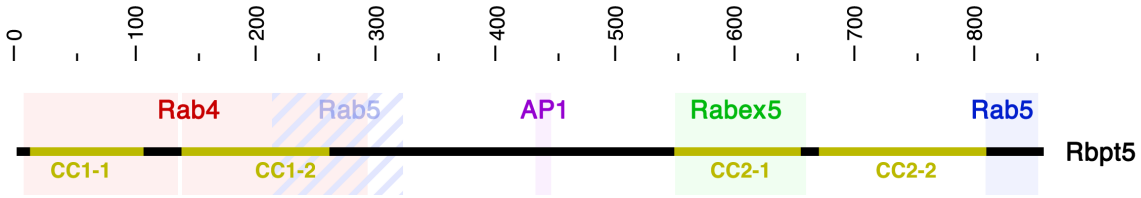

Fig. 15. **Domain organization of Rabaptin5**
Rabaptin5 dimerizes through the indicated coiled coil structures (CC1-1, CC1-2, and CC2-1, CC2-2). At the N-terminus the Rab4 and one Rab5 binding domain are located. An AP1 binding site is in the middle of the protein, whereas Rabex5 binds to CC2-1 region. A second Rab5 binding domain is found in the C-terminus of the protein.

Rabaptin5 was originally identified in a yeast two-hybrid screen using GTPase-deficient Rab5 as a bait (Stenmark et al., 1995). It got its name from the Greek word apto, which means touch: Rabaptin5 is in touch with Rab5.

A conserved 73 amino acid sequence at the C-terminus of Rabaptin5 was shown to be necessary and sufficient for the interaction between Rab5 and Rabaptin5 (Vitale et al., 1998). A later crystallization of Rab5 together with the C-terminal domain of Rabaptin5 could narrow this interaction to only 20 amino acids at the very C-terminal end of Rabaptin5 (Zhu et al., 2004). For a long time, this was thought to be the only Rab5 binding domain. In 2006, however, Korobko et al. found in a yeast two-hybrid screen a second, N-terminal Rab5 binding domain comprising amino acids 216-318 (Korobko et al., 2006).

As mentioned in the Rabex5 chapter, Rabaptin5 forms a stable complex with Rabex5 (Horiuchi et al., 1997) and plays an important role in early endosome fusion. A widely accepted model has been described by Zerial et al. (2001). Initial Rabex5 recruitment to early/sorting endosome occurs either via its early endosome targeting domain or via the interaction with

ubiquitinated cargo (see Rabex5 chapter). Rabex5 then recruits Rab5 to the endosome and converts it to its active GTP-bound form, which becomes anchored to the membrane. The active Rab5 in turn is then able to interact with its effectors, including Rabaptin5. Rabaptin5 via the bound Rabex5 increases the production of Rab5-GTP. These interactions generate a positive feedback loop, which counteracts inactivation of Rab5 through its GAP (Grosshans et al., 2006). In this way, activated Rab5 is specifically concentrated at the early endosome (Fig. 16). Among the Rab5 effectors recruited to Rab5-GTP is VPS34, a phosphoinositol-3-kinase (PI(3)K), which causes an enrichment of PI(3)P on early endosomes (Zerial and McBride, 2001). The concomitant presence of Rab5-GTP and PI(3)P allows then the recruitment of the Rab5 effectors early endosome antigen 1 (EEA1) and Rabenosyn5, which are important for docking and early endosome fusion (Fig. 16) (Zerial and McBride, 2001).

Vitale et al. (1998) found in a yeast two-hybrid screen a second Rab-binding domain, which is located from amino acid 5 to 135 in the N-terminus of Rabaptin5 and mediates the direct interaction with GTP-bound Rab4. A later study, however, showed an interaction of Rabaptin5 with Rab4 between amino acid 140 and 295 with a GST-Rab4 pull-down (Deneka et al., 2003). This is in agreement with the observation of Korobko et al. (2005) that the splice variant Rabaptin5δ, missing residues 187 to 226, cannot interact with Rab4. All agree on a Rab4 binding domain in the N-terminal third of Rabaptin5, but the exact position is still under debate. The contribution of the Rab4-binding domain in Rabaptin5 appeared to be reflected in an observed increase of Rab4 and Rab5 double-positive endosomes (de Renzis et al., 2002), supporting the notion of Rabaptin5 coordinating or coupling these two Rabs and their effector networks.

In vitro and *in vivo* studies both showed that the Rabaptin5/Rabex5 complex interacts with γ-ear domain of AP1 and with GGAs (Mattera et al., 2003). There are two interaction sites between GGAs and Rabaptin5. The GGA-GAT domain binds to the C-terminal coiled-coils of Rabaptin5 (residues 551-862). The second interaction of GGA lies in the GAE domain that recognizes an FGPLV sequence (residues 439-443) in a predicted unstructured segment of Rabaptin5. The FGPLV sequence in Rabaptin5 is made up of hydrophobic amino acid residues that bind to the hydrophobic grooves on the GGA-GAE and γ-adaptin ear domains of AP1 (Mattera et al., 2003). Interestingly the GGA-Rabaptin5 interaction reduces binding of clathrin to the hinge domain of GGA. This could suggest that binding of Rabaptin5/Rabex5 may induce the release of clathrin from GGA-coated intermediates or prevent clathrin binding, thereby inhibiting vesicle formation (Mattera et al., 2003).

Another group investigated the role of Rabaptin5α (splice variant of Rabaptin5) and its putative partner γ_1-adaptin in membrane recycling (Deneka et al., 2003). In agreement with Mat-

tera et al. (2003), they could show that the binding site for γ_1-adaptin is in the hinge region of Rabaptin5α. Co-expression of Rabaptin5α and γ_1-adaptin showed a colocalization in a Rab4-dependent manner on recycling endosomes (Deneka et al., 2003). Cells transfected with Rabaptin-5α alone were unable to support recycling of internalized transferrin receptor. But receptor recycling could be restored by overexpression of Rabaptin-5α together with γ_1-adaptin.

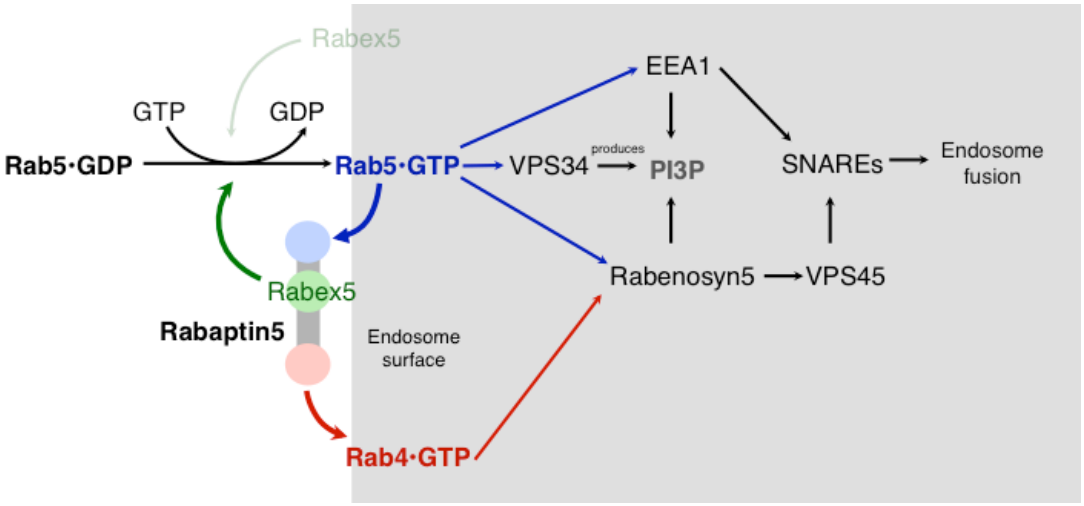

Fig. 16. **Model of Rab5 activation on early endosomes**
Rabex5 activates Rab5 on early endosomes. Rab5-GTP is then able to interact with Rabaptin5. Rabaptin5 in turn binds to Rabex5 and increases the production of Rab5-GTP. These interactions generate a positive feedback loop. Active Rab5 also activates VPS34, which converts PI into PI(3)P. This phosphorylated PI together with Rab5 allows the recruitment of EEA1 and Rabenosyn5, which finally leads to membrane fusion. As Rabaptin5 interacts with Rab5 and Rab4 through independent sites, it is supposed to function as a molecular linker between endocytic and recycling traffic (according to Zerial and McBride 2001).

7.2. VPS34

VPS34 is a phosphoinositol-3-kinase (PI(3)K), which catalyzes the phosphorylation of phosphoinositol (PI) to phosphoinositol-3-phosphate (PI(3)P). It is thought to be one of the first Rab5 effectors recruited to early endosomes (Christoforidis et al., 1999b). Through the presence of Rab5-GTP and the production of PI(3)P, other Rab effectors such as EEA1 (Lawe et al., 2000) or Rabenosyn5 (Nielsen et al., 2000) are specifically recruited to early endosomes. VPS34 plays a crucial role in early endosome function since treatment of cells with the PI(3)K inhibitors Wortmannin (Ui et al., 1995) and LY294002 (Vlahos et al., 1994) prevented localization of PI(3)P-binding proteins (Patki et al., 1997) and impaired transferrin trafficking from early endosomes (van Dam et al., 2002).

7.3. Early endosome antigen 1 (EEA1)

Originally identified as a Lupus autoantigen with restricted localization to early endosomes, EEA1 consists of an N-terminal FYVE domain, four long heptad repeats with the Rab5 interaction site and a C-terminal region containing a calmodulin binding (IQ) motif (Fig. 17) (Mu et al., 1995). It forms a parallel coiled-coil homodimer in cells (Callaghan et al., 1999) similar to Rabaptin5. Endosomal localization requires the interaction of PI(3)P with the FYVE domain on EEA1 (Stenmark et al., 1996), since mutations of conserved residues in the FYVE domain disrupt PI(3)P binding and localization to endosomes. In addition to the FYVE domain, EEA1 also needs its Rab5 binding domain for endosome targeting, showing the importance of the dual interaction of EEA1 with Rab5 and PI(3)P for efficient membrane recruitment (Lawe et al., 2000). EEA1, in coordination with SNARE proteins, is essential for early endosome fusion *in vivo* (Mills et al., 1998). It can directly interact with syntaxin6 (Simonsen et al., 1999) and syntaxin13 (McBride et al., 1999), two target-SNAREs that mediate homotypic early endosome fusion, but the exact mechanism is still under debate.

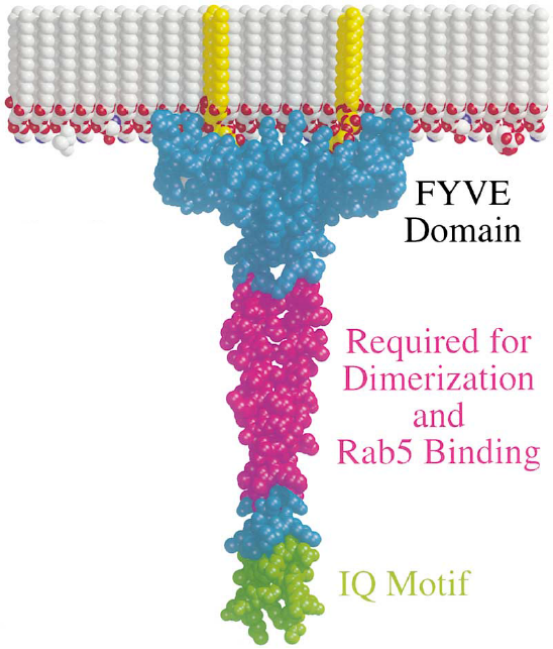

Fig. 17. **Model for multivalent membrane binding by homodimeric EEA1**
EEA1 is targeted to early endosomes via the interaction with PI(3)P and Rab5-GTP. The region required for both dimerization and interaction with Rab5 is highlighted in magenta, while the putative IQ motif is highlighted in green. (Dumas et al., 2001)

7.4. Rabenosyn5

Rabenosyn5 is another FYVE-domain-containing Rab5 effector that, similar to EEA1, is recruited in a Rab5- and PI(3)P-dependent fashion to early endosomes. Via the interaction with VPS45, a member of the Sec1 family of SNARE regulators, Rabenosyn5 is supposed to function in docking and fusion of early endosomes (Nielsen et al., 2000). In addition, Rabenosyn5 was found to bind to Rab4-GTP, thus showing, similar to Rabaptin5, dual Rab5 and Rab4 effector activity (de Renzis et al., 2002). Overexpression of Rabenosyn5 increased transferrin recycling from sorting endosomes but reduced the transport to recycling endosomes suggesting a role of Rabenosyn5 in the coordination of protein sorting with the fast recycling of cargo directly form sorting endosomes (de Renzis et al., 2002). Another study showed an interaction of Rabenosyn5 with EHD1, which regulates recycling of cargo from recycling endosomes to the plasma membrane. They suggest that Rabenosyn5 and EHD1 act sequentially in the transport of proteins from sorting to recycling endosome and back to the plasma membrane (Naslavsky et al., 2004). Rabenosyn5 might serve as a Rab effector linking sorting events at early endosomes to recycling. Whether the recycling occurs directly from sorting endosomes or via recycling endosomes needs to be established.

8. Rab conversion during endosome maturation

A keystep in early-to-late endosome maturation is the Rab conversion, in which Rab5 present on early endosomes is replaced by the late endosomal Rab7 (Rink et al., 2005). Rab conversion can be blocked by expressing dominant negative Rab5, resulting in the formation of hybrid endosomal compartment with markers for both early and late endosomes (Hirota et al., 2007). Rab5 removal from early endosomes requires the inhibition of the positive feedback loop described above (see Rabaptin5 chapter) as well as a GAP activation to hydrolyze GTP on Rab5. Del Conte-Zerial et al. (2008) described a so called cutoff switch model, where Rab5 activates Rab7, which in turn supresses Rab5 via interaction with effectors and GAPs (Del Conte-Zerial et al., 2008). The exact mechanism is starting to emerge, but there are still a lot of open questions. The keyplayers for the Rab conversion include the Mon1/Ccz1 complex (Sand1 in C. elegans) (Poteryaev et al., 2010). Mon1/Ccz1 can bind to Rab5 and promotes Rab7 binding by potentially displacing the GDI from Rab7 or activating the HOPS complex, which in yeast has been proposed to have GEF activity (Wurmser et al., 2000). In mammalian cells, however, the components of the HOPS complex do not possess GEF activity towards Rab7 (Peralta et al., 2010), but the Mon1/Ccz1 complex could be the GEF itself as shown in yeast (Nordmann et al., 2010).

In addition, Mon1/Ccz1 interacts with Rabex5 and displaces it from endosomal membranes, thus interrupting the positive feedback loop of Rab5 activation (Poteryaev et al., 2010). To inactivate Rab5, a GAP has to be recruited to the endosome, which has not been identified yet. There have been reports about TBC-2, a Rab5-GAP in C. elegans, to be recruited to endosomes only when Rab7 is present (Chotard et al., 2010), but this could not be confirmed in mammalian cells. There the closest human homologue of TBC-2, Armus, showed GAP activity towards Rab7 instead of Rab5 (Frasa et al., 2010).

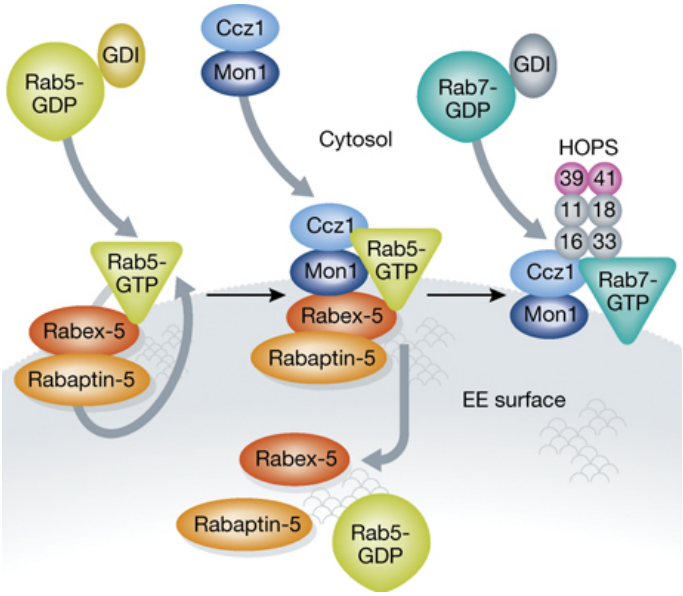

Fig. 18. **Rab conversion during endosome maturation**
To interrupt the positive feedback loop of Rab5 acitvation, Mon1/Ccz1 bind to Rab5 and Rabex5, causing dissociation of Rabex5 from the endosome membrane. In a next step, the Mon1/Ccz1 complex promotes the recruitment and activation of Rab7, which in turn binds to the HOPS complex finally leading to late endosome fusion (Huotari and Helenius, 2011).

Aim of the thesis

Rabaptin5 is one of the better-studied Rab effectors with a widely accepted function in early endosomes fusion involving the Rab5 positive feedback loop. However, Rabaptin5 is a complex protein with several interactors, including Rab4, Rab5, Rabex5 and AP1, and a thorough analysis of the contributions of each domain has been missing.

The aim of this work is to investigate the role of Rabaptin5 in endosomal homeostasis. We analyse the function of Rabaptin5 in more detail taking into account all interaction partners by mutagenesis of the different interaction domains or motifs and expression of the mutant proteins in HeLa cells. Firstly, the contribution of the different interaction domains to Rabaptin5 recruitment to endosomes and to endosome morphology was studied. Secondly, changes in Rabaptin5 localization were determined by coexpression or silencing of Rabaptin5 interactors. Some of our results clearly contradict the widely cited feedback model, in which Rab5 controls its own activity, and lead to new models of Rabaptin5 function.

Material and Methods

Material

Primary Antibodies

Antibody	Host	Used for	IF	Supplier
α-actin	Mouse monoclonal	WB	1:500'000	Millipore
α-CHMP2B	Rabbit polyclonal	IF	1:200	Abcam
α-HA	Mouse monoclonal	IP	5 µl	Hybridoma 12CA5
α-Rab4	Mouse monoclonal	WB	1:1000	BD Transduction Laboratories
α-Rab5	Mouse monoclonal	WB	1:1000	Hybridoma CL621.3
α-Rabaptin5	Mouse monoclonal	WB	1:2000	BD Transduction Laboratories
α-Rabaptin5	Mouse monoclonal	IF	1:1000	BD Transduction Laboratories
α-Rabaptin5 (Rabep1)	Rabbit polyclonal	IP	5 µl	Novus Biologicals
α-Rabex5	Mouse monoclonal	WB	1:1000	BD Transduction Laboratories
α-Rabex5	Mouse monoclonal	IF	1:500	BD Transduction Laboratories

Secondary Antibodies

Antibody	Host	Western blot	IF	Supplier
α-mouse-Alexa488	goat		1:200	Molecular Probes
α-mouse-Alexa568	goat		1:200	Molecular Probes
α-rabbit-Alexa488	goat		1:200	Molecular Probes
α-rabbit-Alexa568	goat		1:200	Molecular Probes
α-mouse-HRP	goat	1:4000		Sigma Immunochemicals
α-rabbit-HRP	goat	1:4000		Sigma Immunochemicals

Fluorochromes

Fluorochromes	Specificity	IF	Supplier
Bisbenzimide H33342	Nuclei	1:1000	Hoechst
DAPI	Nuclei	1:10’000	Sigma
DY-647-phalloidin	Actin filaments	1:200	Dyomics
EGF, biotinylated, complexed to Alexa488 Streptavidin	EGF receptor	2 µg/ml	Invitrogen
Transferrin Alexa488	Tf receptor	20 µg/ml	Molecular Probes
Transferrin Alexa568	Tf receptor	20 µg/ml	Molecular Probes

CellLight reagents

Reagent	Specificity	IF	Supplier
CellLight Early endosomes (RFP-Rab5a)	Early endosomes	5 µl for a 12 well	Invitrogen
CellLight Late endosomes (GFP-Rab7a)	Late endosomes	7 µl for a 12 well	Invitrogen
CellLight Lysosomes (GFP-Lamp1)	Lysosomes	6 µl for a 12 well	Invitrogen

Methods

Cloning

All polymerase chain reactions (PCR) were performed using the iproof high fidelity polymerase (Bio-RAD). PCR products were purified from agarose gels with the NucleoSpin Gel and PCR Clean-up kit (Machery Nagel) according to manufacturer's protocol. The purified constructs were cut with the corresponding restriction enzymes and ligated using the T4 DNA ligase (Roche). The resulting constructs were transformed into *E. coli* UT580.

The cDNA encoding human Rabaptin5 cloned in the pHAT vector was a gift from Marino Zerial (Max Planck Institute, Dresden, Germany). Wildtype Rabaptin5 and all the mutants were cloned into pcDNA3 (Invitrogen). To generate Rbpt5Δ5/1, Rbpt5Δ4/1 and Rbpt5Δ4 codons 1-814, 136-862 and 268-862 were cloned into the vector. For Rbpt5Δ4/2, Rbpt5δ, Rbpt5Δ5/2 and Rbpt5ΔX, codons 140-262, 187-226, 216-318 and 547-666 respectively were deleted by PCR mutagenesis. Rbpt5Δ5 was produced by deleting codon 815-862 from Rbpt5Δ5/2. To generate Rbpt5(AAA), the codons for Asp^{438}, Phe^{439} and Gly^{440} were substituted by alanine residues.

The coding sequence of Rabex5 was amplified from a mouse brain cDNA library. HA-Rx5 was constructed by the addition of the respective epitope-encoding sequences to the 5'-end of the coding sequence and cloned into pcDNA3.

Human Rab4a wildtype and Rab4aS22N in pcDNA3.1 were a gift from Peter van der Sluijs (University of Utrecht, Utrecht, The Netherlands). Human Rab5a and Rab5aS34N in pECFP-C1 were provided by Elizabeth Smythe (University of Sheffield, Sheffield, England, UK).

MultiLabel

For consistent coexpression of multiple proteins, we used the MultiLabel system as described by Kriz et al. (2010). Wildtype and mutant Rbpt5 in pcDNA3 were amplified from the CMV promoter to the poly-A sequence with the iproof high fidelity polymerase (Bio-RAD) and cloned into pSI-DST2cx with T4 DNA Ligase (Roche), resulting in a donor plasmid with untagged Rbpt5. Wildtype and mutant Rab4a, Rab5a, and Rabex5 were ligated into the acceptor vectors pSI-AAL6 or pSI-AAR6 for N-terminal fusion of a mCitrine or a mCherry tag, respectively.

Acceptor plasmids containing a pUC origin of replication were propagated in UT580 cells, while donor plasmids with an R6Kγ origin of replication in Pir1 cells (Invitrogen). The

Cre/*LoxP* recombination reaction was performed at 37°C for 60 minutes (New England Bio-Labs). The unpurified Cre reaction mixture was used to transform UT580 cells by electroporation.

Cell culture and transfection

HeLa α and A431 cells were grown in Dulbecco's modified Eagle's medium (DMEM) supplemented with 10% fetal calf serum (FCS), 100 units/ml penicillin, 100 units/ml streptomycin and 2 mM L-glutamine at 37°C in 7.5% and 5% CO_2, respectively. Cells were transiently transfected using Fugene HD (Promega) and in some cases infected with CellLight reagents 36 h posttransfection (see Materials)

RNA Interference

HeLa α cells were grown as described above. Cells were reverse transfected with 20 nM ON-TARGETplus human Rabaptin5 siRNA (3'UTR), ON-TARGETplus SMARTpool human Rabex5, ON-TARGETplus SMARTpool human Rab4a, ON-TARGETplus SMARTpool human Rab5a or ON-TARGETplus non-targeting control pool siRNA (Dharmacon Thermo Scientific) using lipofectamine RNAiMAX (Invitrogen). Cells were used after three days. For some experiments, the cells were transfected with expression plasmids using Fugene HD (Promega) after one day and cultured for another two days. Protein silencing was tested by immunoblot analysis or used for crosslinking, co-immunoprecipitation or immunofluorescence.

Crosslinking

To test dimer formation of wildtype or mutant Rbpt5, transfected cells were incubated with 0.1 mM membrane-permeant, non-cleavable disuccinimidyl suberate (DSS; ProteoChem) in PBS for 45 min at room temperature followed by quenching with 50 mM Tris-HCl, pH 7.5, for 15 min. The cells were harvested in lysis buffer (0.5% DOC, 1% Triton, 2 mM PMSF, 1 x PIC) for 1 h at 4°C and subjected to immunoblot analysis.

Co-immunoprecipitation

Transfected cells expressing wildtype or mutant Rbpt5 together with HA-Rabex5 were lysed 48 h posttransfection with lysis buffer (0.5% DOC, 1% Triton, 2 mM PMSF, 1 x PIC) for 1 h at 4°C. Post-nuclear supernatants were incubated with anti-Rbpt5 or anti-HA antibodies overnight at 4°C, and antigen-antibody complexes were collected with protein A-Sepharose for 2 h, washed 4 times with lysis buffer and PBS, and subjected to immunoblot analysis.

SDS-PAGE and Immunoblotting

Proteins were separated on 7.5% or 10% polyacrylamide gels and transferred to an Immobilon-P^{SQ} membrane (Millipore). After blocking with 5% nonfat dry milk in TBST for 1 h, the membrane was incubated for 2 h with primary antibody in TBST containing 5% BSA at room temperature. After a few washes, the membrane was incubated with HRP-coupled secondary antibody in 5% nonfat dry milk/TBST for 1h at room temperature. For protein detection Immobilon Western Chemiluminescent HRP Substrate (Millipore) was used and membranes were exposed to Kodak Biomax XAR films.

In vivo recycling assay

To assess recycling, cells were starved for 2 h in uptake medium (medium supplemented with 20 mM HEPES, pH7.2), incubated for 1 h at 37°C with 50 µg/ml Alexa-Fluor tagged transferrin in uptake medium, and washed three times with ice-cold PBS and twice with stripping buffer (150 mM NaCl, 50 mM Na-Acetate, pH 3.5) to release surface transferrin. The cells were then quickly warmed to 37°C and internalized transferrin was chased for up to 20 min in uptake medium supplemented with 50 mM deferoxamine mesylate salt (Sigma). To stop the chase, the cells were fixed with 3% paraformaldehyde in PBS, quenched with 50mM NH4Cl in PBS for 5 min, permeabilized with 0.1% Triton X-100 for 5 min, and stained with 1 unit/ml Alexa-Fluor-tagged phalloidin (Dyomics) and 10 µM bisbenzimide H33342 (Hoechst) for 30 min. Image acquisition was done automatically with an ImageXpress Micro (Molecular Devices) and image analysis was performed with the CellProfiler software (Carpenter et al., 2006).

EGF uptake assay

Transfected A431 cells were grown on coverslips and washed with pre-chilled, serum-free growth medium supplemented with 20 mM HEPES, pH7.2. The coverslips were then incubated for 30 min at 4°C in serum-free growth medium containing 1% BSA, 20 mM HEPES, pH7.2 and 2 µg/ml Alexa488-EGF (Invitrogen), washed three times in ice-cold PBS to remove excess ligand and transferred into pre-warmed growth medium. The chase was performed at 37°C and 5% CO_2 for 10 min, 30 min and 3 h. After each time-point, the coverslips were fixed with 3% paraformaldehyde and processed for immunofluorescence.

Immunofluorescence

Transfected cells were grown on coverslips for 48 h and fixed with 3% paraformaldehyde (PFA) for 10 min at room temperature. To quench the reaction, fixed cells were incubated for 5 min in 50 mM NH_4Cl. In some experiments, the cells were pre-permeabilized with 40 µg/ml digitonin (Serva) in 110 mM potassium acetate, 20 mM HEPES pH 7.2, 2 mM $MgCl_2$ for 5 min at 4°C to release the free cytosolic proteins prior to fixation. For the transferrin staining, cells were allowed to internalize 20 µg/ml Alexa-Fluor tagged transferrin in medium supplemented with 20mM HEPES, pH7.2 for 1h.

Fixed cells were washed with PBS and permeabilized with 0.1% Triton X-100 (Applichem) for 10 min. After blocking with 1% BSA in PBS for 15 min, cells were incubated for 2 h with primary antibodies in PBS containing 1% BSA, washed, and stained for 30 min with fluorescently tagged secondary antibodies in PBS containing 1% BSA. After a 5 min staining with DAPI and several washes with PBS, coverslips were mounted in Fluoromount-G (Southern Biotech). Used Antibodies are described in the table above. Staining patterns were analyzed using a Point Scanning Confocal Zeiss LSM700 upright.

Endosome size measurements

Endosome size was measured in 4 cells per condition with nicely separated endosomes. Pictures were analysed with Bregman segmentation of the Mosaic plugin in Fiji, provided by the group of Kurt Ballmer from the PSI. Background was substracted with a rolling ball radius of 10 pixels and cell masks were set to 0.075 to identify transfected cells. The resulting size values in pixel were translated into μm^2 and plotted with Prism6.

Results

Rabaptin5 constructs and expression levels

To investigate the role of Rabaptin5 in endosome homeostasis, a mutation analysis was performed (Fig. 19). C-terminal truncations of the well-characterized Rab5 and Rabex5 binding domain as well as N-terminal deletions of the two individual, putative and the entire Rab4 binding domain were generated. In a second step also the putative N-terminal Rab5 binding domain was deleted. The AP1 binding site, including the tripeptide sequence DFG, was inactivated by mutation to three alanine residues (AAA). A combination of different mutated sites lead to the following constructs (Fig. 19):

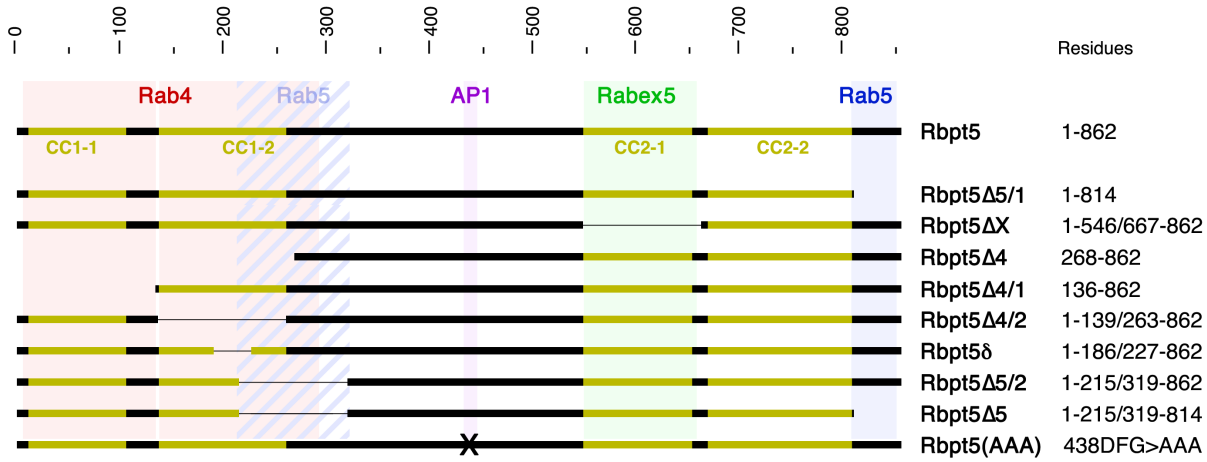

Fig. 19. **Illustration of the domain organization of wildtype Rabaptin5 and mutant constructs**
Coiled coil segments are shown in yellow. Coloured backgrounds highlight the segments reported to interact with Rab4 (red), Rab5 (blue), Rabex5 (green), or AP1 (purple)

To check the expression levels of the different constructs, endogenous Rabpatin5 was knocked down with a siRNA against the 3'UTR and the mutant constructs expressed in HeLa cells. The absence of the full-size Rabaptin5 in cells transfected with the deletion constructs demonstrated efficient knockdown of endogenous Rabaptin5. Western blot analysis compared endogenous levels of Rabaptin5 with the mutant constructs. All constructs showed a 2-3 fold higher expression than the endogenous protein (Fig. 20). Taking into account a transfection efficiency of around 10%, resulted in a 20-30 fold higher concentration of the transfected construct over endogenous Rabaptin5 per cell. Rbpt5(AAA) was the only construct with an expression level similar to the endogenous levels of Rabaptin5, which will be important for the further studies (Fig. 20, lane 10).

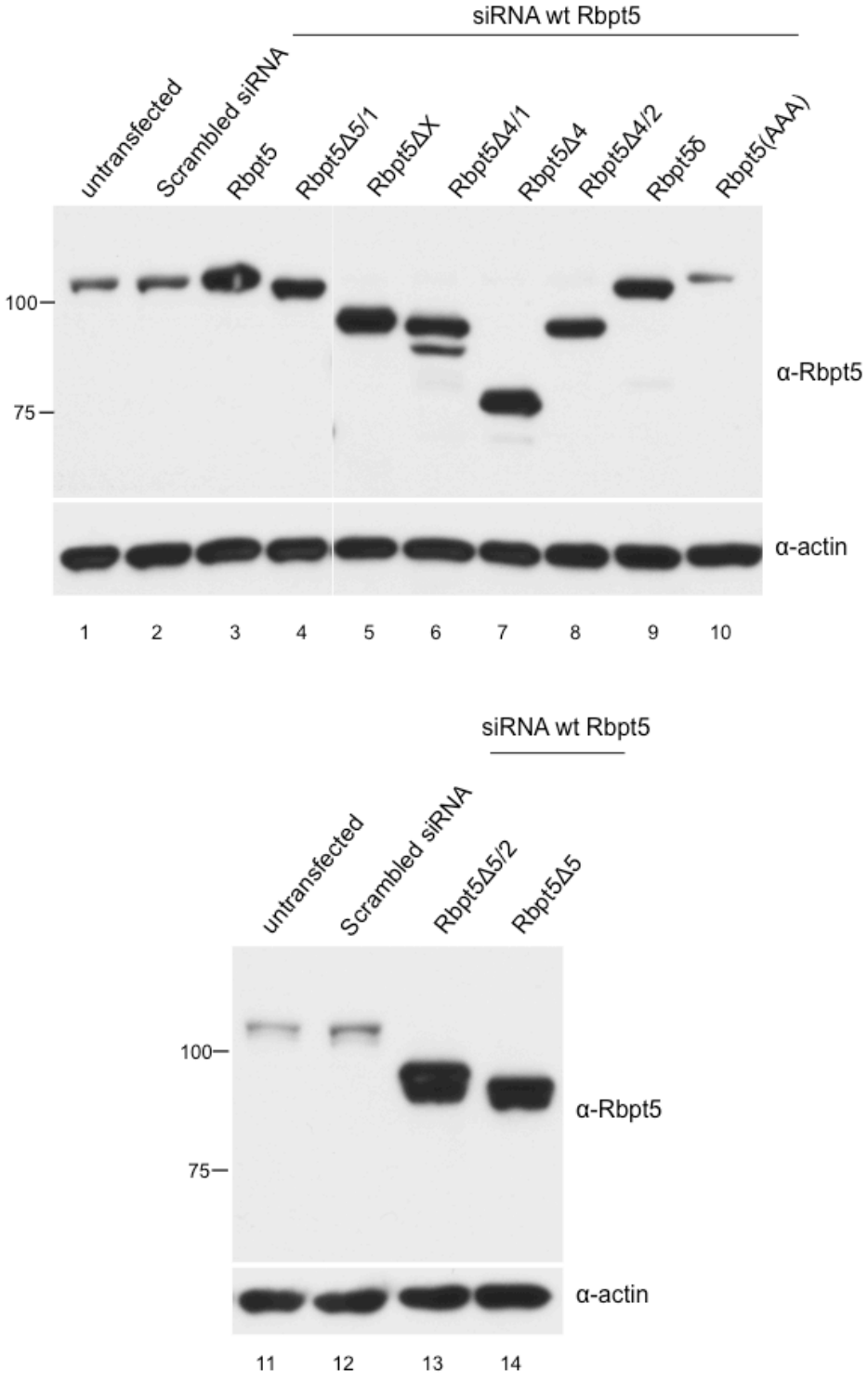

Fig. 20. **Expression levels of the different mutants**

Expression of Rabaptin5 constructs in Rabaptin5 wildtype silenced HeLa cells was assessed by SDS-PAGE of extracts and immunoblotting with an anti-Rabaptin5 antibody. Expression levels were in a similar range for the majority of the constructs. Rbpt5(AAA) expressed a little less then the other constructs. Actin was used to ensure equal loading. Numbers on the left indicate the position of molecular mass markers (in kilodaltons).

Rabaptin5 localizes to early endosomes

Endogenous levels of Rabaptin5 in HeLa cells were not detected by immunofluorescence microscopy with available antibodies. Since addition of any fluorescent protein tag to the Rabaptin5 sequence caused aggregation of the protein, Rabaptin5 was expressed in HeLa cells without tag and detected with an anti-Rabaptin5 antibody (see Material and Methods). Upon transient transfection, Rabaptin5 was observed in the cytosol and on membrane structures containing internalized fluorescent transferrin (Tf) as a marker for early endosomes (Fig. 21A). After a brief digitonin permeabilization of the plasma membrane before fixation, only endosome-bound Rabaptin5 was retained (Fig. 21B). Silencing of the endogenous Rabaptin5 did not affect the localization of the exogenously expressed protein (Fig. 21C). In addition, the size of Tf-positive endosomes did not change upon Rabaptin5 expression (Fig. 21E). To assess endosome size, the arithmetic mean plus its standard deviation did not represent an adequate presentation of the data, since the endosome size was spread over a large range better described with a box plot. A box plot depicts 50% of the values in the middle box plus minimum and maximum values on both sides (Fig. 21E). 50% of the endosomes in control HeLa cells had a size between 7-20 nm^2, which is not affected by the moderate expression of Rabaptin5 wildtype (Fig. 21E).

An increase in endosome size has been previously reported in cells treated with butyrate to stimulate gene expression (Deneka et al., 2003) or using the T7 RNA polymerase vaccinia virus expression system (Vitale et al., 1998). Indeed in butyrate-treated cells, we could reproduce endosome enlargement by Rabaptin5 (Fig. 21D). Endosome size increased from 7-20 nm^2 to 14-75 nm^2 with a maximum up to 15 μm^2 (Fig. 21E). As indicated by the spindly appearance (Fig. 21D), the cells suffered during the butyrate treatment even leading to cell death and thus showing this treatment was toxic to the cells. This indicates that transfection of cells without butyrate treatment provides comparatively moderate protein expression.

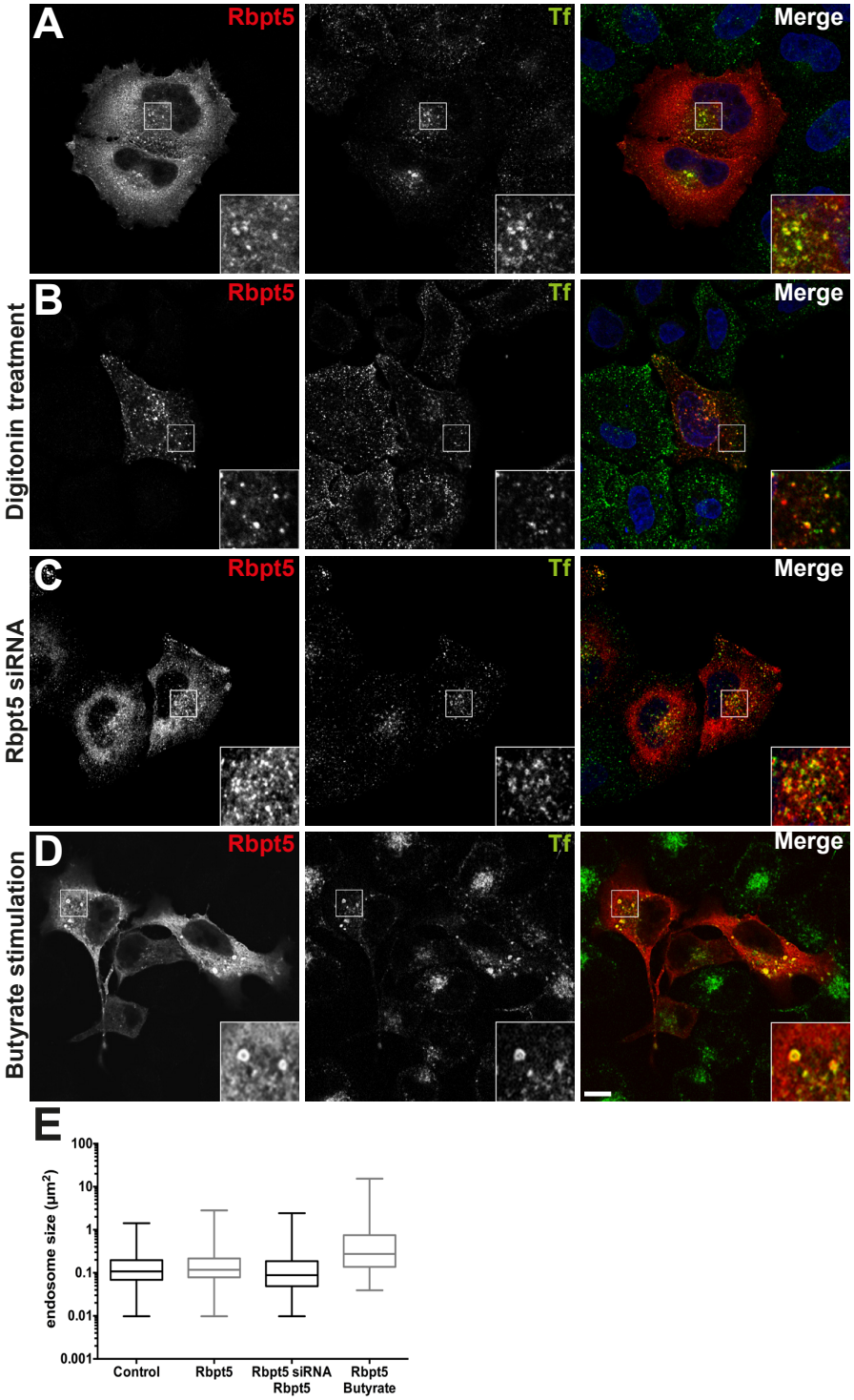

Fig. 21. **Rabaptin5 colocalizes with Tf-positive endosomes in transfected HeLa cells**

A) Rbpt5 transfected HeLa cells were allowed to internalize fluorescent Tf for 1h and stained with an anti-Rbpt5 antibody. **B**) With digitonin permeabilization prior to fixation, cytosolic Rbpt5 was released. **C**) Knockdown of endogenous Rbpt5 prior to transfection did not change exogenous Rbpt5 distribution. **D**) Butyrate treatment caused endosome enlargement. **E**) Quantification of Tf positive endosome size. Box plots show median value in the centre, each box represents 50% of all values (25% quartile to 75% quartile) and whiskers indicate minimal and maximal values, respectively (N=4). Bars, 10 µm. Nuclei were stained with DAPI (blue).

Rab4a enhances membrane recruitment of Rabaptin5

For coexpression and colocalization analysis of two proteins, we used MultiLabel, a modular plasmid-based eukaryotic expression system (Kriz et al., 2010), that allows similar expression levels from identical promotors at a constant ratio in all transfected cells. In some cases, the BacMam technology was used to express a second gene. This technique is based on a insect virus (baculovirus), that has been modified for transgene expression in mammalian cells. This virus does not replicate in mammalian cells and thus no extra safety measures have to be taken. Cells expressing the Rabaptin5 constructs were infected with this baculovirus one night before fixation.

Expression of Rabex5 alone or together with Rbpt5 increased the average endosome size from 7-18 nm^2 to 8-40 nm^2 with maximum values up to 47 μm^2 (Fig. 22A, B and B′), in agreement with previous reports (Mattera and Bonifacino, 2008; Zhu et al., 2007) and consistent with GEF stimulated Rab5 endosome fusion. Coexpressed Rbpt5 and Rabex5 (mCherry-tagged) colocalized on endosomes (Fig. 22B), still leaving a considerable amount of cytosolic Rbpt5.

In contrast to Rabex5, expression of Rab5a or coexpression of Rbpt5/Rab5a did not change the overall endosome size compared to untransfected cells or Rbpt5 transfected cells (Fig. 22C, D and D′). Coexpressed Rbpt5 and Rab5a (RFP-tagged) colocalized on endosomes (Fig. 22D), as did Rbpt5 and Rab4a (tagged with citrine) (Fig. 22F). Rab4a expression, both with and without Rbpt5, increased the range of endosome size (Fig. 22E, F and F′). The majority of endosomes still had a size of 8-20 nm^2, but the maxima increased up to 14 μm^2. In addition, Rab4a drastically reduced the cytosolic pool of Rbpt5 (Fig. 22F) compared to Rabex5 and Rab5a, showing an enhanced membrane recruitment of Rbpt5, potentially via its Rab4-binding domain.

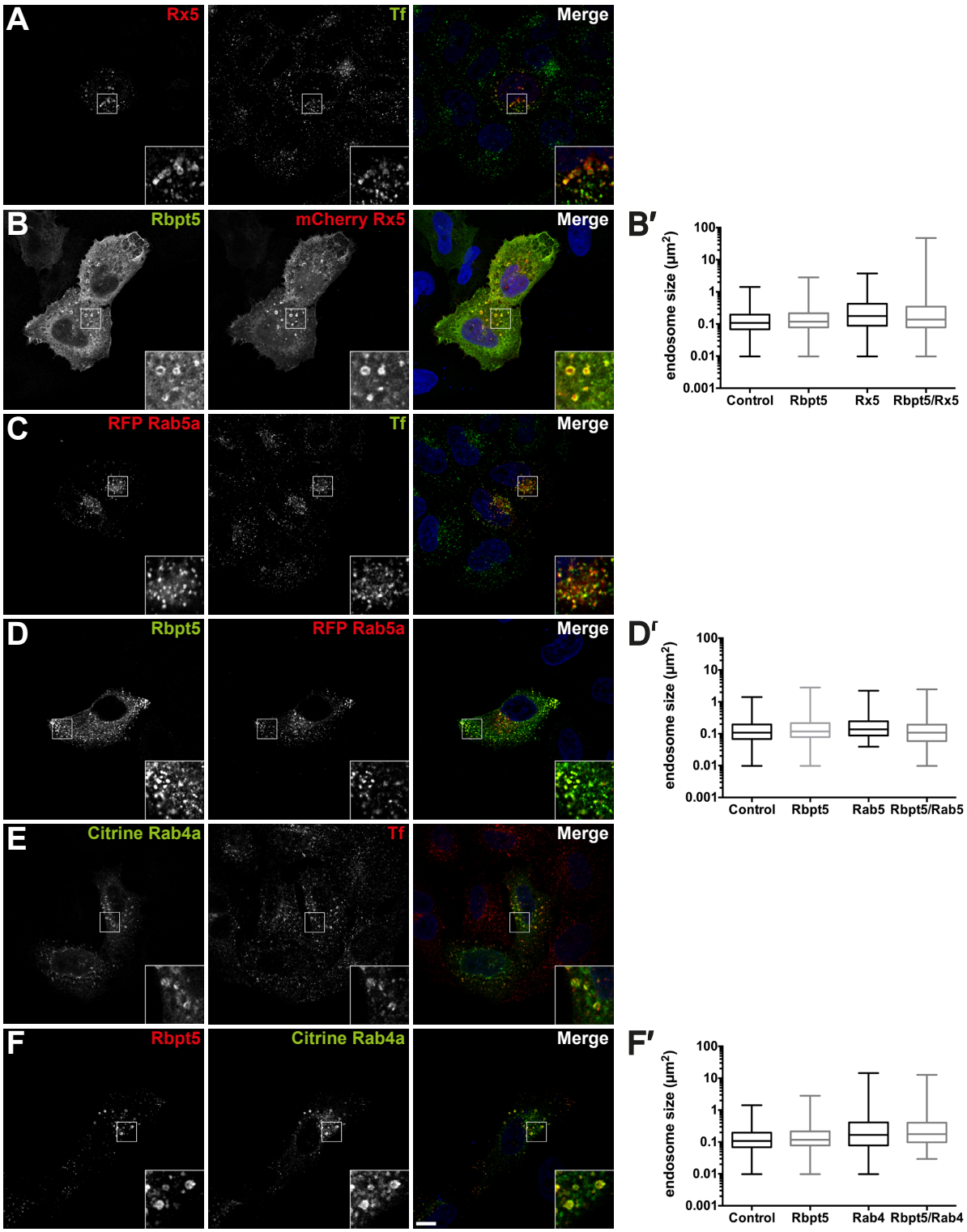

Fig. 22. **Coexpression of Rab4a enhances membrane recruitment of Rbpt5**

Expression of Rx5 alone (**A**) or Rx5 together with Rbpt5 (**B**) increased the endosome size (**B′**), while Rab5a (**C**) or Rbpt5/Rab5a (**D**) did not (**D′**). Rab4a (**E**) and Rbpt5/Rab4a (**F**) increased the overall range of endosome size (**F′**). Only expression with Rab4a decreased the cytosolic pool of Rbpt5. Bars, 10 µm. Nuclei were stained with DAPI (blue).

Rbpt5 knockdown or Rbpt5 expression do not affect Tf recycling

In a first attempt to investigate the role of Rabaptin5 in transferrin recycling, endogenous Rbpt5 was silenced (Fig. 23A, lane 5) and cells were allowed to internalize fluorescent Tf for 1 h to fill the endosomal compartment to steady-state. Tf was chased from the cells in the presence of 50 µM deferoxamine and recycling was stopped every 2 min for 20 min. Rbpt5 knockdown did neither affect the recycling rate of transferrin (Fig. 23C) nor endosome size (Fig. 23B)

Secondly, Rbpt5 was expressed in HeLa cells and Tf recycling in transfected cells was compared to untransfected cells. As illustrated in Fig. 23E, the distribution of fluorescent transferrin in Rbpt5 expressing versus non-transfected cells is similar at 0 min recycling. After 20 min of recycling, essentially all the Tf was recycled back to the plasma membrane regardless of expressing or non-expressing cells (Fig. 23F). This result was also reflected by the recycling curve shown in Fig. 23D. Increased Rbpt5 expression in HeLa cells did not dramatically affect the Tf recycling rate. In the first 5 min, transferrin recycling might be a little slower in Rbpt5 expressing cells, although not significantly different from untransfected cells. After 5 min the two curves merge again and no difference is observable anymore, suggesting no involvement of wildtype Rbpt5 in the recycling pathway back to the plasma membrane.

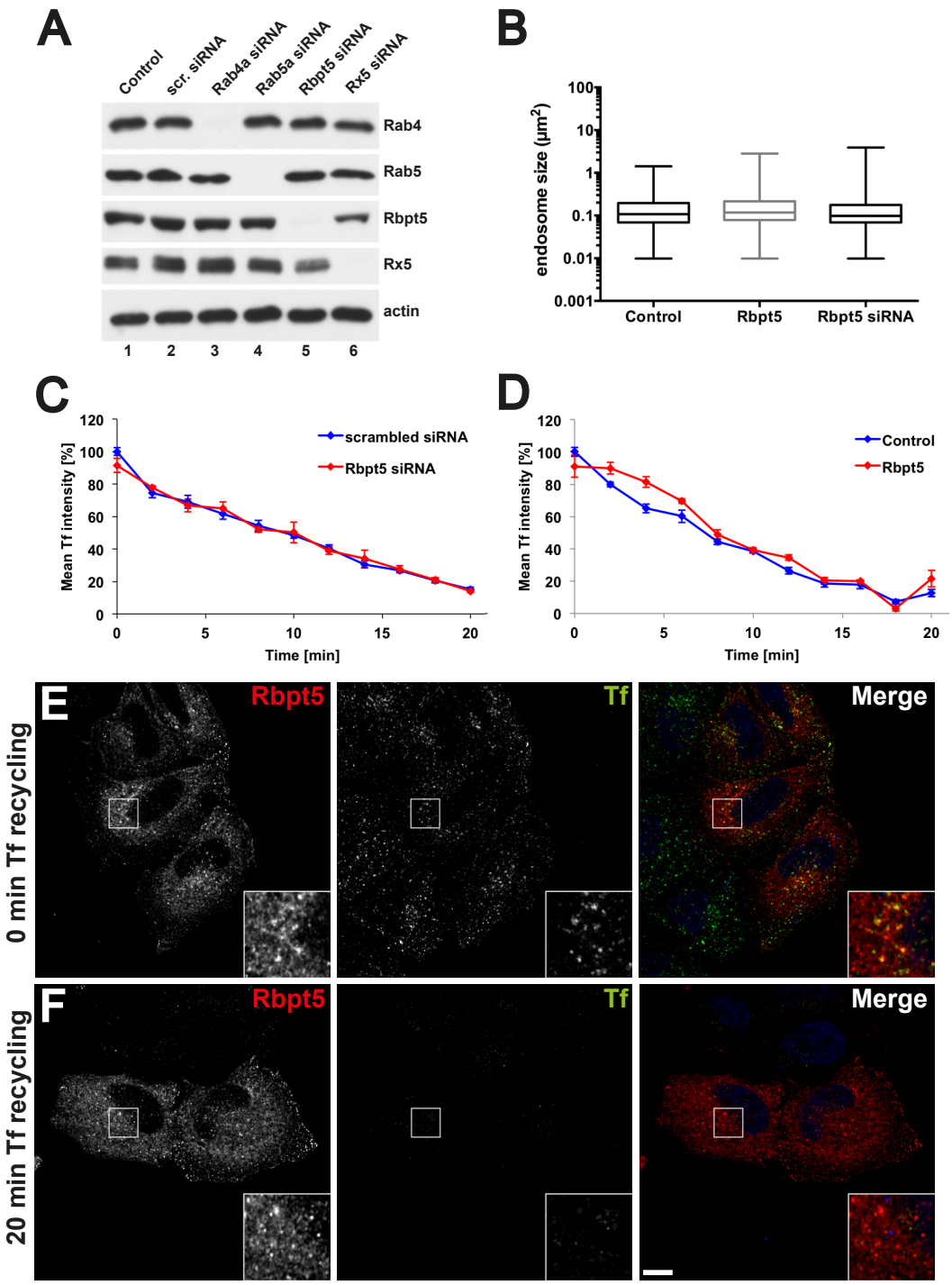

Fig. 23. **Rbpt5 knockdown or Rbpt5 expression do not affect Tf recycling**

A) siRNA knockdown of Rbpt5 and the three interactors Rab4a, Rab5a and Rx5. **B**) Quantification of endosome size. **C**) Transferrin recycling curves for Rbpt5 siRNA and scrambled siRNA knockdown HeLa cells. Graph represents the mean value and standard deviation of 4 assay wells. **D**) Transferrin recycling curve for Rbpt5 expressing or untransfected HeLa cells. Graph represents the mean value and standard deviation of 6 assay wells. **E+F**) Representative pictures of **D** after 0 min or 20 min Tf recycling. Bars, 10 µm. Nuclei were stained with DAPI (blue).

Mutation of the AP1/GGA interaction motif has no effect on Rabaptin5 recruitment and endosome morphology

Since AP1 is known to act at the TGN and endosomes, the interaction motif in Rbpt5 was mutated. To ensure proper functionality of the mutant, the dimerization ability of the protein was checked by *in vivo* crosslinking with DSS and immunoblot analysis. The efficiency of producing covalent dimers was the same for Rbpt5(AAA) as for wildtype Rbpt5 (Fig. 24A).

Upon transfection of HeLa cells, Rbpt5(AAA) was observed in the cytosol and on transferrin-positive endosomes (Fig. 24B) identical with the wildtype situation (Fig. 21A). Since Rbpt5(AAA) was not as highly expressed as other mutants (Fig. 20, lane 12), endogenous wildtype Rbpt5 might interfere and form heterodimers with Rbpt5(AAA), thus masking a potential phenotype. To exclude this scenario, endogenous Rbpt5 was knocked down prior to transfection of the mutant. The absence of endogenous Rbpt5 had no effect on Rbpt5(AAA) recruitment and endosome morphology (Fig. 24C), also reflected in no change in endosome size compared to untransfected or Rbpt5 expressing cells (Fig. 24D). AP1 does not seem to be involved in recruitment to endosome.

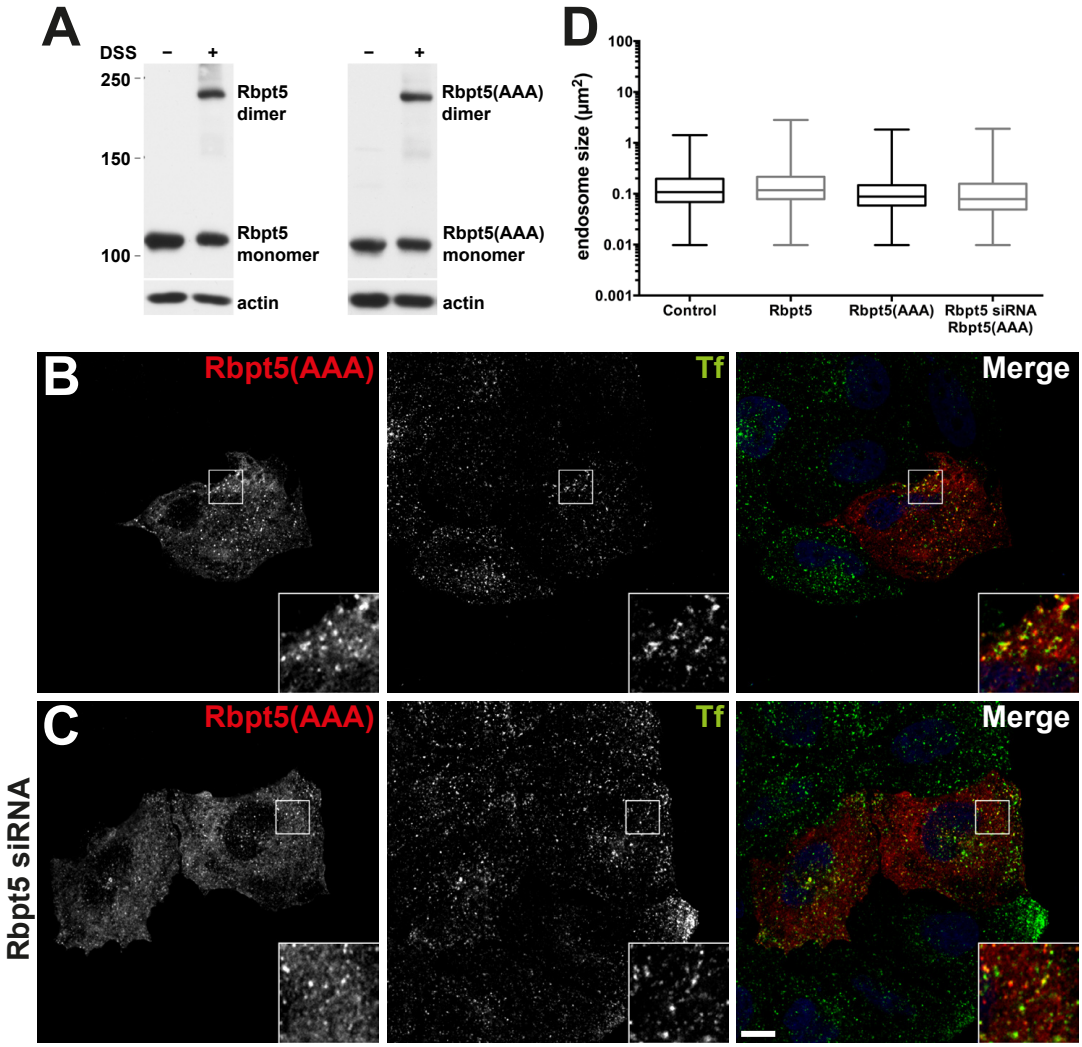

Fig. 24. **Mutation of the AP1 interaction motif has no effect on Rbpt5 recruitment to endosomes**
A) *In vivo* crosslinking with DSS to show dimerization of Rbpt5(AAA). **B**) Rbpt5(AAA) transfected HeLa cells were allowed to internalize fluorescent Tf for 1h and stained with an anti-Rbpt5 antibody. **C**) Knock-down of endogenous Rbpt5 prior to transfection did not change Rbpt5(AAA) localization. **D**) Quantification of endosome size. Bars, 10 µm. Nuclei were stained with DAPI (blue).

Rabaptin5 recruitment to endosomes requires Rabex5

In a next step, the interaction between Rabaptin5 and Rabex5 was studied by deletion of the Rabex5 interaction domain in the coiled-coil CC2-1 of Rbpt5. Since it is known that Rbpt5 homodimerizes via its coiled-coil domains, proper dimer formation was tested to ensure functionality of the protein. *In vivo* crosslinking revealed very efficient dimerization of Rbpt5ΔX (Fig. 25A).

Deletion of the Rabex5 binding domain resulted in a completely cytosolic distribution of the protein (Fig. 25B) and had no effect on endosome size compared to untransfected and Rbpt5 transfected cells (Fig. 25C). That this is due to the lack of Rabex5 binding and not to an indirect structural effect of the deletion was confirmed by siRNA-mediated silencing of endogenous Rabex5 expression (Fig. 23A, lane 6). Rabex5 knockdown also abolished Rbpt5 wildtype recruitment to endosomes (Fig. 25D). In addition, coexpression of Rabex5 could not rescue membrane recruitment of Rbpt5ΔX (Fig. 25E), indicating that the interaction with Rabex5 is required for membrane association.

Interestingly, coexpression of Rab5a induced a minimal membrane recruitment (Fig. 25F), while Rab4a rescued the entire phenotype (Fig. 25G). Even without the Rabex5 binding domain, Rab4a is a potent Rbpt5 endosome recruiter apparent from the complete disappearance of the cytosolic pool of the protein in Fig. 25G.

Fig. 25. **Rabex5 is required for Rbpt5 recruitment to endosomes**

A) Dimerization assay for Rbpt5ΔX. **B**) Rbpt5ΔX transfected HeLa cells show no endosome recruitment and **C**) no changes in endosome size. **D**) siRNA mediated knockdown of Rx5 caused a cytosolic distribution of Rbpt5 wildtype. **E**) Coexpression with Rx5 did not rescue endosome recruitment, while **F**) Rab5a partially and **G**) Rab4a completely could. Bars, 10 µm. Nuclei were stained with DAPI (blue). ↓

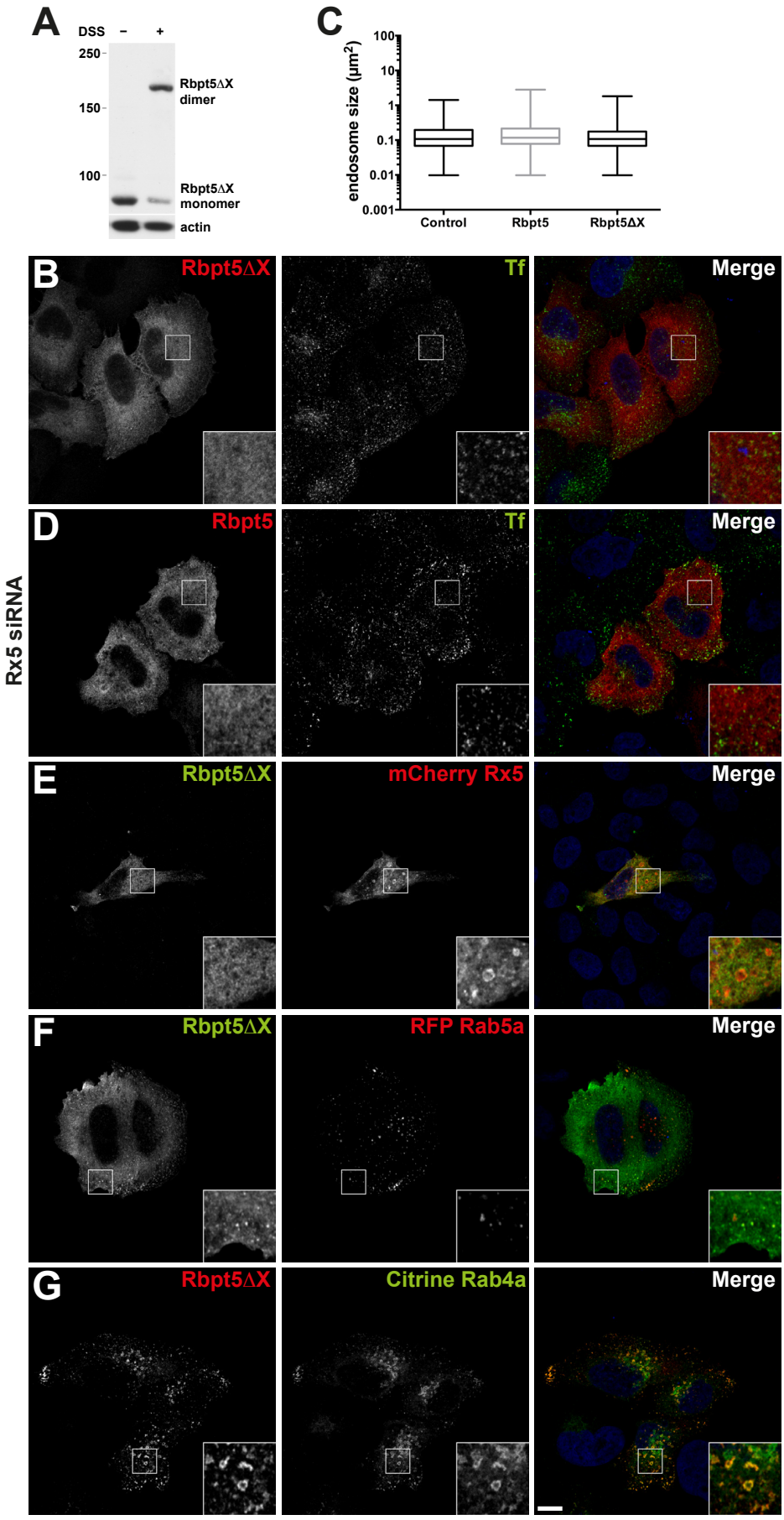
A
DSS – +
250
150
100
Rbpt5ΔX dimer
Rbpt5ΔX monomer
actin
C
endosome size (µm²)
100
10
1
0.1
0.01
0.001
Control
Rbpt5
Rbpt5ΔX
B
Rbpt5ΔX
Tf
Merge
D
Rbpt5
Tf
Merge
Rx5 siRNA
E
Rbpt5ΔX
mCherry Rx5
Merge
F
Rbpt5ΔX
RFP Rab5a
Merge
G
Rbpt5ΔX
Citrine Rab4a
Merge

Rabaptin5 recruitment to endosomes also requires Rab4a

In the construct Rbpt5Δ4, the N-terminal 285 residues including all published Rab4-binding sequences have been deleted. Since this mutant could not be crosslinked by DSS, the dimerization state was tested by coimmunoprecipitation with Rabex5, the binding of which is critically dependent on the coiled-coil formation in the segment CC2-1 of Rbpt5. As shown by immunoblot analysis in Fig. 26A, Rabex5 was coimmunoprecipitated with Rbpt5Δ4 and vice versa as efficiently as the wildtype protein, demonstrating efficient complex formation. However, Rbpt5Δ4 was not recruited to endosomes, but showed a cytosolic distribution (Fig. 26B) and did not influence endosome size (Fig. 26C). Upon brief digitonin permeabilization prior to fixation, no signal was retained on cellular membranes (Fig. 26D). Transfected cells were identified by coexpression of mCherry, which partially localized to the nucleus and remained trapped during digitonin pre-permeabilization. As expected, coexpression of Rab4a could not rescue membrane recruitment of Rbpt5Δ4 (Fig. 26E). On the other hand, coexpression of Rabex5 (Fig. 26F) or Rab5a (Fig. 26G) could partially induce membrane recruitment.

To directly assess the involvement of Rab4a in endosome recruitment of Rbpt5, we analyzed the effects of silencing or inactivating Rab4a on the membrane recruitment of wildtype Rbpt5. Inactivation of Rab4a by expression of the dominant negative mutant Rab4aS22N completely prevented membrane binding of Rbpt5 (Fig. 27A). The same result was obtained by siRNA-mediated silencing of Rab4a (Fig. 27B and Fig. 23A, lane 3). These and the findings from the previous chapter indicate that endosome recruitment of Rbpt5 is mediated by Rabex5 and Rab4a-GTP.

Fig. 26. **Deletion of the Rab4 binding domain of Rbpt5 abolishes Rbpt5 membrane recruitment.**
A) Dimerization of Rbpt5Δ4 was shown by coimmunoprecipitation with Rx5 and vice versa. **B**) Rbpt5Δ4 transfected HeLa cells show no endosome recruitment and **C**) no changes in endosome size. **D**) With digitonin permeabilization prior to fixation, the cytosolic Rbpt5Δ4 was released. **E**) Coexpression with Rab4a did not rescue endosome recruitment, while **F**) Rx5 and **G**) Rab5a partially could. Bars, 10 µm. Nuclei were stained with DAPI (blue). ↓

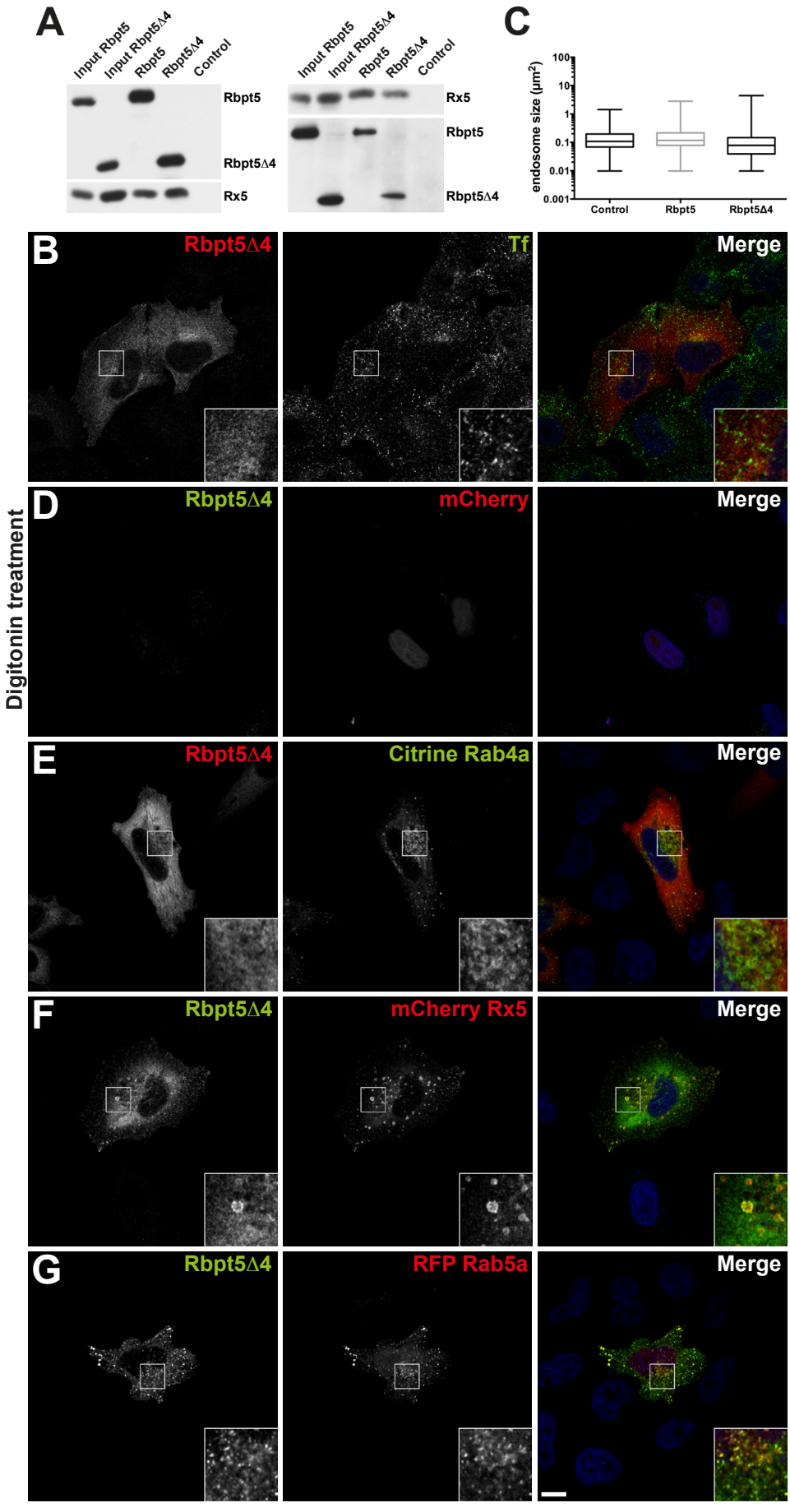
A
Input Rbpt5
Input Rbpt5Δ4
Rbpt5
Rbpt5Δ4
Control
Rbpt5
Rbpt5Δ4
Rx5
Input Rbpt5
Input Rbpt5Δ4
Rbpt5
Rbpt5Δ4
Control
Rx5
Rbpt5
Rbpt5Δ4
C
endosome size (µm²)
100
10
1
0.1
0.01
0.001
Control
Rbpt5
Rbpt5Δ4
B
Rbpt5Δ4
Tf
Merge
Digitonin treatment
D
Rbpt5Δ4
mCherry
Merge
E
Rbpt5Δ4
Citrine Rab4a
Merge
F
Rbpt5Δ4
mCherry Rx5
Merge
G
Rbpt5Δ4
RFP Rab5a
Merge

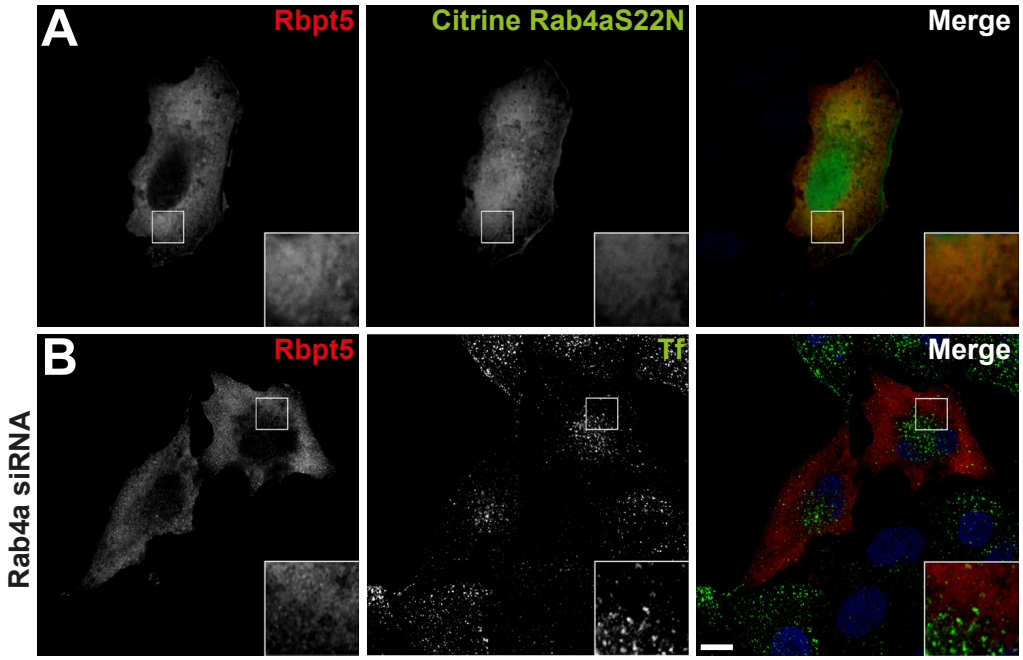

Fig. 27. **Rab4a inactivation inhibits Rbpt5 endosome recruitment**
A) No endosome recruitment of Rbpt5 with dominant negative Rab4aS22N or **B**) upon Rab4a siRNA silencing. Bars, 10 µm. Nuclei were stained with DAPI (blue).

Two distinct Rab4 interaction domains in the N-terminal portion of Rabaptin5

While previous studies agreed that the N-terminal third of Rbpt5 binds to Rab4-GTP as detected by yeast two-hybrid analysis (Korobko et al., 2005; Vitale et al., 1998) or GST-Rab4 pull-down experiments (Deneka et al., 2003), they differed in the location of the interacting sequence(s) within this segment. Vitale et al. (1998) observed activity for residues 5–135 (including the coiled-coil domain CC1-1), whereas Deneka et al. (2003) and Korobko et al. (2005) did not. Instead they observed binding to residues 140–295 (including CC1-2). Analyzing the deletion constructs Rbpt5Δ4/1 lacking residues 1–135 and Rbpt5Δ4/2 lacking residues 140–262 (illustrated in Fig. 19), we found both efficiently recruited to Tf-containing endosomes (Fig. 28A and B), suggesting that both segments were able to bind Rab4a independently. The two deletions, however, differed in that only Rbpt5Δ4/2 caused the formation of giant endosomes increasing the average range of endosome size from 7-18 nm^2 to 12-55 nm^2 with maximas up to 8.5 μm^2. It has to be kept in mind that the deletion in Rbpt5Δ4/2 also overlaps with the segment including residues 216–318 that had been reported to interact with Rab5a in a yeast two-hybrid analysis (Korobko et al., 2006). Rbpt5Δ4/2 may thus reduce interaction with Rab5a, which could cause the different phenotype. Evidence hinting in this direction is that expression of Rbpt5δ, a natural splice variant lacking residues 187–226 that

hardly cut into the Rab5 interacting sequence (Fig. 19), did not cause endosome enlargement (Fig. 28C).

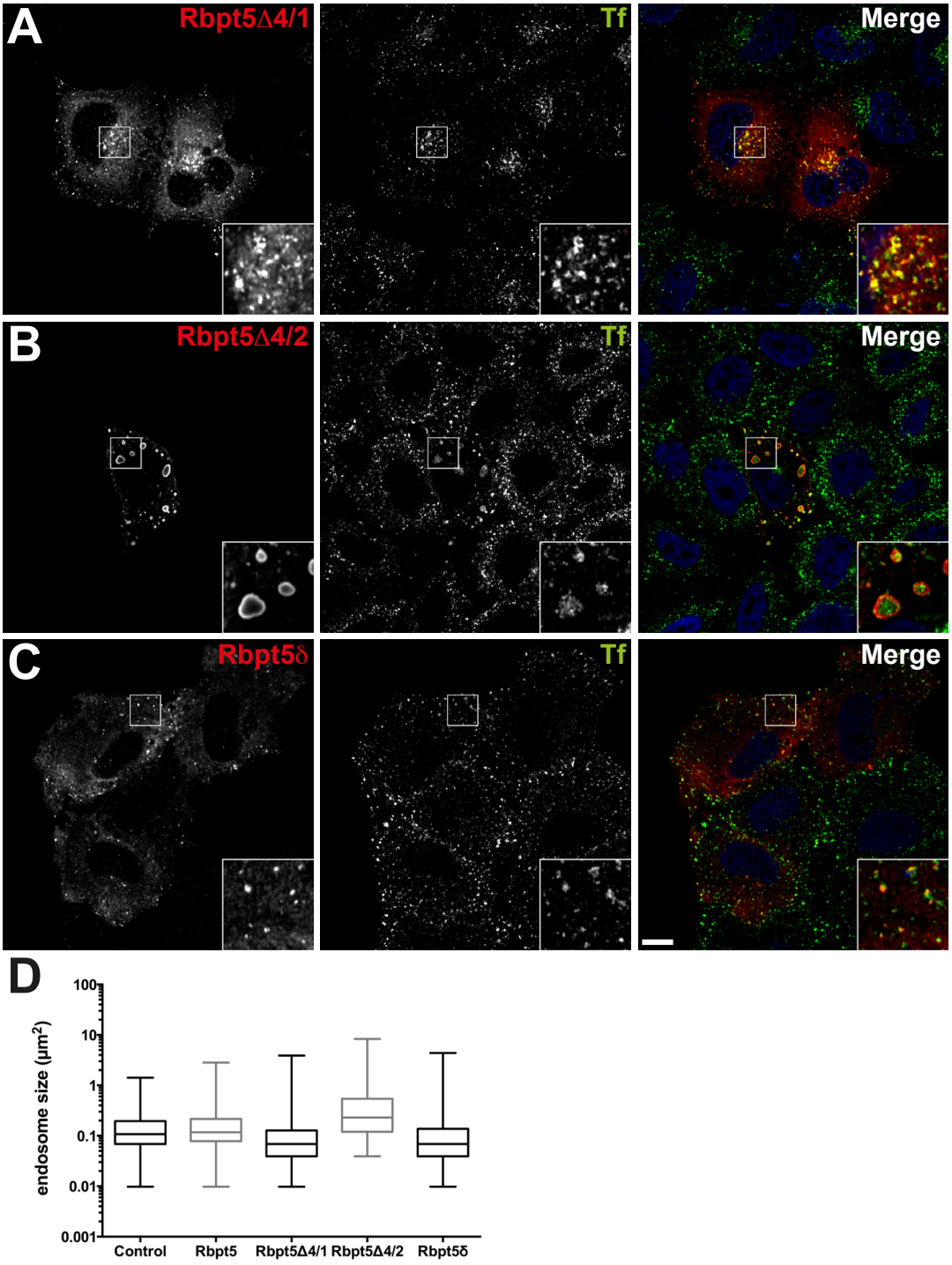

Fig. 28. **Dissection of the Rab4 interaction sequences in Rbpt5**

A) Rbpt5Δ4/1 and **B**) Rbpt5Δ4/2 are both independently able to bind Rab4a, **C**) as well as the natural splice variant Rbpt5δ, but only **D**) Rbpt5Δ4/2 induced enlarged endosomes. Bars, 10 µm. Nuclei were stained with DAPI (blue).

Rabaptin5 recruitment to endosomes does not depend on Rab5a

To verify the hypothesis that reduced Rab5a binding to Rbpt5 could cause endosome enlargement, as mentioned above, the Rab5 binding domains were mutated. Deletion of the C-terminal residues 815–862 containing the better characterized Rab5 binding domain did not affect the ability of the protein to dimerize as shown by *in vivo* crosslinking with DSS and immunoblot analysis (Fig. 29A). Expressed Rbpt5Δ5/1 still recruited to Tf-containing endosomes (Fig. 29B) that in addition were dramatically enlarged, increasing the average range of endosome size from 7-18 nm^2 to 17-113 nm^2 with maxima up to 18 μm^2 (Fig. 29F). This indicated that binding to Rab5a via the C-terminal domain is not essential for membrane recruitment of Rbpt5 and might even be inhibitory to endosome enlargement. The giant Rbpt5Δ5/1-decorated endosomes were still positive for Rab5a, as was shown by coexpression with RFP-Rab5a (Fig. 29C). Surprisingly, however, both Tf and Rab5a were frequently found inside these Rbpt5Δ5/1-positive membranes. In contrast, coexpressed mCherry-labeled Rx5 and Citrine-labeled Rab4a decorated the Rbpt5Δ5/1 endosomes only externally (Fig. 29D and E) and decreased endosome size to the levels of the expression of Rx5 and Rab4a alone (Fig. 29F and Fig. 22B′/F′). Only coexpression with Rab4a reduced the cytosolic pool of Rbpt5Δ5/1, again indicating improved recruitment to endosomes by increased levels of Rab4a (Fig. 29E).

To directly assess the role of Rab5a in membrane recruitment of Rbpt5, Rab5a was inactivated either by expression of the dominant negative Rab5aS34N mutant or by siRNA-mediated silencing (Fig. 23A, lane 4). In both cases, endosome recruitment of both wildtype Rbpt5 and Rbpt5Δ5/1 remained unaffected and both still caused the dramatic endosome enlargement (Fig. 30). These results argue against a role of Rab5a in membrane association of Rbpt5 as proposed by the feedback model. They further suggest that endosome enlargement by Rbpt5Δ5/1 is not dependent on Rab5-induced endosome fusion.

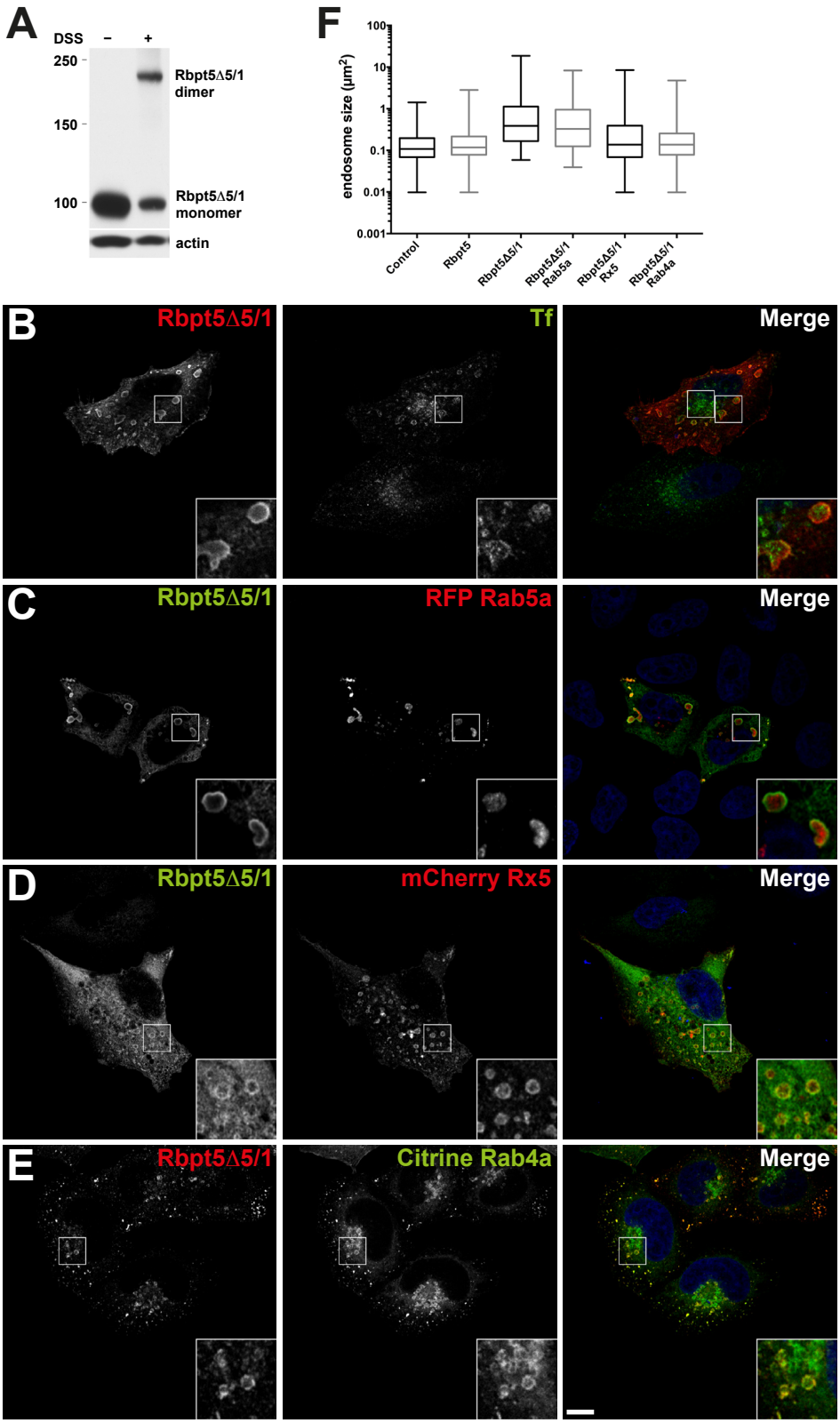

Fig. 29. **Deletion of the C-terminal Rab5-binding domain of Rbpt5 stimulates endosome enlargement**
A) Dimerization assay for Rbpt5Δ5/1. Rbpt5Δ5/1 recruits to **B**) Tf- and **C**) Rab5a-positive enlarged endosomes. Coexpressed with **D**) Rx5 and **E**) Rab4a decreases endosome size to the level of the single expression of these proteins (**F**), while only Rab4a improves endosome recruitment. Bars, 10 µm. Nuclei were stained with DAPI (blue).

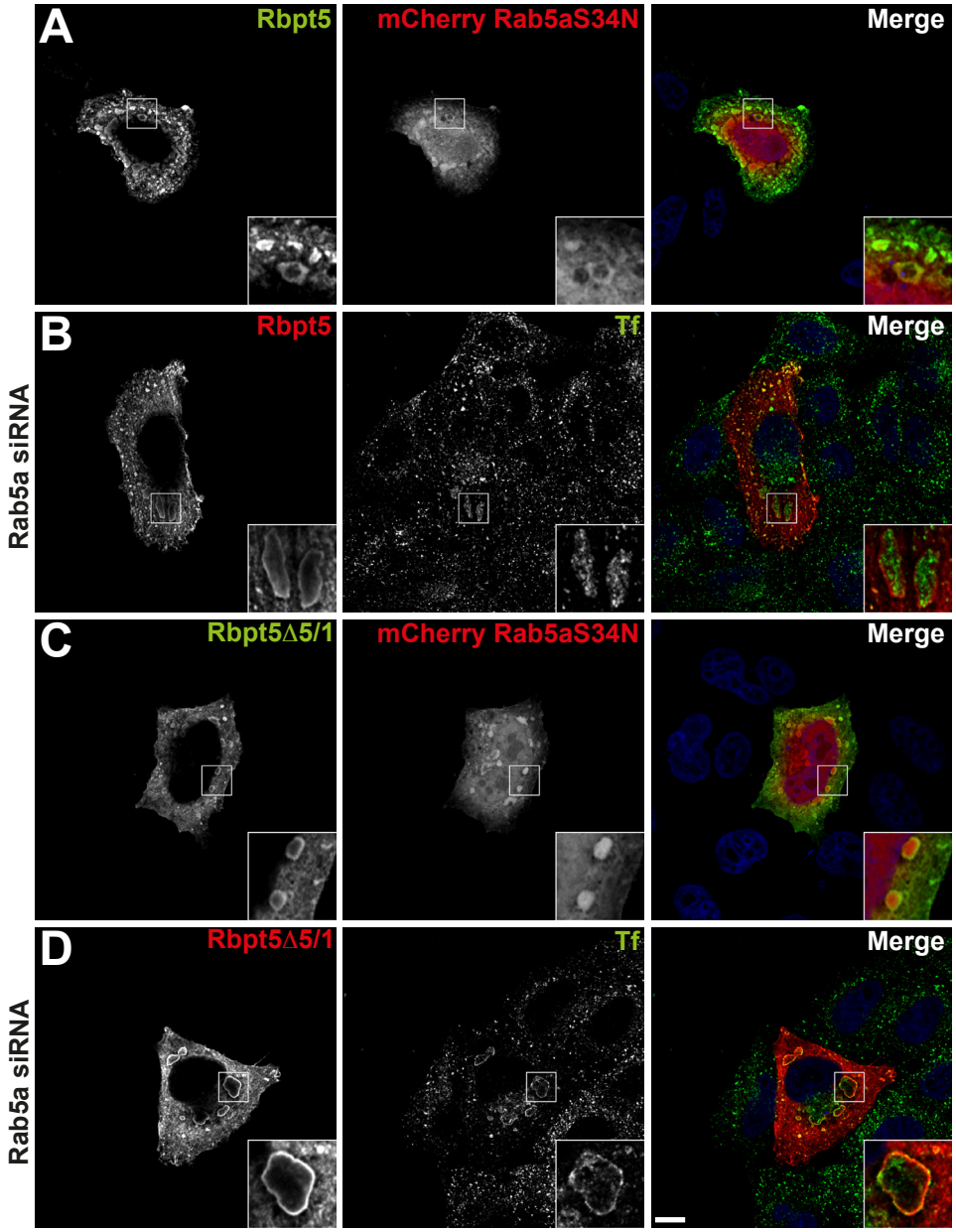

Fig. 30. **Elimination of Rab5a does not affect membrane recruitment of Rbpt5, but allows the formation of giant endosomes.**

A) Upon coexpression of Rab5aS34N or **B**) Rab5a siRNA knockdown, Rbpt5 still localizes to endosome and allows the formation of giant endosomes. **C**) The same was true for Rbpt5Δ5/1 expresses together with Rab5aS34N or **D**) Rab5a siRNA knockdown. Bars, 10 µm. Nuclei were stained with DAPI (blue).

Since there are reports of a second more N-terminal Rab5-binding domain on Rbpt5, also this binding sequence was deleted and the mutant analyzed (Fig. 19). *In vivo* crosslinking showed the same efficiency in producing covalent dimers as Rbpt5Δ5/1 (Fig. 31A). Expressed Rbpt5Δ5/2 also recruited to Tf-containing endosomes (Fig. 31B), which showed the same drastic endosome enlargement as Rbpt5Δ5/1 (Fig. 31C). Rab5a was frequently found inside these giant endosomes (Fig. 31D), while Rab4a only decorated the outside and in-

creased endosome recruitment (Fig. 31E). In summary, Rbpt5Δ5/2 behaves exactly the same as Rbpt5Δ5/1.

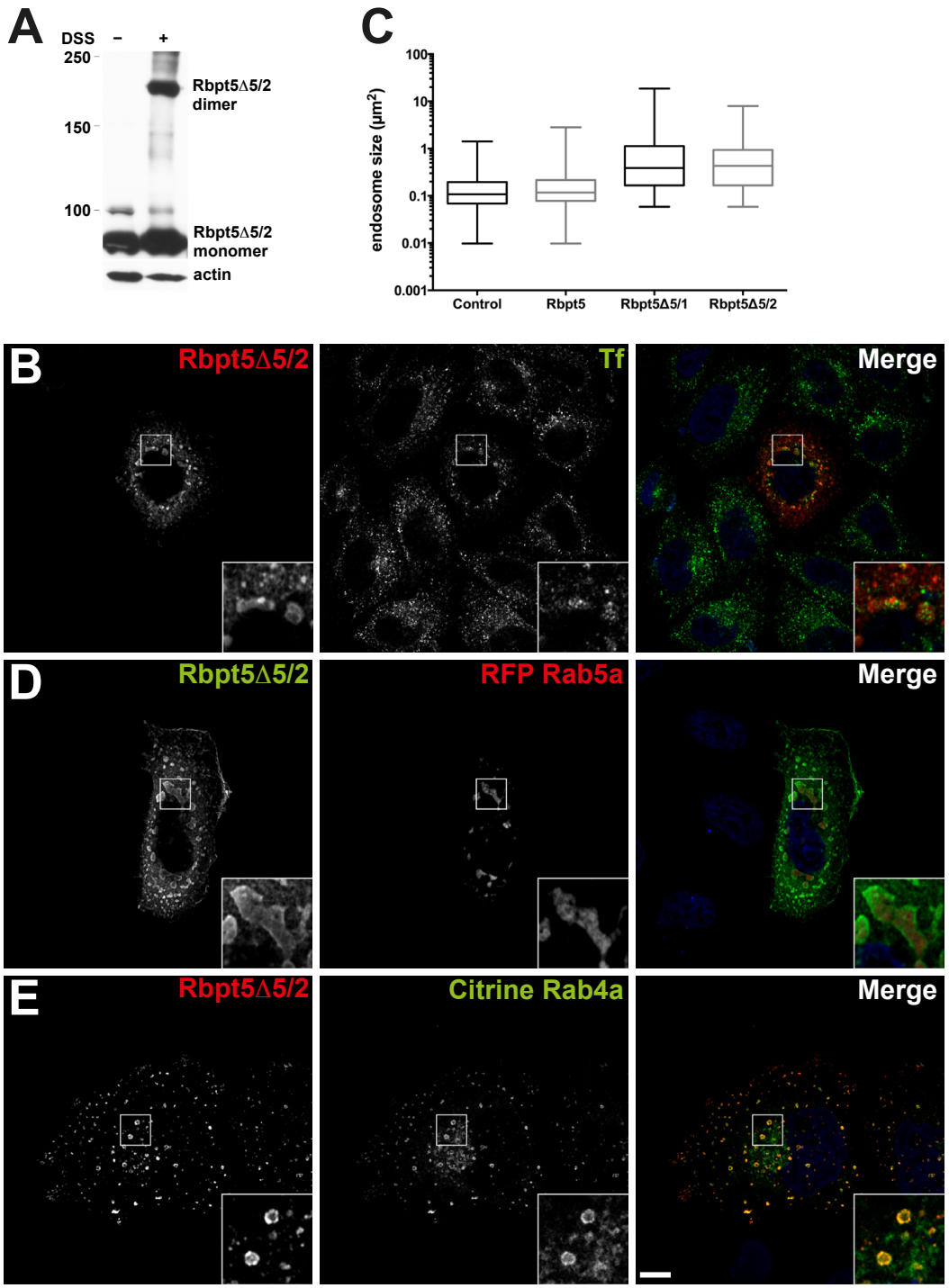

Fig. 31. **Deletion of the N-terminal Rab5-binding domain of Rbpt5 stimulates endosome enlargement like Rbpt5Δ5/1**

A) Dimerization assay for Rbpt5Δ5/2. Rbpt5Δ5/2 recruits to **B**) Tf-positive endosome **C**) highly enlarged in size like Rbpt5Δ5/1. **D**) Rab5a is often found inside these structures, while **E**) Rab4a increases membrane recruitment. Bars, 10 µm. Nuclei were stained with DAPI (blue).

Deletion of the individual Rab5-binding domains on Rabaptin5 induce early/late endosome chimeras

As mentioned above, Rbpt5Δ5/1 and Rbpt5Δ5/2 showed early endosome characteristics by colocalizing with Tf, Rab5a and Rab4a, but surprisingly Tf and Rab5a were often found inside these endosomes instead of just decorating them on the outside. The latter properties are typically found in multivesicular bodies where parts of endosomal membranes are invaginated with their associated proteins for later degradation in lysosomes. Responsible for intraluminal vesicle formation is the ESCRT machinery including CHMP2B/VPS2B, which is part of the ESCRTIII complex. The giant endosomes produced by Rbpt5Δ5/1 were indeed positive for the CHMP2B (Fig. 32A). The same was also observed for Rbpt5Δ5/2 (data not shown). Coexpressed Rab7a was found in the perinuclear region, where late endosomes are typically located, but also inside the Rbpt5Δ5/1-induced giant endosomes (Fig. 32B). Similar to the coexpression with Rab7a, Lamp1 accumulated in the perinuclear region, but also on the giant endosomes (Fig. 32C). Lamp1 is primarily a marker for lysosomes, but is also partially found on late endosomes. The rather weak staining of Lamp1 on the giant structures compared to the perinuclear lysosomal staining points more to a late endosomal than lysosomal characteristics of the giant structures.

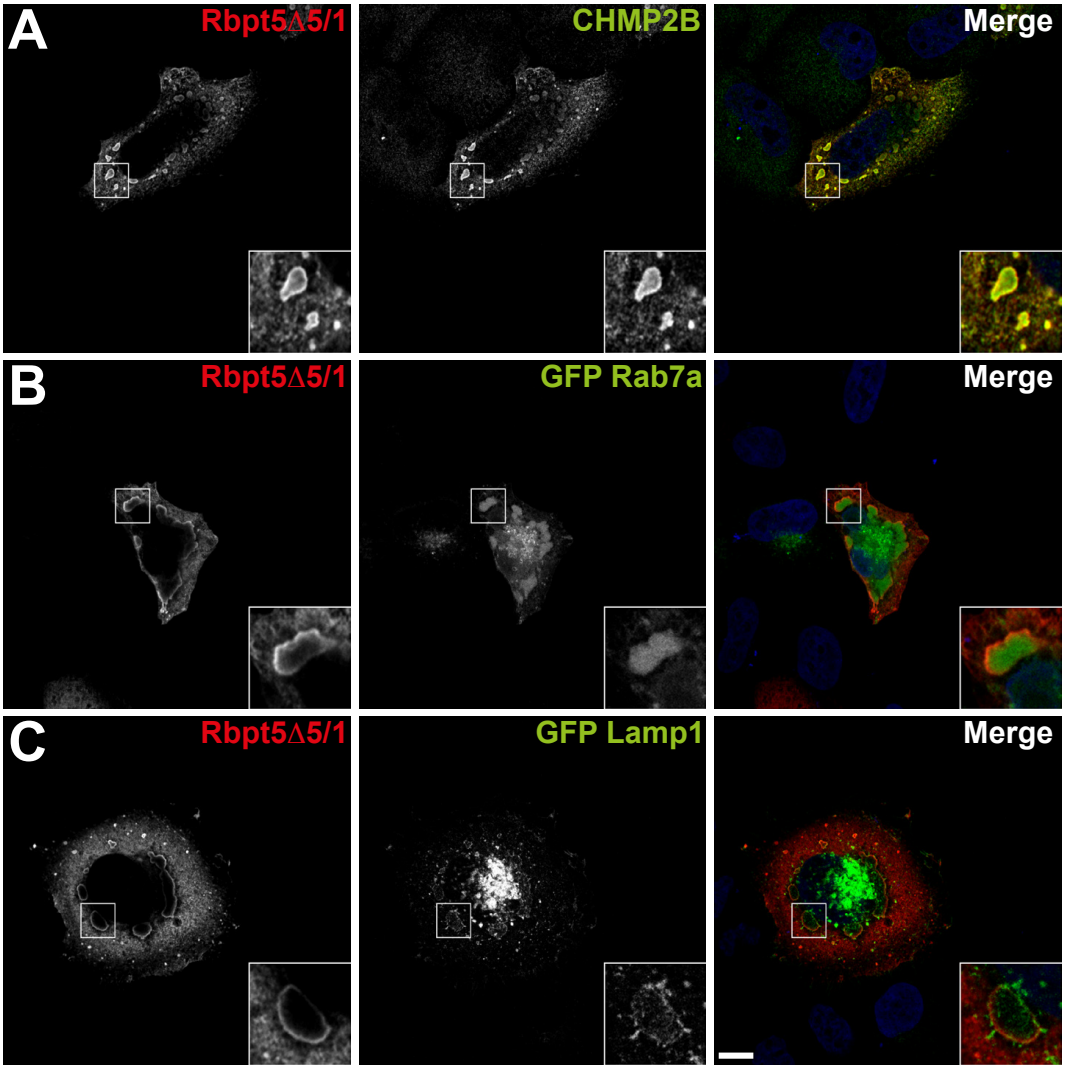

Fig. 32. **Rbpt5Δ5/1-induced giant endosomes show late endosomal characteristics**

Giant endosomes induced by Rbpt5Δ5/1 colocalize with **A**) CHMP2B, a component of the ESCRT machinery, **B**) the late endosomal marker Rab7a and **C**) Lamp1. Bars, 10 µm. Nuclei were stained with DAPI (blue).

To further assess the endolysosomal identity of the giant endosomes, an epidermal growth factor (EGF) uptake assay was performed (Fig. 33). For this experiment, A431 cells were used, which express high levels of EGF receptor (EGFR). The cells were allowed to bind fluorescently labelled EGF at 4°C at the surface and were than chased for different timepoints at 37°C. After 10 min of internalization, EGF typically labelled early endosomes at the periphery of the cell, but did not colocalize with Rbpt5Δ5/2-induced giant endosomes (Fig. 33A). Only after 30 min, the giant endosomes were at least partially labelled with fluorescent EGF, again indicating late endosomal characteristics of these structures (Fig. 33B). After 3 h of uptake, EGF migrated to lysosomal structures, where it is degraded and did not

colocalize with the giant endosomes any more (Fig. 33C). The results from this and the previous chapters suggest a defect in the maturation process from early to late endosomes resulting in giant chimeric endosomes with early and late endosomal characteristics.

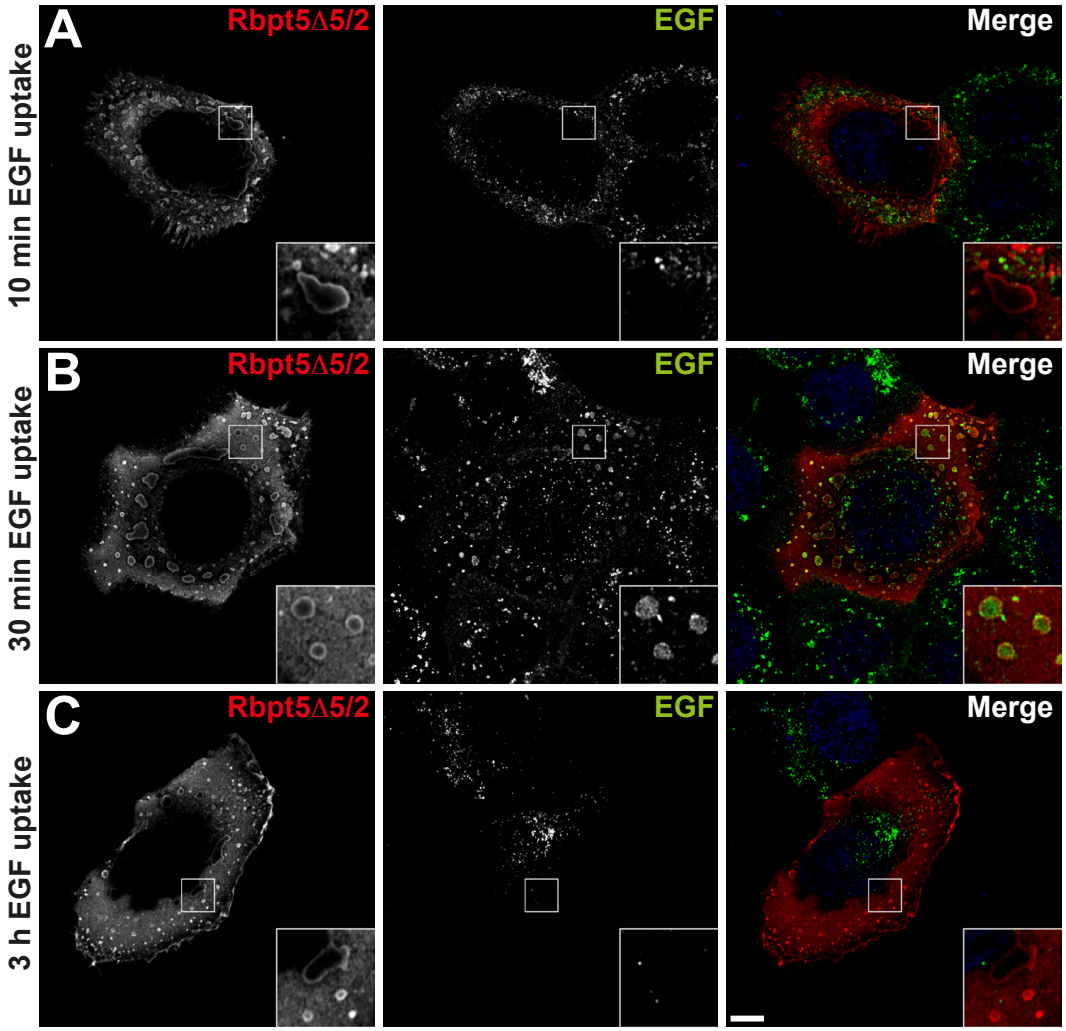

Fig. 33. **Rbpt5Δ5/2-induced giant endosomes colocalize with late endosomal EGF after 30 min of uptake** Fluorescently labelled EGF was bound on ice to the surface of A431 cells and chased for 10 min, 30 min or 3 h at 37°C. **A**) Early endosomal EGF does not colocalize with Rbpt5Δ5/2-induced giant endosomes, while **B**) late endosomal EGF does. **C**) After 3 h of chase, fluorescent EGF migrates to lysosomes for degradation and is not found on the giant endosomes any more. Bars, 10 µm. Nuclei were stained with DAPI (blue).

Transferrin recycling is affected by Rbpt5Δ5/1 and Rbpt5Δ5/2

To investigate the consequences of the massive endosome enlargement induced by Rbpt5Δ5/1 and Rbpt5Δ5/2, qualitative and quantitative Tf recycling was performed. For the qualitative analyses, 0 and 20 min of Tf recycling were studied. After loading the cells for 1 h with fluorescent transferrin to steady-state, the giant endosomes of both Rbpt5Δ5/1 and Rbpt5Δ5/2 were filled with Tf (Fig. 34A and C). 20 min of recycling completely emptied un-transfected cells, while in the expressing cells retained transferrin was easily detected exclusively within giant endosomes (Fig. 34B and D). Quantitative analysis of transferrin recycling in Rbpt5Δ5/2 expressing cells showed unaffected recycling in the first 5 min, while the recycling rate moderately decreased in the following 15 min (Fig. 34E). This could be interpreted as a mild reduction of transferrin recycling from early endosomes. More likely though, the reduced recycling rate is caused by an indirect effect of transferrin uptake into intraluminal vesicles of the early/late endosome chimeras as shown above, thus prohibiting transferrin recycling back to the plasma membrane.

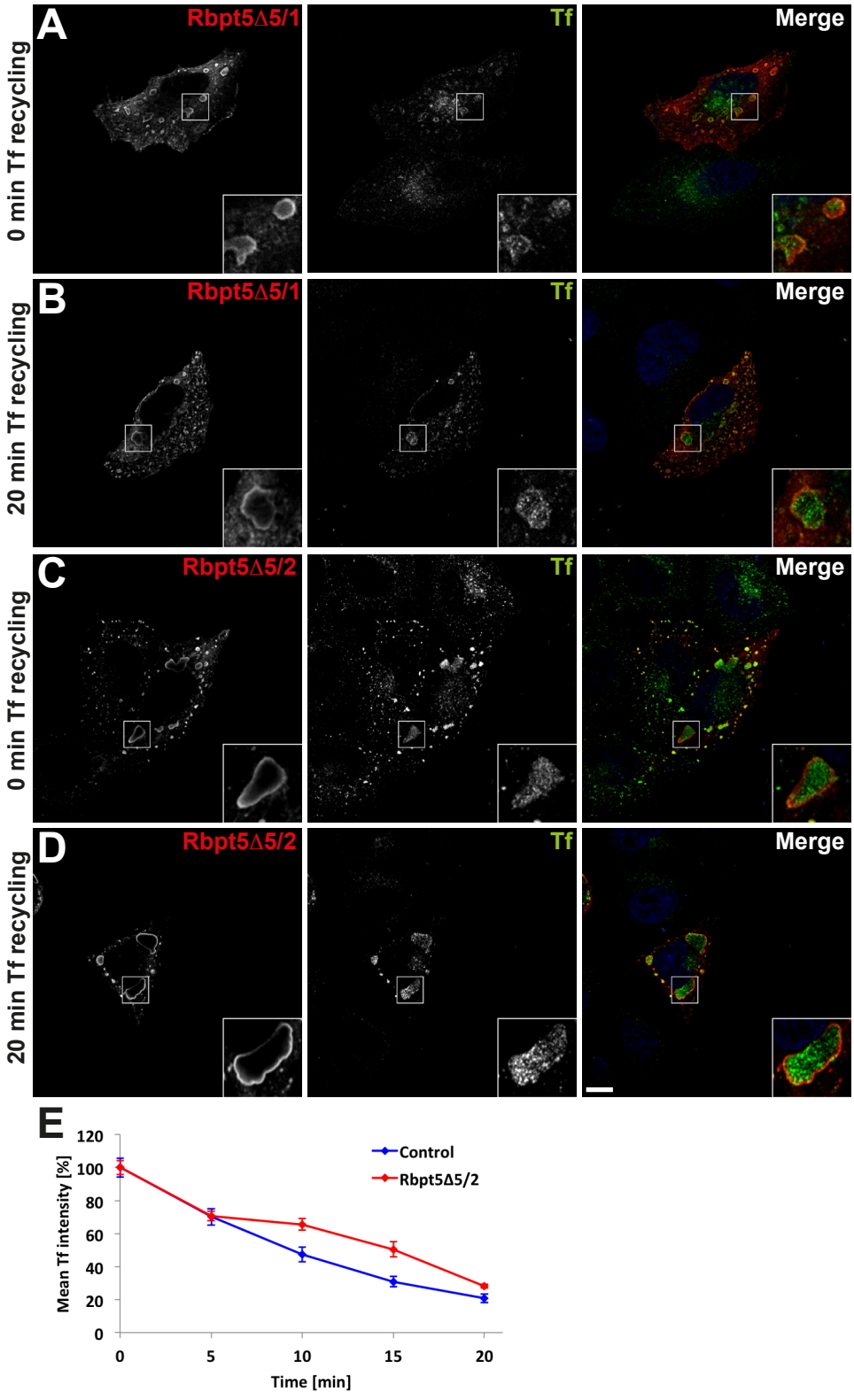

Fig. 34. **Rbpt5Δ5/1 and Rbpt5Δ5/2 both reduce Tf recycling**

Transferrin recycling for Rbpt5Δ5/1 **A**) at 0 min and **B**) 20 min recycling. **C** and **D**) show representative pictures for 0 min and 20 min Tf recycling for Rbpt5Δ5/2. **E**) Quantitative anlaysis of Tf recycling in Rbpt5Δ5/2-positive cells. Graph represents the mean value and standard deviation of 6 assay wells. Bars, 10 µm. Nuclei were stained with DAPI (blue).

Rabaptin5 missing both Rab5 binding domains only shows late endosomal properties

An obvious sequel to studying the two Rab5 binding domains on Rabaptin5 individually, was the analysis of the double mutant. Also Rbpt5Δ5 showed a high efficiency of producing covalent dimers (Fig. 35A) and induced giant endosome similar in size to the single Rab5 binding domain mutants (Fig. 35B). Interestingly, the giant endosomes induced by Rbpt5Δ5 were negative for transferrin and Rab5 (Fig. 35C and D) indicating a loss of the early endosome characteristics. In contrast, staining for CHMP2B appeared on the giant endosomes as did coexpressed Rab7a (Fig. 35E and F), suggesting late endosomal morphology. However, Lamp1, which faintly stained the giant endosomes of the single mutants, did not colocalize at all (Fig. 35G). Rbpt5Δ5 seems to induce large endosomes with late endosome character excluding early endosomal and lysosomal markers.

Fig. 35. **Deletion of both Rab5 binding domains on Rbpt5 induces giant endosomes with late endosomal properties**

A) Dimerization assay for Rbpt5Δ5 and **B**) quantitation of endosomes size. Rbpt5Δ5 induced giant endosomes were negative for **C**) Tf and **D**) Rab5a, but colocalized with **E**) CHMP2B and **F**) Rab7a. **G**) The lysosomal marker Lamp1 was excluded from the giant endosomes. Bars, 10 µm. Nuclei were stained with DAPI (blue). ↓

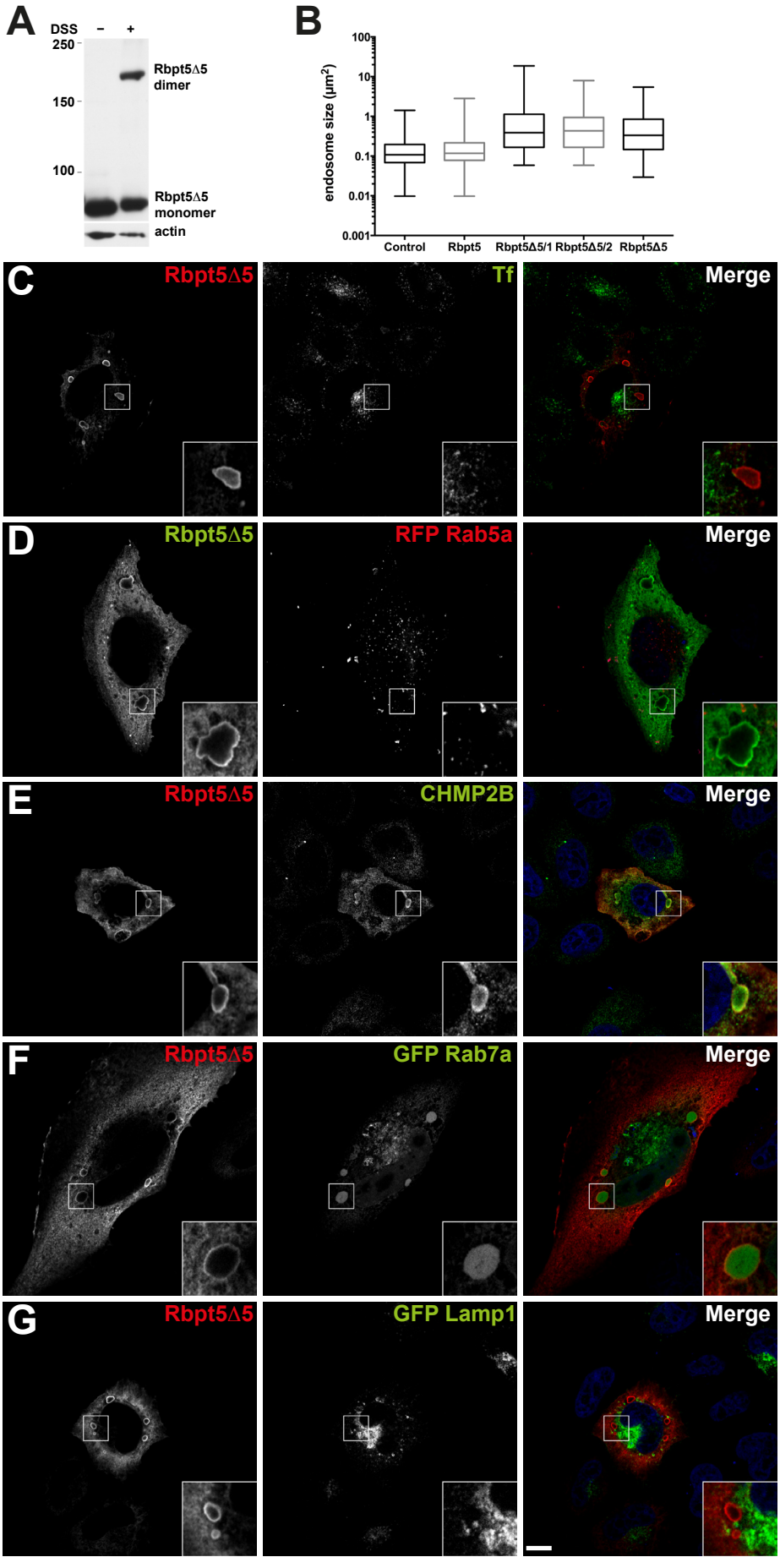
A
DSS – +
250
150
100
Rbpt5Δ5 dimer
Rbpt5Δ5 monomer
actin
B
endosome size (µm²)
100
10
1
0.1
0.01
0.001
Control
Rbpt5
Rbpt5Δ5/1
Rbpt5Δ5/2
Rbpt5Δ5
C
Rbpt5Δ5
Tf
Merge
D
Rbpt5Δ5
RFP Rab5a
Merge
E
Rbpt5Δ5
CHMP2B
Merge
F
Rbpt5Δ5
GFP Rab7a
Merge
G
Rbpt5Δ5
GFP Lamp1
Merge

Rabaptin5 mutant phenotypes can be observed in other cell lines

The Rabaptin5 mutation analysis was carried out in HeLa cells. To exclude cell type specific effects, another cell line was analysed. A431 cells were transfected with wildtype or mutant Rabaptin5 and loaded with fluorescent transferrin to steady-state. Wildtype Rabaptin5 was observed in the cytosol and on transferrin positive early endosomes (Fig. 36A), while Rbpt5ΔX and Rbpt5Δ4 showed a cytosolic distribution (Fig. 36B and C). As described in HeLa cells, Rbpt5Δ5/1 and Rbpt5Δ5/2, where the two Rab5 binding domain were deleted individually, and the double deletion mutant Rbpt5Δ5 induced giant endosomes with similar size (Fig. 36G). Rbpt5Δ5/1 and Rbpt5Δ5/2 still contained fluorescent transferrin (Fig. 36D and E) showing early endosomal features, while Rbpt5Δ5 was devoid of it (Fig. 36F).

In summary, A431 cells show the same phenotypes as HeLa cells. Individual mutants were additionally expressed in Cos1 cells, even belonging to a different species and also reproduced the same phenotypes (data not shown). This leads to the conclusion that our observations are conserved in different cell types and even species.

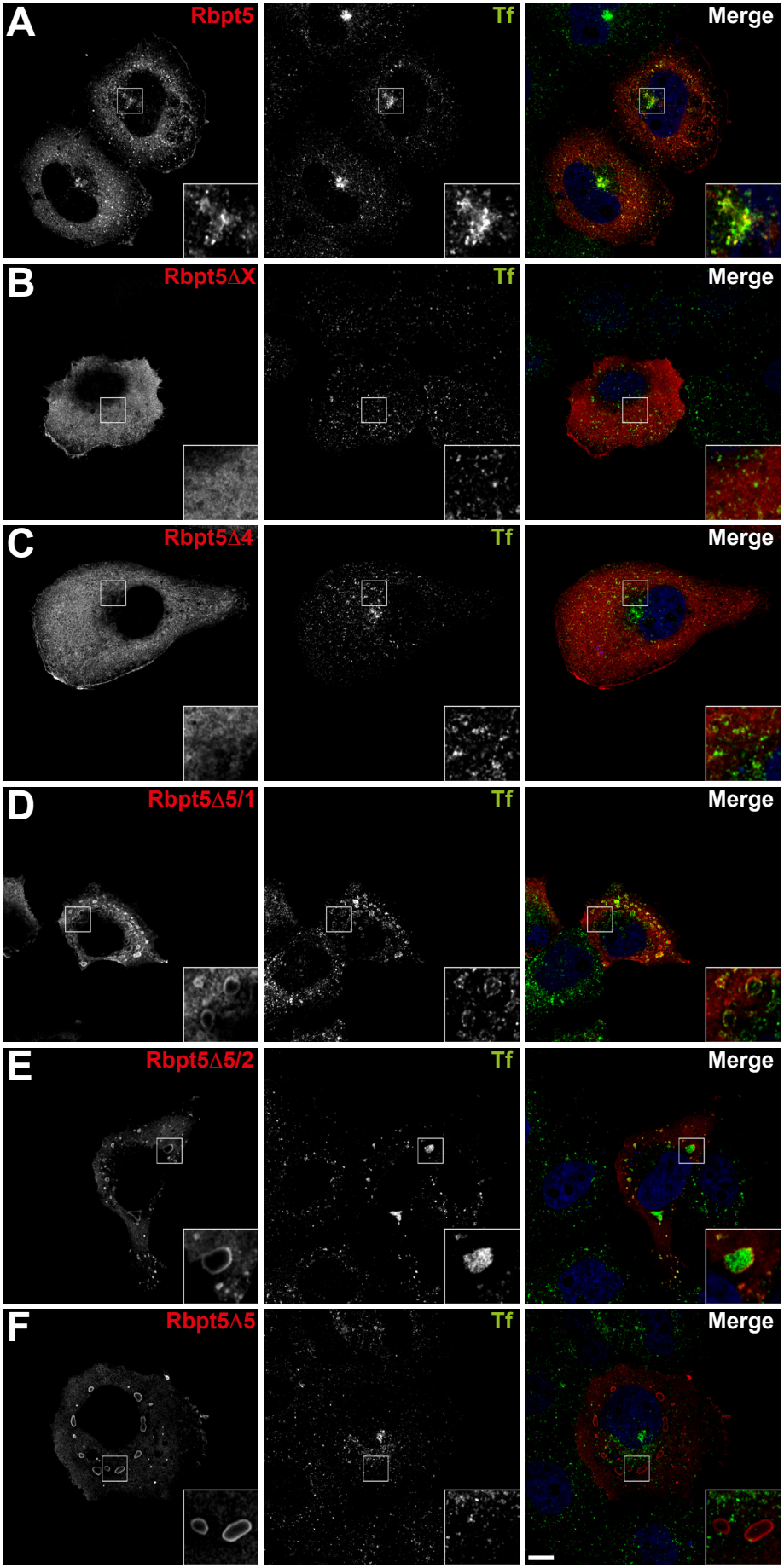
A
Rbpt5
Tf
Merge
B
Rbpt5ΔX
Tf
Merge
C
Rbpt5Δ4
Tf
Merge
D
Rbpt5Δ5/1
Tf
Merge
E
Rbpt5Δ5/2
Tf
Merge
F
Rbpt5Δ5
Tf
Merge

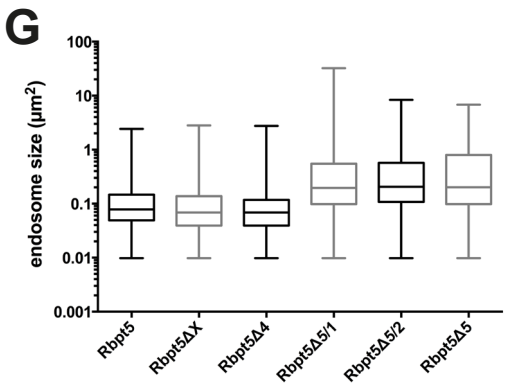

Fig. 36. **A431 cells show the same phenotypes for wildtype and mutant Rbpt5 as in HeLa cells**
A) Wildtype Rbpt5 was observed in the cytosol and on early endosome, in contrast to **B**) Rbpt5ΔX and **C**) Rbpt5Δ4 with a primarily cytosolic distribution. While **D**) Rbpt5Δ5/1 and **E)** Rbpt5Δ5/2 induced Tf-positive giant endosome, the huge endosome induced by **F**) Rbpt5Δ5 were devoid of Tf. **G**) Quantitation of endosome size. Bars, 10 µm. Nuclei were stained with DAPI (blue).

Discussion

Rabaptin5 was extensively studied by several groups for more than 10 years starting with its discovery in 1995 (Stenmark et al., 1995). With the establishment of the positive feedback loop by the Zerial group, the function of Rabaptin5 was supposed to be solved and the protein moved out of the focus. With the findings in this thesis, the well-established view is challenged in serveral ways.

Wildtype Rabaptin5 shows different effects in several studies

Previous studies using immunofluorescence microscopy usually boosted Rabaptin5 expression by either adding sodium butyrate before analysis (Deneka et al., 2003) or using the T7 RNA polymerase vaccinia virus expression system (Vitale et al., 1998) leading to Rabaptin5 induced enlarged endosomes. We could reproduce the phenotype induced by butyrate (Fig. 21D), but decided to abstain from this treatment, since endosome enlargement already visible for the wildtype could mask more prominent phenotypes of the mutant proteins or other interactors. Moderate expression of Rabaptin5 together with Rabex5 or Rab4a could show that endosome enlargement was induced by Rabex5 or Rab4a, respectively, and not by Rabaptin5 (Fig. 22). Massive overexpression of Rabaptin5 would have masked this effect and would not allow drawing correct conclusions.

Deneka et al. (2003) also performed transferrin recycling assays upon either Rabaptin5α silencing or wildtype Rabaptin5α overexpression. In their case, Rbpt5 siRNA knockdown decreased endocytosis resulting in little transferrin in endosomes at steady-state and thus made it difficult to assess Tf recycling. We, however, could not observe a change in endocytosis since recycling in silenced and control cells started at similar levels after loading the cells with transferrin to steady-state (Fig. 23C) and transferrin recycling of Rbpt5 knockdown cells was not affected either. Instead of analysing only a few confocal images, we used an automated microscope that takes into account hundreds of cells and resulting in a more quantitative output.

Our transferrin recycling rate was not dramatically changed by a moderate Rabaptin5 expression (Fig. 23D). Deneka et al. (2003), however, showed that Tf recycling was delayed in Rabaptin5α transfected cells, where protein expression was enhanced by butyrate treatment. Butyrate induces higher gene expression in mammalian cells by hyperacetylating histones in chromatin structure (Candido et al., 1978), thereby not only influencing Rabaptin5 expression but also other genes. The transferrin recycling rate may thus be influenced by other upregulated proteins and makes it impossible to compare these two values.

Our results suggest no dramatic influence of Rabaptin5 on transferrin recycling. In addition, the mutation of the AP1 binding site on Rabaptin5 had no influence on Rbpt5 recruitment nor on endosome size (Fig. 24B and D), even though AP1 was known to be involved in the formation of endosome-derived vesicles *in vitro* (Pagano et al., 2004).

Rabaptin5 recruitment to endosomes is mediated by Rabex5 and Rab4a, but not by Rab5a

It has been shown that free Rabex5 (unattached to Rabaptin5) was able to recruit to endosomes directly via an early endosome targeting domain (Zhu et al., 2007) or by binding to ubiquitinated cargo on endosomes via its ubiquitin interacting motif (Mattera and Bonifacino, 2008). This was proposed to kickstart a Rab5 activation loop by recruiting Rabaptin5/Rabex5 complex, which in turn produces even more Rab5-GTP on early endosomes leading to a positive feedback loop (Zerial and McBride, 2001). One study, which supported this feedback model, used a Rabaptin5 mutant missing the entire C-terminal part from amino acid 547 up to the end of the protein. This mutant did not show endosome recruitment, which lead the authors to the assumption that Rab5 recruits Rabaptin5 to endosome via the C-terminal Rab5 binding domain on Rabaptin5 (Vitale et al., 1998).

In agreement with the feedback model, Rabex5 expression caused the formation of large endosomes, which were positive for Rabaptin5 (Fig. 22B). On the other hand, deletion of the Rabex5 binding domain on Rabaptin5 resulted in a cytosolic distribution of the mutant with no endosomal recruitment as did Rabex5 siRNA knockdown for wildtype Rabaptin5 (Fig. 25B and D). From these results, we conclude that Rabex5 is essential for Rabaptin5 endosome recruitment.

However, inconsistent with the positive feedback model were our results about the Rabaptin5/Rab5a interaction. We could show that Rab5a is not responsible for Rabaptin5 endosome recruitment, since wildtype Rabaptin5 could still recruit to endosomes in cells expressing dominant negative Rab5a or in Rab5a knockdown cells (Fig. 30 A/B). In addition, deletion of the Rab5 binding domains on Rabaptin5 did not prevent membrane recruitment (Fig. 29, Fig. 31, Fig. 35).

Going back at the data from Vitale et al. (1998) with the knowledge about the binding domains from nowadays, it could be observed that their mutant was not only lacking the C-terminal Rab5 binding domain but also the Rabex5 binding domain. Most probably the lack of the Rabex5 binding domain in their mutant caused the defect in endosome recruitment and would support our view of Rabaptin5 recruitment via Rabex5 and not Rab5.

Surprisingly, coexpression of Rab4a with wildtype Rbpt5 enhanced membrane recruitment of Rabaptin5 (Fig. 22F), while inactivation of Rab4a by expression of the dominant negative mutant Rab4aS22N (Fig. 27A) or Rab4a siRNA-mediated silencing (Fig. 27B) completely prevented membrane binding of wildtype Rbpt5. This was also shown by the cytosolic distribution of Rbpt5 missing the entire Rab4 binding domain (Fig. 26B). All these results strongly suggest that in addition to Rabex5 also Rab4a is required for endosome recruitment of Rabaptin5.

This clearly contradicts the feedback model, where Rabaptin5 is recruited to endosomes via Rab5-GTP. Rab4, instead, was supposed to be involved in the recycling from the endosome to the plasma membrane. Several publications have attributed Rab4 an involvement in recycling of the transferrin receptor, but its exact function remains elusive. Van der Sluijs et al. (1992) showed that neither Tf uptake nor Tf recycling to the plasma membrane was affected in CHO cells overexpressing wildtype or dominant negative Rab4. In contrast to this finding, it was reported that Tf recycling was strongly inhibited in HeLa cells expressing dominant negative Rab4 and slightly increased in cells expressing wildtype and constitutively active Rab4 (McCaffrey et al., 2001). Unpublished data from our lab showed no effect in Tf recycling for dominant negative nor constitutive active Rab4a. Taking into account these conflicting results of Rab4 involvement in endosomal recycling and the data presented in this thesis would suggest that Rab4 acts in an early step of Rabaptin5 recruitment to endosomes and is probably less important in recycling. Apparent from the presented results, we can reject the established positive feedback model.

The location of the Rab4 binding domain on Rabaptin5 was also a matter of debate. Previous studies agreed that the N-terminal third of Rbpt5 binds to Rab4-GTP as detected by yeast two-hybrid analysis (Korobko et al., 2005; Vitale et al., 1998) or GST-Rab4 pull-down experiments (Deneka et al., 2003), but they differed on the location of the interacting sequence(s) within this segment. Vitale et al. (1998) observed activity for residues 5–135 (including the coiled-coil domain CC1-1) in a yeast two-hybrid screen, whereas Deneka et al. (2003) showed binding to residues 140–295 (including CC1-2) in GST-Rab4 pull-down experiments. Both potential Rab4 binding sites were only analysed with biochemical assays and no *in vivo* localization studies were performed. By analyzing the deletion constructs Rbpt5Δ4/1 lacking residues 1–135 and Rbpt5Δ4/2 lacking residues 140–262 with immunofluorescence, we found both efficiently recruited to Tf-containing endosomes (Fig. 28A and B), suggesting that both segments were able to bind Rab4a independently *in vivo*. In addition, Rbpt5δ, a natural splice variant lacking residues 187–226, was expressed. According to Korobko et al. (2005), Rbpt5δ was not able to bind to Rab4 in a yeast two-hybrid screen and did not colocalize with Rab4 in BHK21 cells. We could not confirm this phenotype, since Rbpt5δ like Rbpt5Δ4/2 was

recruited to endosomes (Fig. 28C). Our findings indicate two independent Rab4 binding domains in the N-terminus of Rabaptin5 where both of them are sufficient to induce endosome recruitment individually and only deletion of both segments leads to dissociation from endosomal membranes.

Interaction between Rabaptin5 and Rab5a on early endosomes inhibits endosome maturation

Studying the interaction between Rabaptin5 and Rab5a did not only demonstrate Rab5-independent endosome recruitment of Rabaptin5, but also showed a new phenotype. Deletion of the individual Rab5 binding domains on Rabaptin5 induced giant endosomes positive for early endosomal markers like Tf, Rab4a and Rab5a (Fig. 29/Fig. 31). In addition, these giant endosomes showed a multivesicular appearance positive for the ESCRT component CHMP2B and the late endosomal markers Rab7a and Lamp1 (Fig. 32). Deletion of one of the two Rab5 binding domains on Rabaptin5 produced giant chimeric early/late endosomes, which suggests a dysregulation in endosome maturation.

In agreement with a defect in endosome maturation is the observation that a deletion of both Rab5 binding domains on Rabaptin5 induces giant endosomes with only late endosomal properties (Fig. 35). In addition, endosome enlargement could also be shown by Rab5a inactivation and subsequent wildtype Rbpt5 expression (Fig. 30). With no Rab5 interaction to Rabaptin5, premature late endosomes were formed.

Our data suggest a new model (Fig. 37). Rabaptin5 is recruited to endosome by Rab4a-GTP and Rabex5 via two independent Rab4 and one Rabex5 binding domain on Rabaptin5. It is not clear, in which way Rabex5 recruits Rabaptin5 to endosomes. Lippé et al. (2001) showed that under physiological conditions, no free Rabex5 is present in the cell. Instead Rabex5 forms a stable complex with one Rabaptin5 homodimer and would thus be recruited to endosomes as a complex (Fig. 37A). Two independent studies, however, demonstrated that free Rabex5 (unattached to Rabaptin5) was able to recruit to endosomes directly via an early endosome targeting domain (Zhu et al., 2007) or by binding to ubiquitinated cargo on endosomes via an ubiquitin interacting motif (Mattera and Bonifacino, 2008). This would suggest that membrane associated Rabex5 could recruit uncomplexed Rabaptin5 (Fig. 37B).

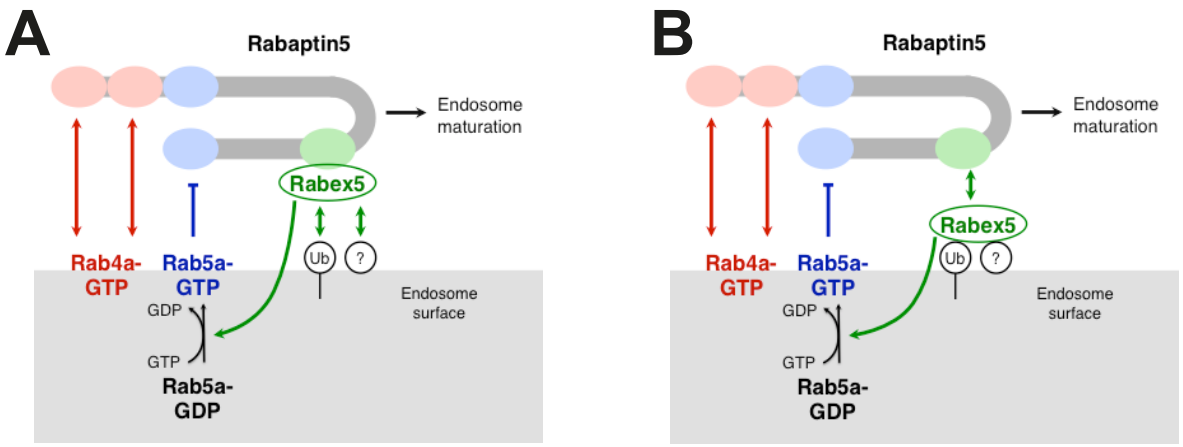

Fig. 37. **Potential models of Rabaptin5 function**

Rabaptin5 is recruited to endosomes by Rab4a-GTP and Rabex5 (indicated by ↔). Membrane bound Rabex5 activates a local pool of Rab5, which in turn inhibits Rabaptin5 driven endosome maturation (indicated by ⊥). It is not clear if Rabaptin5 is recruited to endosomes in complex with Rabex5 (**A**) or via membrane bound Rabex5, which is targeted to endosomal membranes via ubiquinated cargo (Ub) or its early endosome targeting domain (?) (**B**).

Independent of Rabaptin5, membrane associated Rabex5 activates a local pool of Rab5a on endosomes. We speculate that Rab5a-GTP may inhibit Rabaptin5 driven endosome maturation since deletion of the Rab5 binding domains on Rabaptin5 induces a premature maturation process. How Rabaptin5 can promote endosome maturation is absolutely not clear. The current model of endosome maturation involves another Rab5 effector Mon1/Ccz1, which promotes Rab7 binding by potentially displacing the GDI from Rab7 (Poteryaev et al., 2010). So far no interaction between Mon1/Ccz1 and Rabaptin5 has been shown and it will be a challenge to connect Rabaptin5 driven endosome maturation with the model based on Mon1/Ccz1.

Outlook

Our results are mainly based on immunofluorescence microscopy. In general, it would be beneficial to perform some biochemical experiments to show binding between the different proteins. Strong interactions between proteins like Rabaptin5 and Rabex5 can be detected by simple coimmunoprecipitation. Weaker interactions and interaction with only one form of a protein like the GTP-bound form of Rab proteins are more challenging to show. *In vivo* crosslinking with a cleavable crosslinker like dithiobissuccinimidylpropionate (DSP) and subsequent coimmunoprecipitation could be one way to demonstrate interaction between different Rab proteins and the Rabaptin5 mutants. Another possibility is to perform dominant active Rab GST pull-downs with mutant Rabaptin5 lysates followed by western blot analysis.

We could show that Rabaptin5 is recruited to endosomes by Rab4a-GTP and Rabex5. To decipher Rabaptin5 recruitment in the context of Rabex5 membrane association via ubiquitinated cargo the ubiquitin binding site on Rabex5 will be mutated and analysed together with Rabaptin5. In addition, the GEF catalytic core of Rabex5 can be inactivated by a simple point mutation and tested, if Rabaptin5 endosome recruitment is still possible by immunofluorescence.

The Rab5 binding domain in the N-terminal third of Rabaptin5 was identified in a yeast two-hybrid screen compromising a large sequence partially overlapping with the second Rab4 binding domain. It would be of great use to separate these two binding domains. We are currently trying to dissect the Rab5 binding into smaller pieces and will test them for Rabaptin5 recruitment.

The mechanism of Rabaptin5 driven endosome maturation is absolutely unclear. As a starting point colocalization studies could be performed with Mon1/Ccz1, which is supposed to be a keyplayer in endosome maturation. In addition, coimmunoprecipitation experiments could show an interaction between the proteins. Most probably a Rabaptin5/Mon1 interaction is too simple and we suspect so far unknown interactors to be involved. To identify new Rabaptin5 interactors, an unbiased yeast two-hybrid screen with full-length Rabaptin5 as a bait might identify the missing pieces in this complex process. New interactors will then be characterized and analysed together with Rabaptin5.

Abbreviations

AAK1	Adaptor associated kinase 1
ADP	Adenosine diphosphate
AP	Adaptor protein
ARF	ADP ribosylation factor
BAR domain	Bin/Amphiphysin/Rvs domain
CC domain	Coiled-coil domain
CCV	Clathrin coated vesicle
CHC	Clathrin heavy chain
CLC	Clathrin light chain
COPI/II	Coat protein I/II
DAPI	4',6'-Diamidino-2-phenylindole
DSS	Disuccinimidyl suberate
EEA1	Early endosome antigen 1
EET domain	Early endosome targeting domain
EGF	Epidermal growth factor
EGFR	EGF receptor
EPS15	EGFR pathway substrate 15
ER	Endoplasmic reticulum
ESCRT	Endosomal sorting complex required for transport
FCHO protein	Fer/Cip4 homology domain only protein
GAE	γ-adaptin ear
GAP	GTPase activating protein
GAPVD1	GTPase activating protein and VPS9 domain-containing protein 1
GAT	GGA and TOM
GDF	GDI displacement factor
GDI	GDP dissociation inhibitor

GDP	Guanosine diphosphate
GEF	Guanine nucleotide exchange factor
GFP	Green fluorescent protein
GGA	Golgi-localizing, γ-adaptin ear homology domain, Arf-binding proteins
GTP	Guanosine triphoshate
GTPase	GTP hydrolase
HA	Hemagglutinin
HB	Helical bundle
HSP70	Heat shock protein 70
HOPS	Homotypic fusion and vacuole protein sorting
IF	Immunofluorescence
ILV	Intraluminal vesicle
LAMP	Lysosome associated membrane protein
LDL	Low density lipoprotein
LDLR	LDL receptor
LMP	Lysosomal membrane protein
M6P	Mannose-6-phosphate
M6PR	M6P receptor
MBM	Membrane-binding motif
MIU	Motif interacting with ubiquitin
MVB	Multivesicular body
PCR	Polymerase chain reaction
PI	Phosphoinositol
PI(3)K	Phosphoinositol-3-kinase
PI(3)P	Phosphoinositol-3-phosphate
PI(4)P	Phosphoinositol-4-phosphate
$PI(3,5)P_2$	Phosphoinositol-3,5-bisphosphate

$PI(4,5)P_2$	Phosphoinositol-4,5-bisphosphate
$PI(3,4,5)P_3$	Phosphoinositol-3,4,5-triphosphate
PR	Proline-rich region
PX	Phox homology
Rbpt5	Rabaptin5
RFP	Red fluorescent protein
RME6	Receptor mediated endocytosis 6
RNAi	RNA interference
siRNA	Small interfering RNA
Rx5	Rabex5
SNARE	Soluble N-ethylmaleimide-sensitive factor attachment protein receptor
SNX	Sorting nexin
Tf	Transferrin
TfR	Transferrin receptor
TGN	Trans Golgi Network
VPS	Vacuolar protein sorting
VSV G protein	Vesicular stomatitis virus G protein
ZnF motif	Zinc-finger motif

References

Babst, M. (2011). MVB vesicle formation: ESCRT-dependent, ESCRT-independent and everything in between. Curr Opin Cell Biol *23*, 452–457.

Behnia, R., and Munro, S. (2005). Organelle identity and the signposts for membrane traffic. Nature *438*, 597–604.

Blümer, J., Rey, J., Dehmelt, L., Mazel, T., Wu, Y.-W., Bastiaens, P., Goody, R.S., and Itzen, A. (2013). RabGEFs are a major determinant for specific Rab membrane targeting. J Cell Biol *200*, 287–300.

Boehm, M., Aguilar, R.C., and Bonifacino, J.S. (2001). Functional and physical interactions of the adaptor protein complex AP-4 with ADP-ribosylation factors (ARFs). Embo J *20*, 6265–6276.

Bonfanti, L., Mironov, A.A., Martínez-Menárguez, J.A., Martella, O., Fusella, A., Baldassarre, M., Buccione, R., Geuze, H.J., Mironov, A.A., and Luini, A. (1998). Procollagen traverses the Golgi stack without leaving the lumen of cisternae: evidence for cisternal maturation. Cell *95*, 993–1003.

Bonifacino, J.S., and Glick, B.S. (2004). The mechanisms of vesicle budding and fusion. Cell *116*, 153–166.

Bonifacino, J.S., and Hurley, J.H. (2008). Retromer. Curr Opin Cell Biol *20*, 427–436.

Bonifacino, J.S., and Rojas, R. (2006). Retrograde transport from endosomes to the trans-Golgi network. Nat Rev Mol Cell Biol *7*, 568–579.

Brodsky, F.M. (2012). Diversity of clathrin function: new tricks for an old protein. Annu Rev Cell Dev Biol *28*, 309–336.

Bucci, C., Parton, R.G., Mather, I.H., Stunnenberg, H., Simons, K., Hoflack, B., and Zerial, M. (1992). The small GTPase rab5 functions as a regulatory factor in the early endocytic pathway. Cell *70*, 715–728.

Burgos, P.V., Mardones, G.A., Rojas, A.L., daSilva, L.L.P., Prabhu, Y., Hurley, J.H., and Bonifacino, J.S. (2010). Sorting of the Alzheimer's disease amyloid precursor protein mediated by the AP-4 complex. Dev Cell *18*, 425–436.

Callaghan, J., Simonsen, A., Gaullier, J.M., Toh, B.H., and Stenmark, H. (1999). The endosome fusion regulator early-endosomal autoantigen 1 (EEA1) is a dimer. Biochem J *338 (Pt 2)*, 539–543.

Canagarajah, B.J., Ren, X., Bonifacino, J.S., and Hurley, J.H. (2013). The clathrin adaptor complexes as a paradigm for membrane-associated allostery. Protein Sci. *22*, 517–529.

Candido, E.P., Reeves, R., and Davie, J.R. (1978). Sodium butyrate inhibits histone deacetylation in cultured cells. Cell *14*, 105–113.

Carpenter, A.E., Jones, T.R., Lamprecht, M.R., Clarke, C., Kang, I.H., Friman, O., Guertin, D.A., Chang, J.H., Lindquist, R.A., Moffat, J., et al. (2006). CellProfiler: image analysis software for identifying and quantifying cell phenotypes. Genome Biol. *7*, R100.

Chavrier, P., Gorvel, J.P., Stelzer, E., Simons, K., Gruenberg, J., and Zerial, M. (1991). Hypervariable C-terminal domain of rab proteins acts as a targeting signal. Nature *353*, 769–772.

Chen, W., Feng, Y., Chen, D., and Wandinger-Ness, A. (1998). Rab11 is required for trans-golgi network-to-plasma membrane transport and a preferential target for GDP dissociation inhibitor. Mol Biol Cell *9*, 3241–3257.

Chotard, L., Mishra, A.K., Sylvain, M.-A., Tuck, S., Lambright, D.G., and Rocheleau, C.E. (2010). TBC-2 regulates RAB-5/RAB-7-mediated endosomal trafficking in Caenorhabditis elegans. Mol Biol Cell *21*, 2285–2296.

Christoforidis, S., McBride, H.M., Burgoyne, R.D., and Zerial, M. (1999a). The Rab5 effector EEA1 is a core component of endosome docking. Nature *397*, 621–625.

Christoforidis, S., Miaczynska, M., Ashman, K., Wilm, M., Zhao, L., Yip, S.C., Waterfield, M.D., Backer, J.M., and Zerial, M. (1999b). Phosphatidylinositol-3-OH kinases are Rab5 effectors. Nat Cell Biol *1*, 249–252.

Cocucci, E., Aguet, F., Boulant, S., and Kirchhausen, T. (2012). The first five seconds in the life of a clathrin-coated pit. Cell *150*, 495–507.

Conner, S.D., and Schmid, S.L. (2003). Regulated portals of entry into the cell. Nature *422*, 37–44.

Cremona, O., Di Paolo, G., Wenk, M.R., Lüthi, A., Kim, W.T., Takei, K., Daniell, L., Nemoto, Y., Shears, S.B., Flavell, R.A., et al. (1999). Essential role of phosphoinositide metabolism in synaptic vesicle recycling. Cell *99*, 179–188.

D'Souza-Schorey, C., Li, G., Colombo, M.I., and Stahl, P.D. (1995). A regulatory role for ARF6 in receptor-mediated endocytosis. Science *267*, 1175–1178.

D'souza-Schorey, C., and Chavrier, P. (2006). ARF proteins: roles in membrane traffic and beyond. Nat Rev Mol Cell Biol *7*, 347–358.

de Renzis, S., Sönnichsen, B., and Zerial, M. (2002). Divalent Rab effectors regulate the sub-compartmental organization and sorting of early endosomes. Nat Cell Biol *4*, 124–133.

Del Conte-Zerial, P., Brusch, L., Rink, J.C., Collinet, C., Kalaidzidis, Y., Zerial, M., and Deutsch, A. (2008). Membrane identity and GTPase cascades regulated by toggle and cut-out switches. Mol. Syst. Biol. *4*, 206.

Dell'Angelica, E.C. (2001). Clathrin-binding proteins: got a motif? Join the network! Trends Cell Biol *11*, 315–318.

Dell'Angelica, E.C., Klumperman, J., Stoorvogel, W., and Bonifacino, J.S. (1998). Association of the AP-3 adaptor complex with clathrin. Science *280*, 431–434.

Dell'Angelica, E.C., Mullins, C., and Bonifacino, J.S. (1999). AP-4, a novel protein complex related to clathrin adaptors. J Biol Chem *274*, 7278–7285.

Dell'Angelica, E.C., Ohno, H., Ooi, C.E., Rabinovich, E., Roche, K.W., and Bonifacino, J.S. (1997). AP-3: an adaptor-like protein complex with ubiquitous expression. Embo J *16*, 917–928.

Dell'Angelica, E.C., Puertollano, R., Mullins, C., Aguilar, R.C., Vargas, J.D., Hartnell, L.M., and Bonifacino, J.S. (2000). GGAs: a family of ADP ribosylation factor-binding proteins related to adaptors and associated with the Golgi complex. J Cell Biol *149*, 81–94.

Delprato, A., and Lambright, D.G. (2007). Structural basis for Rab GTPase activation by VPS9 domain exchange factors. Nat Struct Mol Biol *14*, 406–412.

Delprato, A., Merithew, E., and Lambright, D.G. (2004). Structure, exchange determinants, and family-wide rab specificity of the tandem helical bundle and Vps9 domains of Rabex-5. Cell *118*, 607–617.

Deneka, M., Neeft, M., Popa, I., van Oort, M., Sprong, H., Oorschot, V., Klumperman, J., Schu, P., and van der Sluijs, P. (2003). Rabaptin-5alpha/rabaptin-4 serves as a linker between rab4 and gamma(1)-adaptin in membrane recycling from endosomes. Embo J *22*, 2645–2657.

Díaz, E., and Pfeffer, S.R. (1998). TIP47: a cargo selection device for mannose 6-phosphate receptor trafficking. Cell *93*, 433–443.

Donaldson, J.G., and Jackson, C.L. (2011). ARF family G proteins and their regulators: roles in membrane transport, development and disease. Nat Rev Mol Cell Biol *12*, 362–375.

Doray, B., Ghosh, P., Griffith, J., Geuze, H.J., and Kornfeld, S. (2002). Cooperation of GGAs and AP-1 in packaging MPRs at the trans-Golgi network. Science *297*, 1700–1703.

Dumas, J.J., Merithew, E., Sudharshan, E., Rajamani, D., Hayes, S., Lawe, D., Corvera, S., and Lambright, D.G. (2001). Multivalent endosome targeting by homodimeric EEA1. Mol. Cell *8*, 947–958.

Echard, A., Jollivet, F., Martinez, O., Lacapère, J.J., Rousselet, A., Janoueix-Lerosey, I., and Goud, B. (1998). Interaction of a Golgi-associated kinesin-like protein with Rab6. Science *279*, 580–585.

Edeling, M.A., Smith, C., and Owen, D. (2006). Life of a clathrin coat: insights from clathrin and AP structures. Nat Rev Mol Cell Biol *7*, 32–44.

Feng, Y., Press, B., and Wandinger-Ness, A. (1995). Rab 7: an important regulator of late endocytic membrane traffic. J Cell Biol *131*, 1435–1452.

Ferguson, S.M., Ferguson, S., Raimondi, A., Paradise, S., Shen, H., Mesaki, K., Ferguson, A., Destaing, O., Ko, G., Takasaki, J., et al. (2009). Coordinated actions of actin and BAR proteins upstream of dynamin at endocytic clathrin-coated pits. Dev Cell *17*, 811–822.

Fouraux, M.A., Deneka, M., Ivan, V., van der Heijden, A., Raymackers, J., van Suylekom, D., van Venrooij, W.J., van der Sluijs, P., and Pruijn, G.J.M. (2004). Rabip4' is an effector of rab5 and rab4 and regulates transport through early endosomes. Mol Biol Cell *15*, 611–624.

Fölsch, H., Ohno, H., Bonifacino, J.S., and Mellman, I. (1999). A novel clathrin adaptor complex mediates basolateral targeting in polarized epithelial cells. Cell *99*, 189–198.

Frasa, M.A.M., Maximiano, F.C., Smolarczyk, K., Francis, R.E., Betson, M.E., Lozano, E., Goldenring, J., Seabra, M.C., Rak, A., Ahmadian, M.R., et al. (2010). Armus is a Rac1 effector that inactivates Rab7 and regulates E-cadherin degradation. Curr Biol *20*, 198–208.

Gaidarov, I., and Keen, J.H. (1999). Phosphoinositide-AP-2 interactions required for targeting to plasma membrane clathrin-coated pits. J Cell Biol *146*, 755–764.

Gaidarov, I., Chen, Q., Falck, J.R., Reddy, K.K., and Keen, J.H. (1996). A functional phosphatidylinositol 3,4,5-trisphosphate/phosphoinositide binding domain in the clathrin adaptor AP-2 alpha subunit. Implications for the endocytic pathway. J Biol Chem *271*, 20922–20929.

Glick, B.S., and Luini, A. (2011). Models for Golgi Traffic: A Critical Assessment. Cold Spring Harbor Perspectives in Biology *3*, a005215–a005215.

Glick, B.S., and Malhotra, V. (1998). The curious status of the Golgi apparatus. Cell *95*, 883–889.

Gorvel, J.P., Chavrier, P., Zerial, M., and Gruenberg, J. (1991). rab5 controls early endosome fusion in vitro. Cell *64*, 915–925.

Grosshans, B.L., Ortiz, D., and Novick, P. (2006). Rabs and their effectors: achieving specificity in membrane traffic. Proc Natl Acad Sci USA *103*, 11821–11827.

Gruenberg, J. (2001). The endocytic pathway: a mosaic of domains. Nat Rev Mol Cell Biol *2*, 721–730.

Haar, ter, E., Harrison, S.C., and Kirchhausen, T. (2000). Peptide-in-groove interactions link target proteins to the beta-propeller of clathrin. Proc Natl Acad Sci USA *97*, 1096–1100.

Hanson, P.I., Roth, R., Lin, Y., and Heuser, J.E. (2008). Plasma membrane deformation by circular arrays of ESCRT-III protein filaments. J Cell Biol *180*, 389–402.

Hao, M., and Maxfield, F.R. (2000). Characterization of rapid membrane internalization and recycling. J Biol Chem *275*, 15279–15286.

Henne, W.M., Buchkovich, N.J., and Emr, S.D. (2011). The ESCRT pathway. Dev Cell *21*, 77–91.

Henne, W.M., Boucrot, E., Meinecke, M., Evergren, E., Vallis, Y., Mittal, R., and McMahon, H.T. (2010). FCHo proteins are nucleators of clathrin-mediated endocytosis. Science *328*, 1281–1284.

Hirano, S., Kawasaki, M., Ura, H., Kato, R., Raiborg, C., Stenmark, H., and Wakatsuki, S. (2006). Double-sided ubiquitin binding of Hrs-UIM in endosomal protein sorting. Nat Struct Mol Biol *13*, 272–277.

Hirota, Y., Kuronita, T., Fujita, H., and Tanaka, Y. (2007). A role for Rab5 activity in the biogenesis of endosomal and lysosomal compartments. Biochem. Biophys. Res. Commun. *364*, 40–47.

Hirst, J., and Robinson, M.S. (1998). Clathrin and adaptors. Biochim. Biophys. Acta *1404*, 173–193.

Hirst, J., Bright, N.A., Rous, B., and Robinson, M.S. (1999). Characterization of a fourth adaptor-related protein complex. Mol Biol Cell *10*, 2787–2802.

Hirst, J., Lui, W.W., Bright, N.A., Totty, N., Seaman, M.N., and Robinson, M.S. (2000). A family of proteins with gamma-adaptin and VHS domains that facilitate trafficking between the trans-Golgi network and the vacuole/lysosome. J Cell Biol *149*, 67–80.

Hirst, J., Barlow, L.D., Francisco, G.C., Sahlender, D.A., Seaman, M.N.J., Dacks, J.B., and Robinson, M.S. (2011). The fifth adaptor protein complex. PLoS Biol. *9*, e1001170.

Hirst, J., Borner, G.H.H., Antrobus, R., Peden, A.A., Hodson, N.A., Sahlender, D.A., and Robinson, M.S. (2012). Distinct and overlapping roles for AP-1 and GGAs revealed by the "knocksideways" system. Curr Biol *22*, 1711–1716.

Hirst, J., Irving, C., and Borner, G.H.H. (2013). Adaptor protein complexes AP-4 and AP-5: new players in endosomal trafficking and progressive spastic paraplegia. Traffic *14*, 153–164.

Hirst, J., Motley, A., Harasaki, K., Peak Chew, S.Y., and Robinson, M.S. (2003). EpsinR: an ENTH domain-containing protein that interacts with AP-1. Mol Biol Cell *14*, 625–641.

Horiuchi, H., Giner, A., Hoflack, B., and Zerial, M. (1995). A GDP/GTP exchange-stimulatory activity for the Rab5-RabGDI complex on clathrin-coated vesicles from bovine brain. J Biol Chem *270*, 11257–11262.

Horiuchi, H., Lippé, R., McBride, H.M., Rubino, M., Woodman, P., Stenmark, H., Rybin, V., Wilm, M., Ashman, K., Mann, M., et al. (1997). A novel Rab5 GDP/GTP exchange factor complexed to Rabaptin-5 links nucleotide exchange to effector recruitment and function. Cell *90*, 1149–1159.

Huotari, J., and Helenius, A. (2011). Endosome maturation. Embo J *30*, 3481–3500.

Jovic, M., Sharma, M., Rahajeng, J., and Caplan, S. (2010). The early endosome: a busy sorting station for proteins at the crossroads. Histol. Histopathol. *25*, 99–112.

Keen, J.H., Willingham, M.C., and Pastan, I.H. (1979). Clathrin-coated vesicles: isolation, dissociation and factor-dependent reassociation of clathrin baskets. Cell *16*, 303–312.

Kirchhausen, T. (1999). Adaptors for clathrin-mediated traffic. Annu Rev Cell Dev Biol *15*, 705–732.

Korobko, E.V., Kiselev, S.L., and Korobko, I.V. (2002). Multiple Rabaptin-5-like transcripts. Gene *292*, 191–197.

Korobko, E.V., Palgova, I.V., Kiselev, S.L., and Korobko, I.V. (2006). Apoptotic cleavage of rabaptin-5-like proteins and a model for rabaptin-5 inactivation in apoptosis. Cell Cycle *5*, 1854–1858.

Korobko, E., Kiselev, S., Olsnes, S., Stenmark, H., and Korobko, I. (2005). The Rab5 effector Rabaptin-5 and its isoform Rabaptin-5delta differ in their ability to interact with the small GTPase Rab4. Febs J. *272*, 37–46.

Kostelansky, M.S., Schluter, C., Tam, Y.Y.C., Lee, S., Ghirlando, R., Beach, B., Conibear, E., and Hurley, J.H. (2007). Molecular architecture and functional model of the complete yeast ESCRT-I heterotetramer. Cell *129*, 485–498.

Kriz, A., Schmid, K., Baumgartner, N., Ziegler, U., Berger, I., Ballmer-Hofer, K., and Berger, P. (2010). A plasmid-based multigene expression system for mammalian cells. Nat Commun *1*, 120–120.

Kuroda, T.S., and Fukuda, M. (2004). Rab27A-binding protein Slp2-a is required for peripheral melanosome distribution and elongated cell shape in melanocytes. Nat Cell Biol *6*, 1195–1203.

Lawe, D.C., Patki, V., Heller-Harrison, R., Lambright, D., and Corvera, S. (2000). The FYVE domain of early endosome antigen 1 is required for both phosphatidylinositol 3-phosphate and Rab5 binding. Critical role of this dual interaction for endosomal localization. J Biol Chem *275*, 3699–3705.

Lee, S., Tsai, Y.C., Mattera, R., Smith, W.J., Kostelansky, M.S., Weissman, A.M., Bonifacino, J.S., and Hurley, J.H. (2006). Structural basis for ubiquitin recognition and autoubiquitination by Rabex-5. Nat Struct Mol Biol *13*, 264–271.

Lippé, R., Miaczynska, M., Rybin, V., Runge, A., and Zerial, M. (2001). Functional synergy between Rab5 effector Rabaptin-5 and exchange factor Rabex-5 when physically associated in a complex. Mol Biol Cell *12*, 2219–2228.

Luzio, J.P., Pryor, P.R., and Bright, N.A. (2007). Lysosomes: fusion and function. Nat Rev Mol Cell Biol *8*, 622–632.

Massol, R.H., Boll, W., Griffin, A.M., and Kirchhausen, T. (2006). A burst of auxilin recruitment determines the onset of clathrin-coated vesicle uncoating. Proc Natl Acad Sci USA *103*, 10265–10270.

Mattera, R., and Bonifacino, J.S. (2008). Ubiquitin binding and conjugation regulate the recruitment of Rabex-5 to early endosomes. Embo J *27*, 2484–2494.

Mattera, R., Arighi, C.N., Lodge, R., Zerial, M., and Bonifacino, J.S. (2003). Divalent interaction of the GGAs with the Rabaptin-5-Rabex-5 complex. Embo J *22*, 78–88.

Mattera, R., Tsai, Y.C., Weissman, A.M., and Bonifacino, J.S. (2006). The Rab5 guanine nucleotide exchange factor Rabex-5 binds ubiquitin (Ub) and functions as a Ub ligase through an atypical Ub-interacting motif and a zinc finger domain. J Biol Chem *281*, 6874–6883.

Maxfield, F.R., and Mcgraw, T.E. (2004). Endocytic recycling. Nat Rev Mol Cell Biol *5*, 121–132.

McBride, H.M., Rybin, V., Murphy, C., Giner, A., Teasdale, R., and Zerial, M. (1999). Oligomeric complexes link Rab5 effectors with NSF and drive membrane fusion via interactions between EEA1 and syntaxin 13. Cell *98*, 377–386.

McCaffrey, M.W., Bielli, A., Cantalupo, G., Mora, S., Roberti, V., Santillo, M., Drummond, F., and Bucci, C. (2001). Rab4 affects both recycling and degradative endosomal trafficking. FEBS Lett *495*, 21–30.

McGough, I.J., and Cullen, P.J. (2011). Recent advances in retromer biology. Traffic *12*, 963–971.

McLauchlan, H., Newell, J., Morrice, N., Osborne, A., West, M., and Smythe, E. (1998). A novel role for Rab5-GDI in ligand sequestration into clathrin-coated pits. Curr Biol *8*, 34–45.

McMahon, H.T., and Boucrot, E. (2011). Molecular mechanism and physiological functions of clathrin-mediated endocytosis. Nat Rev Mol Cell Biol *12*, 517–533.

Mellman, I. (1996). Endocytosis and molecular sorting. Annu Rev Cell Dev Biol *12*, 575–625.

Meyer, C., Zizioli, D., Lausmann, S., Eskelinen, E.L., Hamann, J., Saftig, P., Figura, von, K., and Schu, P. (2000). mu1A-adaptin-deficient mice: lethality, loss of AP-1 binding and rerouting of mannose 6-phosphate receptors. Embo J *19*, 2193–2203.

Méresse, S., Gorvel, J.P., and Chavrier, P. (1995). The rab7 GTPase resides on a vesicular compartment connected to lysosomes. J Cell Sci *108 (Pt 11)*, 3349–3358.

Miele, A.E., Watson, P.J., Evans, P.R., Traub, L.M., and Owen, D.J. (2004). Two distinct interaction motifs in amphiphysin bind two independent sites on the clathrin terminal domain beta-propeller. Nat Struct Mol Biol *11*, 242–248.

Mills, I.G., Jones, A.T., and Clague, M.J. (1998). Involvement of the endosomal autoantigen EEA1 in homotypic fusion of early endosomes. Curr Biol *8*, 881–884.

Mills, I.G., Jones, A.T., and Clague, M.J. (1999). Regulation of endosome fusion. Mol Membr Biol *16*, 73–79.

Mironov, A.A., Beznoussenko, G.V., Nicoziani, P., Martella, O., Trucco, A., Kweon, H.S., Di Giandomenico, D., Polishchuk, R.S., Fusella, A., Lupetti, P., et al. (2001). Small cargo proteins and large aggregates can traverse the Golgi by a common mechanism without leaving the lumen of cisternae. J Cell Biol *155*, 1225–1238.

Mitsunari, T., Nakatsu, F., Shioda, N., Love, P.E., Grinberg, A., Bonifacino, J.S., and Ohno, H. (2005). Clathrin adaptor AP-2 is essential for early embryonal development. Mol. Cell. Biol. *25*, 9318–9323.

Mohrmann, K. (2002). rab4 Function in Membrane Recycling from Early Endosomes Depends on a Membrane to Cytoplasm Cycle. Journal of Biological Chemistry *277*, 32029–32035.

Mohrmann, K., and van der Sluijs, P. (1999). Regulation of membrane transport through the endocytic pathway by rabGTPases. Mol Membr Biol *16*, 81–87.

Morgan, J.R., Prasad, K., Hao, W., Augustine, G.J., and Lafer, E.M. (2000). A conserved clathrin assembly motif essential for synaptic vesicle endocytosis. J. Neurosci. *20*, 8667–8676.

Möbius, W., van Donselaar, E., Ohno-Iwashita, Y., Shimada, Y., Heijnen, H.F.G., Slot, J.W., and Geuze, H.J. (2003). Recycling compartments and the internal vesicles of multivesicular bodies harbor most of the cholesterol found in the endocytic pathway. Traffic *4*, 222–231.

Mu, F.T., Callaghan, J.M., Steele-Mortimer, O., Stenmark, H., Parton, R.G., Campbell, P.L., McCluskey, J., Yeo, J.P., Tock, E.P., and Toh, B.H. (1995). EEA1, an early endosome-associated protein. EEA1 is a conserved alpha-helical peripheral membrane protein flanked by cysteine “fingers” and contains a calmodulin-binding IQ motif. J Biol Chem *270*, 13503–13511.

Nakatsu, F., and Ohno, H. (2003). Adaptor protein complexes as the key regulators of protein sorting in the post-Golgi network. Cell Struct Funct *28*, 419–429.

Nakayama, K., and Wakatsuki, S. (2003). The structure and function of GGAs, the traffic controllers at the TGN sorting crossroads. Cell Struct Funct *28*, 431–442.

Naslavsky, N., Boehm, M., Backlund, P.S., and Caplan, S. (2004). Rabenosyn-5 and EHD1 interact and sequentially regulate protein recycling to the plasma membrane. Mol Biol Cell *15*, 2410–2422.

Nielsen, E., Christoforidis, S., Uttenweiler-Joseph, S., Miaczynska, M., Dewitte, F., Wilm, M., Hoflack, B., and Zerial, M. (2000). Rabenosyn-5, a novel Rab5 effector, is complexed with hVPS45 and recruited to endosomes through a FYVE finger domain. J Cell Biol *151*, 601–612.

Nielsen, E., Severin, F., Backer, J.M., Hyman, A.A., and Zerial, M. (1999). Rab5 regulates motility of early endosomes on microtubules. Nat Cell Biol *1*, 376–382.

Nordmann, M., Cabrera, M., Perz, A., Bröcker, C., Ostrowicz, C., Engelbrecht-Vandré, S., and Ungermann, C. (2010). The Mon1-Ccz1 complex is the GEF of the late endosomal Rab7 homolog Ypt7. Curr Biol *20*, 1654–1659.

Ohno, H., Tomemori, T., Nakatsu, F., Okazaki, Y., Aguilar, R.C., Foelsch, H., Mellman, I., Saito, T., Shirasawa, T., and Bonifacino, J.S. (1999). Mu1B, a novel adaptor medium chain expressed in polarized epithelial cells. FEBS Lett *449*, 215–220.

Olusanya, O., Andrews, P.D., Swedlow, J.R., and Smythe, E. (2001). Phosphorylation of threonine 156 of the mu2 subunit of the AP2 complex is essential for endocytosis in vitro and in vivo. Curr Biol *11*, 896–900.

Ooi, C.E., Dell'Angelica, E.C., and Bonifacino, J.S. (1998). ADP-Ribosylation factor 1 (ARF1) regulates recruitment of the AP-3 adaptor complex to membranes. J Cell Biol *142*, 391–402.

Owen, D.J., Vallis, Y., Pearse, B.M., McMahon, H.T., and Evans, P.R. (2000). The structure and function of the beta 2-adaptin appendage domain. Embo J *19*, 4216–4227.

Owen, D.J., Collins, B.M., and Evans, P.R. (2004). Adaptors for clathrin coats: structure and function. Annu Rev Cell Dev Biol *20*, 153–191.

Pagano, A., Crottet, P., Prescianotto-Baschong, C., and Spiess, M. (2004). In vitro formation of recycling vesicles from endosomes requires adaptor protein-1/clathrin and is regulated by rab4 and the connector rabaptin-5. Mol Biol Cell *15*, 4990–5000.

Patki, V., Virbasius, J., Lane, W.S., Toh, B.H., Shpetner, H.S., and Corvera, S. (1997). Identification of an early endosomal protein regulated by phosphatidylinositol 3-kinase. Proc Natl Acad Sci USA *94*, 7326–7330.

Pearse, B.M. (1976). Clathrin: a unique protein associated with intracellular transfer of membrane by coated vesicles. Proc Natl Acad Sci USA *73*, 1255–1259.

Pelham, H.R.B. (2004). Membrane traffic: GGAs sort ubiquitin. Curr Biol *14*, R357–R359.

Penengo, L., Mapelli, M., Murachelli, A.G., Confalonieri, S., Magri, L., Musacchio, A., Di Fiore, P.P., Polo, S., and Schneider, T.R. (2006). Crystal structure of the ubiquitin binding domains of rabex-5 reveals two modes of interaction with ubiquitin. Cell *124*, 1183–1195.

Peralta, E.R., Martin, B.C., and Edinger, A.L. (2010). Differential effects of TBC1D15 and mammalian Vps39 on Rab7 activation state, lysosomal morphology, and growth factor dependence. J Biol Chem *285*, 16814–16821.

Pevsner, J., Volknandt, W., Wong, B.R., and Scheller, R.H. (1994). Two rat homologs of clathrin-associated adaptor proteins. Gene *146*, 279–283.

Pfeffer, S.R. (2013). Rab GTPase regulation of membrane identity. Curr Opin Cell Biol *25*, 414–419.

Poteryaev, D., Datta, S., Ackema, K., Zerial, M., and Spang, A. (2010). Identification of the switch in early-to-late endosome transition. Cell *141*, 497–508.

Poupart, M.-E., Fessart, D., Cotton, M., Laporte, S.A., and Claing, A. (2007). ARF6 regulates angiotensin II type 1 receptor endocytosis by controlling the recruitment of AP-2 and clathrin. Cell Signal *19*, 2370–2378.

Press, B., Feng, Y., Hoflack, B., and Wandinger-Ness, A. (1998). Mutant Rab7 causes the accumulation of cathepsin D and cation-independent mannose 6-phosphate receptor in an early endocytic compartment. J Cell Biol *140*, 1075–1089.

Puertollano, R., Aguilar, R.C., Gorshkova, I., Crouch, R.J., and Bonifacino, J.S. (2001). Sorting of mannose 6-phosphate receptors mediated by the GGAs. Science *292*, 1712–1716.

Rabouille, C., and Klumperman, J. (2005). Opinion: The maturing role of COPI vesicles in intra-Golgi transport. Nat Rev Mol Cell Biol *6*, 812–817.

Raiborg, C., Bache, K.G., Mehlum, A., Stang, E., and Stenmark, H. (2001a). Hrs recruits clathrin to early endosomes. Embo J *20*, 5008–5021.

Raiborg, C., Bremnes, B., Mehlum, A., Gillooly, D.J., D'Arrigo, A., Stang, E., and Stenmark, H. (2001b). FYVE and coiled-coil domains determine the specific localisation of Hrs to early endosomes. J Cell Sci *114*, 2255–2263.

Raiborg, C., and Stenmark, H. (2002). Hrs and endocytic sorting of ubiquitinated membrane proteins. Cell Struct Funct *27*, 403–408.

Raiborg, C., and Stenmark, H. (2009). The ESCRT machinery in endosomal sorting of ubiquitylated membrane proteins. Nature *458*, 445–452.

Ren, M., Xu, G., Zeng, J., De Lemos-Chiarandini, C., Adesnik, M., and Sabatini, D.D. (1998). Hydrolysis of GTP on rab11 is required for the direct delivery of transferrin from the pericentriolar recycling compartment to the cell surface but not from sorting endosomes. Proc Natl Acad Sci USA *95*, 6187–6192.

Ricotta, D., Conner, S.D., Schmid, S.L., Figura, von, K., and Höning, S. (2002). Phosphorylation of the AP2 mu subunit by AAK1 mediates high affinity binding to membrane protein sorting signals. J Cell Biol *156*, 791–795.

Rink, J., Ghigo, E., Kalaidzidis, Y., and Zerial, M. (2005). Rab conversion as a mechanism of progression from early to late endosomes. Cell *122*, 735–749.

Roosterman, D., Schmidlin, F., and Bunnett, N.W. (2003). Rab5a and rab11a mediate agonist-induced trafficking of protease-activated receptor 2. Am J Physiol, Cell Physiol *284*, C1319–C1329.

Rothman, J.E., and Wieland, F.T. (1996). Protein sorting by transport vesicles. Science *272*, 227–234.

Saftig, P., and Klumperman, J. (2009). Lysosome biogenesis and lysosomal membrane proteins: trafficking meets function. Nat Rev Mol Cell Biol *10*, 623–635.

Saint-Pol, A., Yélamos, B., Amessou, M., Mills, I.G., Dugast, M., Tenza, D., Schu, P., Antony, C., McMahon, H.T., Lamaze, C., et al. (2004). Clathrin adaptor epsinR is required for retrograde sorting on early endosomal membranes. Dev Cell *6*, 525–538.

Saksena, S., Wahlman, J., Teis, D., Johnson, A.E., and Emr, S.D. (2009). Functional reconstitution of ESCRT-III assembly and disassembly. Cell *136*, 97–109.

Sato, M., Sato, K., Fonarev, P., Huang, C.-J., Liou, W., and Grant, B.D. (2005). Caenorhabditis elegans RME-6 is a novel regulator of RAB-5 at the clathrin-coated pit. Nat Cell Biol *7*, 559–569.

Schlossman, D.M., Schmid, S.L., Braell, W.A., and Rothman, J.E. (1984). An enzyme that removes clathrin coats: purification of an uncoating ATPase. J Cell Biol *99*, 723–733.

Semerdjieva, S., Shortt, B., Maxwell, E., Singh, S., Fonarev, P., Hansen, J., Schiavo, G., Grant, B.D., and Smythe, E. (2008). Coordinated regulation of AP2 uncoating from clathrin-coated vesicles by rab5 and hRME-6. J Cell Biol *183*, 499–511.

Sever, S. (2002). Dynamin and endocytosis. Curr Opin Cell Biol *14*, 463–467.

Simmen, T., Höning, S., Icking, A., Tikkanen, R., and Hunziker, W. (2002). AP-4 binds basolateral signals and participates in basolateral sorting in epithelial MDCK cells. Nat Cell Biol *4*, 154–159.

Simonsen, A., Gaullier, J.M., D'Arrigo, A., and Stenmark, H. (1999). The Rab5 effector EEA1 interacts directly with syntaxin-6. J Biol Chem *274*, 28857–28860.

Sobo, K., Chevallier, J., Parton, R.G., Gruenberg, J., and van der Goot, F.G. (2007). Diversity of raft-like domains in late endosomes. PLoS ONE *2*, e391.

Spang, A. (2008). The life cycle of a transport vesicle. Cell. Mol. Life Sci. *65*, 2781–2789.

Stamnes, M.A., and Rothman, J.E. (1993). The binding of AP-1 clathrin adaptor particles to Golgi membranes requires ADP-ribosylation factor, a small GTP-binding protein. Cell *73*, 999–1005.

Stenmark, H., Aasland, R., Toh, B.H., and D'Arrigo, A. (1996). Endosomal localization of the autoantigen EEA1 is mediated by a zinc-binding FYVE finger. J Biol Chem *271*, 24048–24054.

Stenmark, H., Parton, R.G., Steele-Mortimer, O., Lütcke, A., Gruenberg, J., and Zerial, M. (1994). Inhibition of rab5 GTPase activity stimulates membrane fusion in endocytosis. Embo J *13*, 1287–1296.

Stenmark, H., Vitale, G., Ullrich, O., and Zerial, M. (1995). Rabaptin-5 is a direct effector of the small GTPase Rab5 in endocytic membrane fusion. Cell *83*, 423–432.

Stenmark, H. (2009). Rab GTPases as coordinators of vesicle traffic. Nat Rev Mol Cell Biol *10*, 513–525.

Stimpson, H.E.M., Toret, C.P., Cheng, A.T., Pauly, B.S., and Drubin, D.G. (2009). Early-arriving Syp1p and Ede1p function in endocytic site placement and formation in budding yeast. Mol Biol Cell *20*, 4640–4651.

Sundborger, A., Soderblom, C., Vorontsova, O., Evergren, E., Hinshaw, J.E., and Shupliakov, O. (2011). An endophilin-dynamin complex promotes budding of clathrin-coated vesicles during synaptic vesicle recycling. J Cell Sci *124*, 133–143.

Swaminathan, S., Amerik, A.Y., and Hochstrasser, M. (1999). The Doa4 deubiquitinating enzyme is required for ubiquitin homeostasis in yeast. Mol Biol Cell *10*, 2583–2594.

Taguchi, T. (2013). Emerging roles of recycling endosomes. J Biochem *153*, 505–510.

Takatsu, H., Yoshino, K., Toda, K., and Nakayama, K. (2002). GGA proteins associate with Golgi membranes through interaction between their GGAH domains and ADP-ribosylation factors. Biochem J *365*, 369–378.

Traub, L.M., Ostrom, J.A., and Kornfeld, S. (1993). Biochemical dissection of AP-1 recruitment onto Golgi membranes. J Cell Biol *123*, 561–573.

Trischler, M., Stoorvogel, W., and Ullrich, O. (1999). Biochemical analysis of distinct Rab5- and Rab11-positive endosomes along the transferrin pathway. J Cell Sci *112 (Pt 24)*, 4773–4783.

Trowbridge, I.S., Collawn, J.F., and Hopkins, C.R. (1993). Signal-dependent membrane protein trafficking in the endocytic pathway. Annu Rev Cell Biol *9*, 129–161.

Ui, M., Okada, T., Hazeki, K., and Hazeki, O. (1995). Wortmannin as a unique probe for an intracellular signalling protein, phosphoinositide 3-kinase. Trends Biochem. Sci. *20*, 303–307.

Ullrich, O., Reinsch, S., Urbé, S., Zerial, M., and Parton, R.G. (1996). Rab11 regulates recycling through the pericentriolar recycling endosome. J Cell Biol *135*, 913–924.

Ungewickell, E., and Branton, D. (1981). Assembly units of clathrin coats. Nature *289*, 420–422.

Urbé, S., Huber, L.A., Zerial, M., Tooze, S.A., and Parton, R.G. (1993). Rab11, a small GTPase associated with both constitutive and regulated secretory pathways in PC12 cells. FEBS Lett *334*, 175–182.

van Dam, E.M., Broeke, Ten, T., Jansen, K., Spijkers, P., and Stoorvogel, W. (2002). Endocytosed transferrin receptors recycle via distinct dynamin and phosphatidylinositol 3-kinase-dependent pathways. J Biol Chem *277*, 48876–48883.

van der Sluijs, P., Hull, M., Webster, P., Mâle, P., Goud, B., and Mellman, I. (1992). The small GTP-binding protein rab4 controls an early sorting event on the endocytic pathway. Cell *70*, 729–740.

van der Sluijs, P., Hull, M., Zahraoui, A., Tavitian, A., Goud, B., and Mellman, I. (1991). The small GTP-binding protein rab4 is associated with early endosomes. Proc Natl Acad Sci USA *88*, 6313–6317.

Vitale, G., Rybin, V., Christoforidis, S., Thornqvist, P., McCaffrey, M., Stenmark, H., and Zerial, M. (1998). Distinct Rab-binding domains mediate the interaction of Rabaptin-5 with GTP-bound Rab4 and Rab5. Embo J *17*, 1941–1951.

Vitelli, R., Santillo, M., Lattero, D., Chiariello, M., Bifulco, M., Bruni, C.B., and Bucci, C. (1997). Role of the small GTPase Rab7 in the late endocytic pathway. J Biol Chem *272*, 4391–4397.

Vlahos, C.J., Matter, W.F., Hui, K.Y., and Brown, R.F. (1994). A specific inhibitor of phosphatidylinositol 3-kinase, 2-(4-morpholinyl)-8-phenyl-4H-1-benzopyran-4-one (LY294002). J Biol Chem *269*, 5241–5248.

Volpicelli-Daley, L.A., Li, Y., Zhang, C.-J., and Kahn, R.A. (2005). Isoform-selective effects of the depletion of ADP-ribosylation factors 1-5 on membrane traffic. Mol Biol Cell *16*, 4495–4508.

Vonderheit, A., and Helenius, A. (2005). Rab7 associates with early endosomes to mediate sorting and transport of Semliki forest virus to late endosomes. PLoS Biol. *3*, e233.

Wasiak, S., Legendre-Guillemin, V., Puertollano, R., Blondeau, F., Girard, M., de Heuvel, E., Boismenu, D., Bell, A.W., Bonifacino, J.S., and McPherson, P.S. (2002). Enthoprotin: a novel clathrin-associated protein identified through subcellular proteomics. J Cell Biol *158*, 855–862.

Wurmser, A.E., Sato, T.K., and Emr, S.D. (2000). New component of the vacuolar class C-Vps complex couples nucleotide exchange on the Ypt7 GTPase to SNARE-dependent docking and fusion. J Cell Biol *151*, 551–562.

Yamamoto, H., Koga, H., Katoh, Y., Takahashi, S., Nakayama, K., and Shin, H.-W. (2010). Functional cross-talk between Rab14 and Rab4 through a dual effector, RUFY1/Rabip4. Mol Biol Cell *21*, 2746–2755.

Zerial, M., and McBride, H. (2001). Rab proteins as membrane organizers. Nat Rev Mol Cell Biol *2*, 107–117.

Zhu, G., Zhai, P., Liu, J., Terzyan, S., Li, G., and Zhang, X.C. (2004). Structural basis of Rab5-Rabaptin5 interaction in endocytosis. Nat Struct Mol Biol *11*, 975–983.

Zhu, H., Zhu, G., Liu, J., Liang, Z., Zhang, X.C., and Li, G. (2007). Rabaptin-5-independent membrane targeting and Rab5 activation by Rabex-5 in the cell. Mol Biol Cell *18*, 4119–4128.

Transferrin recycling experiments in Figure 23C/D and 34E were performed by David Hirschmann